Terry's Nail Identification: A Novel Machine Learning Approach

Umer Hassan

Department of Biomedical Engineering, Faculty of Engineering, Science, Technology, and Management
Ziauddin University
Karachi, Pakistan

umer13504@zu.edu.pk

Saad Jawaid Khan*

Department of Biomedical Engineering, Faculty of Engineering, Science, Technology, and Management
Ziauddin University
Karachi, Pakistan

sj.khan@zu.edu.pk

Syeda Fatima Aijaz

Department of Biomedical Engineering, Faculty of Engineering, Science, Technology, and Management
Ziauddin University
Karachi, Pakistan

syeda13503@zu.edu.pk

Choudhary Sobhan Shakeel

Department of Biomedical Engineering, Faculty of Engineering, Science, Technology, and Management
Ziauddin University
Karachi, Pakistan

sobhanshakeel19@gmail.com

Abstract - **Terry's nail is a condition in which the nail seems to have a kind of leukonychia that is differentiated by the ground glass occlusion of the nail, the pink nail bed at the distal border, and the loss of the lunula. The objective of this study is to use a decision tree-based machine learning algorithm to classify Terry's nails and healthy nails. The study has been executed with the collection of a dataset of a total of 87 nail images. It consists of 48 images of normal, healthy nails and 39 images of Terry's nails. The images are categorized using feature extraction techniques and a decision tree classifier algorithm to help with the classification. A total of 27 nail images were evaluated, yielding an accuracy of 82.5%. As per the results, decision tree approaches have the capability of achieving robust categorization and efficiency.**

Keywords - Nail Image; Nail Disease; Machine Learning; Terry's Nail; Decision Tree;

I. INTRODUCTION

In order to properly diagnose patients, medical practitioners have access to far too many technologies. According to a study, nails are a key indication of a person's overall wellbeing [1]. A lack of oxygen may cause nails to become weak and brittle. Since this is the case, the nails are frequently the first to show signs of illness [2]. As per a study conducted, nails are a reliable predictor of exposure for the last six months [3]. Nail diseases may affect anyone at any age, regardless of their age, gender, or race. But in a recent study, it was found that nail disorders are more frequent in those over the age of 60. In the 60–70 age category, around 15% of the population is afflicted [1].

It may be difficult to tell whether a person has a long-term medical condition by looking at the nail plate and its unit [4]. A number of feature extraction techniques may be used to extract information about an object's appearance, including shape, color, and texture [5]. A machine is able to detect color and texture changes that the human eye is unable to see. When it comes to the processing of health information, such as diagnostic imaging, automated feature extraction does not require any human interaction [6]. One of humanity's greatest challenges is accurately predicting the impact of sickness on human health [2]. The field of medicine has achieved significant development in recent years [7].

Fingernails' color, texture, and shape reveal signs of a disease or nutritional imbalance, so they might be used as a diagnostic tool [8]. Terry's nails, or extensive nail whitening from the lunula to practically every section of the nail, were first associated with cirrhosis [9]. Terry's nails: when detected in younger people, this symptom is more likely to reflect systemic illness [10]. A number of diseases concluded that Terry's nails are recognized in terms of contributing to other health issues, such as diabetes, hearing loss, and chronic renal failure [11–13].

According to research by Safira, Budhi and Casi [14], GLCM feature extraction was used, which characterizes the texture of an image. KNN classification was also used in order to identify Terry's nail. In that study, nails were classified into Terry's nails and safe nails, and the KNN method used in this research yielded a 98.50% accuracy rate. In another study, they predicted many diseases of the nails by determining the average RGB color of nail images. After that, a decision tree was used to predict diseases like Terry's lines, Beau's lines, white nails, dark lines, yellow nails, and pale nails. Only 65% accuracy was achieved using the decision tree [8]. The SVM classification was utilized in research by Priya Maniyan and BL Shivakumar, in which they used it to detect different nail diseases and their related medical issues and attained 89.9% [15]. Another study has identified nail abnormalities such as onchophagia, darier, eczema, lindsays, melanonychioa, and onchocryptosis, as well as other conditions including pachyonychia, koilonychia, and anonychia. The research also examined Terry's disease, clubbing, glomustumor, psoriasis, and Beau's lines in addition to these disorders. Researchers used SVM, multi-class SVM, and KNN to reach an accuracy of 98.75% [16].

The aim of this research is to classify the healthy nail and Terry's nail images by using feature extraction technique and

*Corresponding Author

decision tree classifier algorithm. This is done by utilizing data acquired from internet sources. Sections of this research are listed as follows: Section 1 consists of an introduction; Section 2 contains methodology; experimental findings and discussion can be seen in the third section; and the conclusion is outlined in the fourth section.

II. METHODOLOGY

This research uses a decision tree to diagnose and classify "healthy nails" and "Terry's nails". It is shown in Fig. 1 how the process works. It starts with an image collection and ends with the classification of two classes.
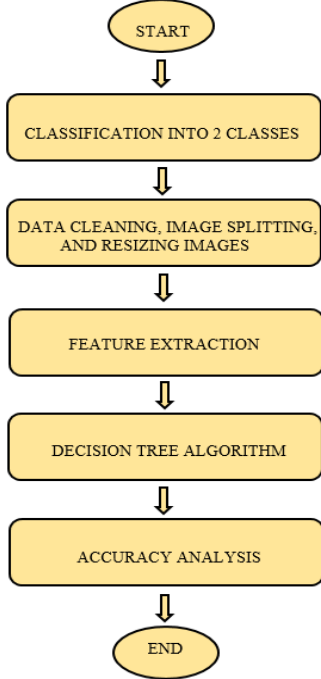
Fig. 1 Proposed Flow Chart of Classification Framework

A. Dataset Sampling

The dataset description is shown in Fig. 2. To build one clear and enhanced dataset, we combined the standard image datasets from two separate data sources, Dermnet and Kaggle. Terry's nail images totaled thirty-nine (39), while normal, healthy nail images totaled forty-eight (48). Eighty-seven (87) images from both classes were gathered in the end. The data was then split and normalized into two distinct files, each representing a distinct class, before being processed and normalized once again.

Each image was scrutinized to see whether it accurately depicted the color, texture, and shape of the two classes, and then the most convincing images were chosen. There were 87 nail images, taken from different sources and then converted to JPEG format. To enhance images, a Python-based system was used. All of the images in this study were segmented using the resize approach. The term "resize operation" refers to the procedure of increasing or lowering the size of a picture by a given quantity. Using the shape function, a NumPy array of the image is rebuilt. It is possible by resizing and deleting the shape

element using the flatten method. As a result, they are combined into one NumPy array that just contains the three colors of the picture, which are red, blue, and green.
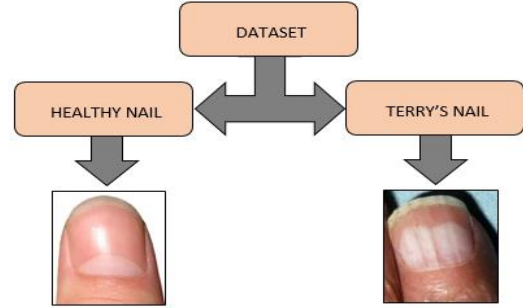
Fig. 2 Illustration of Image Dataset

Data from 70% of each class was utilized for training, while the rest of the data (30%) from each class was tested once the data was cleaned. Overall, there were 87 nail images, 60 of which were training images from both the healthy and Terry's nails, and 27 of which were testing images, as presented in Table 1.

Table 1: Training and Testing Dataset

S. No.	Classes	No. of Training Images	No. of Testing Images
1.	Healthy Nail	33	15
2.	Terry's Nail	27	12
	Total	60	27

B. Extraction of Features

The three features to be extracted are color, shape, and texture from each image dataset, which is a nail image. This is the focus of our research. Features extraction like shape, color, and texture are accomplished via the usage of the libraries of Python CV2 and Skimage.

1) Texture Feature

Python's cv2 and skimage libraries were used in this research to make use of Scikit's image processing capabilities. To determine how local binary patterns (LBPs) appear, an algorithm compares each nail image's pixel to the pixels surrounding it. The equation (1) specifies how the texture was extracted using LBP:

$$\text{LBP}(\text{bpx}, \text{bpy}) = \sum_{p=0}^{p-1} L(\text{bp} - \text{cp}) \times 2^p \qquad (1)$$

In Equation (1), the bordering pixel's intensity is denoted as "bp", and the intensity of the center pixel is signified as "cp". If "x" in L(x) is equal to or greater than 0, then the value is 1, otherwise it is 0.

2) Color Feature

In order to undertake this research, using NumPy, the pictures were turned into a list of red, green, and blue color pixel values, which represent the three color features that make up an image, and the cv2 library was used to determine the average of

each channel. There are three mean values that the CV2 library generates, and they are all for RGB. As an illustration, in the CV2 library, color-space images are saved as NumPy arrays in reverse order, with values corresponding to each channel's RGB values.

3) Shape Feature

The Hu moment shape descriptor has been used to retrieve shape information from the nail images. The Hu moment was imported into the application using a Python library called OpenCV. Equations (2) and (3) indicate the computed Hu moment, where "hu" represents the calculated Hu moment and "c" means the central moment. When calculating Hu moments, the central moment is considered since it contributes to the movement of the dataset's midpoint region toward the centroid area. By measuring the contour of the input, Hu moments were used to analyze photos, resulting in a NumPy array of the pictures. The shape feature vector was created by flattening NumPy arrays using the method "flatten".

$$hu = c_0 + c_1 \quad (2)$$

$$hu_1 = (c_0 + c_1)^2 + 4c^2 \quad (3)$$

C. Decision Tree

There is a promising future for automated identification of species when ML algorithms are applied to biological imaging data. A categorization approach like the decision tree has been shown to be successful in its purpose of extracting relevant, legitimate, and potentially innovative information [17]. A decision tree may generate easy-to-interpret rules and restrictions without jeopardizing the effectiveness of the algorithm [18]. Unknown samples with numerous class labels can also be handled by decision trees [19]. The effectiveness of decision trees is equivalent to that of other algorithms since they are basic and simple to comprehend by humans [18]. In a decision tree, every root is specified by a data-separating sequence until the leaf node has a Boolean conclusion [20, 21]. There are nodes and links in this hierarchical depiction of knowledge linkages. Nodes indicate purposes when relations are used to categorize data [22, 23]. The equation (4) was used in our case to measure the information gain of splitting a node.

$$D = -\sum_{m=2}^{n} k(j_m) \log_2 k(j_m) \quad (4)$$

The m in Equation (4) represents the number of classes. In our study, the number of classes was 2, so here m = 2. Equation (5) shows the actual equation used in this case.

$$D = -(k(TN) \log_2 k(TN)) - (k(HN) \log_2 k(MHN)) \quad (5)$$

Where "k(TN)" is the probability of class Terry's Nails and "k(HN)" for Healthy Nails.

III. RESULTS

The confusion matrix consists of 4 values, which are true positive (TP), false positive (FP), true negative (TN), and false negative (FN). According to a study by Zeng [24], TN is the percentage of negatives that are actually negatives. An accurate count of positives is called a TP, whereas FN is how often positives are mistaken for negatives. And an inaccurately categorized negative as a positive is a FP. In Fig. 3, the classification and performance outcomes of a decision tree are shown in the form of a confusion matrix, where the class "Healthy Nail" is represented by "0" and the "Terry's Nail" class is denoted as "1".

Fig. 3 Decision Tree Confusion Matrix

Fig. 3 shows that 42 of the healthy nail images were classified as true negatives, whereas 13 of Terry's nail images were identified as real positives. 3 of the healthy nail images resulted in false negatives, and 7 of the terry nail images were classified as false positives.

Precision, F1 score, and recall are all metrics that were used in classification systems, which can be shown in Equations (6), (7), and (8). These were applied to assess the categorization framework's success.

$$R = \frac{\sum TP}{\sum(FN+TP)} \times 100 \quad (6)$$

$$P = \frac{\sum TP}{\sum(FP+TP)} \times 100 \quad (7)$$

$$F1\ Score = \frac{2\times(R\times P)}{R+P} \times 100 \quad (8)$$

The recall, precision, and F1 score values for the identification of classes by the decision tree are represented in Table 2.

Table 2: Recall, Precision and F1 Score values by Decision Tree Classifier

S. No.	Classes	Recall (%)	Precision (%)	F1 Score (%)
1.	Healthy Nails (0)	0.97	0.76	0.85
2.	Terry Nails (1)	0.28	1.00	0.43

IV. DISCUSSION

Using a machine learning system, we were able to classify healthy and Terry's nails based on the color, shape, and texture criteria taken from nail photos received from various web

sources, and the results were presented with the highest accuracy. A decision tree may provide rules and restrictions that are simple to comprehend without impairing the overall efficiency of the program [18]. Fig. 4 depicts the reported accuracy of the decision tree classifier.
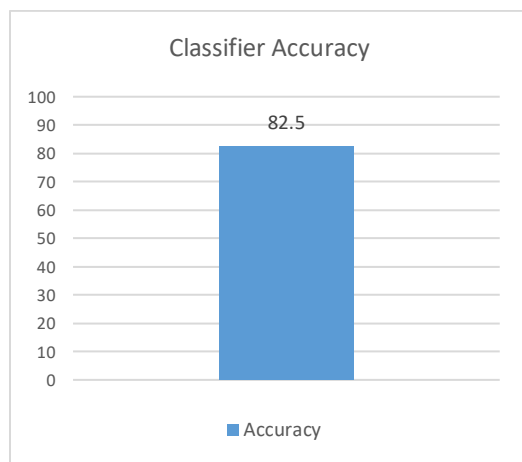
Fig. 4 Accuracy of Decision Tree

In this study, out of the 87 nail images, 69 were correctly categorized, resulting in an accuracy of 82.5%. Thirty-nine images were identified as "Terry's nail," while forty-eight images were classified as "healthy nail." On the other hand, an experiment in which researchers utilized a decision tree classifier along with determining the average RGB color of nail images to predict nail illnesses such as white nails, yellow nails, Terry's lines, pale nails, Beau lines, and dark lines only achieved a 65% accuracy rate [8]. We are the first to use several feature extraction techniques and a decision tree classifier and obtained an accuracy of 82.5% to categorize Terry's nails and healthy nails. Machine learning (ML) methods were used on a small dataset, although no clinical data was obtained in this work. However, deep learning approaches like the convolutional neural network have been extensively reported to provide excellent accuracy [6]. Deep learning applications, on the other hand, do not need image preprocessing or feature extraction. As a result, CNN may be used in the future to generate even better categorization results.

V. Conclusion

In conclusion, the framework used in this research makes use of an image dataset, extracts features like color, shape, and texture, and uses a classifier decision tree to divide the dataset into terry's nails and healthy nails. The efficacy of the proposed classifying framework was demonstrated by the use of this approach, which produced a phenomenal accuracy rate of 82.5%.

The study's satisfying results show that the created framework can correctly categorize two sets of nail images, as indicated by the acquired accuracy. There is, however, still space for further growth and enhancement in this field. Future study might look at using deep learning methodologies, namely

CNN, to improve classification accuracy and give a more detailed analysis of nail conditions.

References

[1] Wollina U, Nenoff P, Haroske G, Haenssle HA. "The diagnosis and treatment of nail disorders." *Deutsches Ärzteblatt International* 113, no. 29-30 (2016): 509.

[2] D. Nithya, S. M. Asha, R. Kurapati, B. S. Priya and D. Divya, Nail based disease analysis at earlier stage using median filter in image processing, *Int. Res. J. Eng. Technol.*, vol.6, no.3, pp.2599-2603, 2019.

[3] Parmar P, Rathod GB. "Forensic Onychology: An essential entity against crime." *Journal of Indian Academy of Forensic Medicine* 34, no. 4 (2012): 355-357.

[4] Pietrangelo, A. (2019). Nail Abnormalities. In.

[5] Sharma V, Shrivastava A. "System for Disease detection by analyzing finger nails Color and Texture." *International Journal of Advanced Engineering Research and Science (IJAERS)* 2, no. 10 (2015).

[6] D. Ravì et al., "Deep learning for health informatics." *IEEE journal of biomedical and health informatics* 21, no. 1 (2016): 4-21.

[7] Ranichitra, A. "Finger Nail Analysis to Diagnose Disease-A Study." *International Journal of Management Technology and Engineering* 8 (2018).

[8] Indi, Trupti S., and Yogesh A. Gunge. "Early stage disease diagnosis system using human nail image processing." *IJ Information Technology and Computer Science* 7 (2016): 30-35.

[9] Masunaga M, Mizumoto J. "Terry's nails due to uncontrolled diabetes mellitus." *The American Journal of Medicine* 134, no. 7 (2021): e428.

[10] Gollins CE, de Berker D. "Nails in systemic disease." *Clinical Medicine* 21, no. 3 (2021): 166.

[11] Ohta R, Sano C. "White nail as a static physical finding: revitalization of physical examination." *Clinics and Practice* 11, no. 2 (2021): 241-245.

[12] Agarwal, R., & Baid, R. (2019). Terry's nails. *The Journal of the Association of Physicians of India*, 67(9), 84-84.

[13] Witkowska AB, Jasterzbski TJ, Schwartz RA. "Terry's nails: a sign of systemic disease." *Indian journal of dermatology* 62, no. 3 (2017): 309.

[14] Safira L, Irawan B, Setianingsih C. "K-Nearest Neighbour Classification and Feature Extraction GLCM for Identification of Terry's Nail." In 2019 *IEEE International Conference on Industry 4.0, Artificial Intelligence, and Communications Technology (IAICT)*, pp. 98-104. IEEE, 2019.

[15] Maniyan P, Shivakumar BL. "Detection of diseases using nail image processing based on multiclass SVM classifier method." *Ijesc* 8, no. 5 (2018): 17382-17390.

[16] Maniyan P, Shivakumar BL. "Early Disease Detection Through Nail Image Processing Based On Ensemble Of KNN Classifier And Image Features." *IOSR Journal of Computer Engineering (IOSR-JCE)* 20, no. 3 (2018).

[17] Woods HA, Kingsolver JG, Fey SB, Vasseur DA. "Uncertainty in geographical estimates of performance and fitness." *Methods in Ecology and Evolution* 9, no. 9 (2018): 1996-2008.

[18] Jena M, Dehuri S.\. "DecisionTree for Classification and Regression: A State-of-the Art Review." *Informatica* 44, no. 4 (2020).

[19] De Caigny A, Coussement K, De Bock KW. "A new hybrid classification algorithm for customer churn prediction based on logistic regression and decision trees." *European Journal of Operational Research* 269, no. 2 (2018): 760-772.

[20] Yang FJ. "An extended idea about decision trees." In *2019 International Conference on Computational Science and Computational Intelligence (CSCI)*, pp. 349-354. IEEE, 2019.

[21] Liang J, Qin Z, Xiao S, Ou L, Lin X. "Efficient and secure decision tree classification for cloud-assisted online diagnosis services." *IEEE Transactions on Dependable and Secure Computing* 18, no. 4 (2019): 1632-1644.

[22] Suresh A, Udendhran R, Balamurgan M. "Hybridized neural network and decision tree based classifier for prognostic decision making in breast cancers." *Soft Computing* 24, no. 11 (2020): 7947-7953.

[23] Priyanka, Kumar D. "Decision tree classifier: a detailed survey." *International Journal of Information and Decision Sciences* 12, no. 3 (2020): 246-269.

[24] Zeng G. "On the confusion matrix in credit scoring and its analytical properties." *Communications in Statistics-Theory and Methods* 49, no. 9 (2020): 2080-2093.

Optimization of Conductive Ink Materials for Designing Cost-Effective Force Sensitive Resistor (FSR) Sensors for Soft Robotics

Amna Jawed Shaikh*

Biomedical Engineering Department
Salim Habib University
Karachi, Pakistan
S21BME22@shu.edu.pk

Gul Munir

Biomedical Engineering Department
Salim Habib University
Karachi, Pakistan
gul.munir@shu.edu.pk

Hassan Ali

Biomedical Engineering Department
Salim Habib University
Karachi, Pakistan
hassan.ali@shu.edu.pk

Tooba Khan

Biomedical Engineering Department

Salim Habib University

Karachi, Pakistan

tooba.khan@shu.edu.pk

Abstract

Force-sensitive resistors or force-sensing resistors play an important part in biomedical engineering as they are frequently used in soft robotics, prosthetics, and other devices that involve pressure detection. Commercially made FSRs are expensive and can be difficult to purchase in bulk for any experiment or research work. FSRs consist of a semi-conductive ink screen printed on them and their accuracy depends on the material used for the ink. Therefore, this study aims to optimize various conductive ink materials and design FSR sensors using the fabricated conductive ink. Furthermore, a comparative analysis is performed to compare the designed FSR sensor using optimized ink material with the commercially available FSR sensor. Results obtained from the study show that the graphite ink showed the least resistance and can be more conductive and the FSR designed using Graphite ink would be more effective for designing inexpensive FSR and has almost the same efficiency as the commercial one.

Keywords— Force sensitive resistor (FSR), Force sensor, Conductive ink, Low-cost force sensor, Soft robotics.

1. Introduction

Piezoresistive sensors measure the change in electrical resistance of its resistor(s) caused by applied pressure. The types of pressure sensors usually[1] used in soft robotics include thin film piezoresistive sensors[1] due to them being thin, flexible, and accessible in different shapes and sizes while remaining tactile[2] A force-sensitive resistor

(FSR) is a type of thin film piezoresistive sensor which means that it changes its resistance when force or pressure is applied on it. The FSR's resistance change is inversely related to pressure. When there is no force or pressure, the sensor may act as an infinite resistor, but as the pressure continues increasing, the resistance value starts to decrease linearly [3].

The force-sensitive resistor is highly useful in the biomedical engineering realm due to it being smaller in size than other pressure sensors and having a high level of sensitivity[3]. It has also been considered effective enough to be used in robotic hands created for gripping and grasping objects specifically[2]. Sensors used in soft grippers usually include electrodes made of graphene and carbon black conductive ink[4]. Studies show that gloves developed using FSRs and flex sensors to measure the force used by the hand while gripping an object presented results with an accuracy of 90.8%[5]. A research had been conducted where a type of low-cost capacitive force sensor was fabricated[4] that had used a commercially available conductive ink for its prototype, however the ink fabricated in this paper is similar and more pocket friendly than the commercial one.

Out of all the FSRs available in the market, very few are commonly used and are proven to be effective and economical[6]. A research was conducted where Electrochemical Paper-based Analytical Devices or ePADs were designed using conductive ink created from graphite powder and PVA based adhesive, which proved to be

---

* Corresponding Author

successful[11] and many studies have focused on designing FSRs and other types of force or bio-sensors using conductive sheets (Velostat)[7], [8], silver nanoparticles[9], [10] and other conductive materials, but this study mainly aims to design FSR using low-cost conductive ink that will prove to be cheaper and an equally effective alternative. Although for creating circuits this ink needs a coating of waterproof acrylic varnish to protect it from smudging or chipping off after drying. The commercially used conductive ink is screen printed to ensure more flexibility[12], so this low-cost conductive ink can also be screen printed and covered with varnish to preserve the circuit for a long time.

The market value of an FSR sensor in Pakistan is investigated for this research which is found to be around 1,000 – 2,000 PKR which is quite expensive for a single sensor. Velostat costs around 4,700 - 13,000 PKR which means that creating an FSR using Velostat would be costlier than buying an actual FSR. The FSRs shown in this paper were made under 500 PKR hence, they are pocket-friendly and can easily be used in place of a commercial FSR.

As stated above, the main objective of this research is to fabricate a low cost conductive ink and design an FSR using it which is easy to construct and as effective in measuring applied force as a commercial FSR.

2. Methodology

Graphene is used for making conductive ink commercially although silver and other conductive metals have been used as well. In this research carbon and graphite were used to fabricate conductive ink because of their cost-effectiveness and great conductive results. Graphite and carbon were used to create a conductive powder that is soluble in water and other substances and can even be printed on 3D circuits and used to make stretchable wireless circuits.

2.1. Preparation of conductive ink

Fabrication of carbon conductive ink was done by opening up dry cell batteries, then the carbon rod found in it was crushed into powder as seen in Figure 1. Graphite was easily obtained with pencils and crushed into powder as represented in figure 2. Carbon and graphite can be used separately to create conductive inks or mixed with a ratio of 1:2. Before using it as an ink, these conductive powders were dissolved in water until they reached an ink-like consistency.
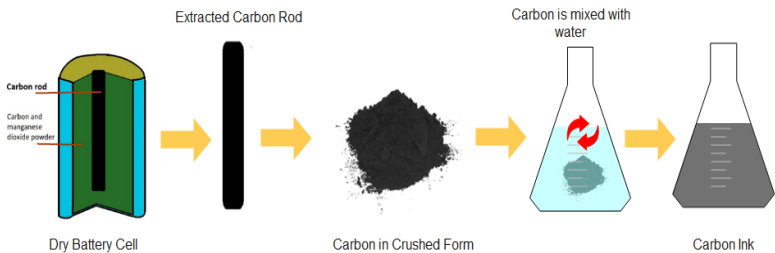
Fig. 1. Carbon extracted from a dry cell battery
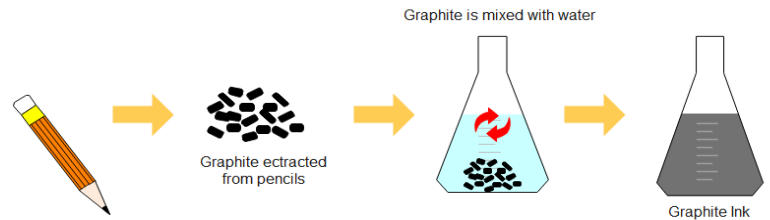
Fig. 2. Graphite extracted from pencils

Three different samples were prepared with different combinations of carbon and graphite as shown in Table 1.

Table 1: Samples of Conductive Ink

S. No.	Samples
1.	Carbon + water ink
2.	Graphite + water ink
3.	Carbon + graphite + water ink

The resistance of fabricated conductive inks is measured using a digital multimeter.

2.2. Model Design of FSR:

The FSR was constructed based on a 3D prototype designed on Fusion360 (see Figures 3-5), hence it was created by taking two sheets of a conductive material (either copper or aluminum) and sandwiching a layer of conductive ink in between. Then it was enclosed in plastic to avoid accidental damage and errors. A thin long piece of each conductive sheet was left uncovered on each side (or can be on one side) to measure the change in resistance of the FSR. The dimensions of these materials can be seen in Table 2 and the finished product is shown in Figure 6.

Table 2: Dimensions of the materials used in FSR

Materials	Length 'cm'	Width 'cm'
Aluminum	6.5cm	4.5cm
Plastic	5.5cm	5.5cm

The final FSR had the dimensions 9.5 x 5.5cm but it can be changed and the size can be reduced as per need.
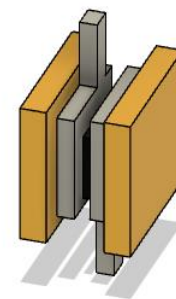
Fig. 3. Prototype model of FSR using Fusion360
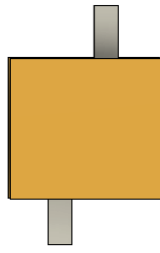
Fig. 4. Front view of FSR prototype model
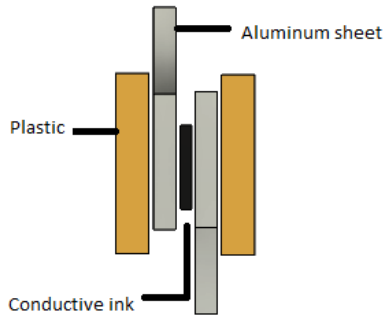
Fig. 5. Side view of FSR prototype model

Fig. 6. FSR based on the prototype

In this research, three FSRs were created, using the designed model, each with a variation of conductive ink in it. The resistance of the designed FSR sensor is measured and analyzed using a digital multimeter.

2.3. Reading FSR Sensor:

The readings of the FSR sensor are measured by connecting the fabricated FSR sensor in the configuration as shown in figure 7. The FSR is connected with a fixed value resistor, which is 2.2kΩ and to 5Volts supply voltage (Vcc). The other end of the 2.2kΩ resistor is connected to the ground and the connection point of FSR and 2.2kΩ resistor is connected to the analog pin of Arduino UNO. This will create a voltage divider circuit configuration and the value of FSR resistance can be obtained by applying the Voltage divider rule in figure 7.
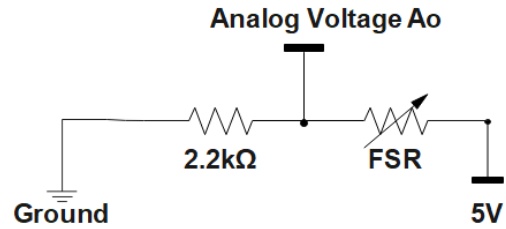
Figure 7: Voltage Divider Configuration

The output voltage of FSR can be calculated using Equation 1.

$$V_O = V_{cc} * \frac{R}{R+FSR} \quad (1)$$

Where,

$V_O = Analog\ Voltage$

$V_{cc} = Supply\ Voltage\ '5V'$

$R = 2.2k\Omega$

When the FSR sensor is squeezed with maximum force, the value of FSR resistance is found to be 25Ω and when no force is applied to FSR the sensor resistance measured via a digital multimeter is found to be 10MΩ.

The Analog Voltage when maximum force is applied to the FSR is found to be by putting the values mentioned above in equation 1:

$$V_O = 5 * \frac{2.2k\Omega}{2.2k\Omega+25\Omega} \quad (2)$$

$$\boldsymbol{V_O = 4.9V}$$

Similarly, the analog voltage when no force is applied to the FSR sensor is found to be:

$$V_O = 5 * \frac{2.2k\Omega}{2.2k\Omega+10M\Omega} \quad (3)$$

$$\boldsymbol{V_O = 0\ V}$$

The calculations above depict that the output voltage varies between 0V-5V depending on the force applied to the FSR sensor. When maximum force is applied to the sensor the output voltage is found to be approximately 5V and when no force is applied to the FSR sensor the output voltage is found to be 0V.

2.4. Analysis of Designed FSR:

For comparative analysis the fabricated and commercially available FSR sensors are connected with Arduino UNO in the same configuration as shown in figure 7, the analog voltage pin is now connected to the Analog pin of Arduino UNO. Arduino Analog to Digital Converter (ADC) will now convert the analog voltage into a 10-bit number ranging from 0 to 1023. The FSR resistance value of both fabricated FSR and the commercially available sensor is obtained via rearranging equation 1 for FSR i.e.

$$FSR = ((V_{cc} - V_o) * R)/V_o \quad (4)$$

$V_O = Analog\ Voltage$

$V_{cc} = Supply\ Voltage\ '5V'$

$R = 2.2k\Omega$

The FSR resistance can be calculated using equation 4 and is utilized for comparative analysis for this study.

3. Results & Discussion

The conductive inks fabricated using different combinations of carbon and graphite were analyzed by measuring their resistance values measured using a digital multimeter as shown in Table 3. Similarly, three different types of force-sensitive resistors (FSR)s were designed using these conductive ink combinations as mentioned below and the resistance values of these FSRs measured via digital multimeter are shown in Table 4.:

1- The first FSR was made using graphite conductive ink and the resistance value observed at rest was 46kΩ and the value decreased to 1.9Ω upon pressure.

2- The second FSR was made using graphite + carbon conductive ink and it gave a resistance of 7.4MΩ which dropped down to 1.6Ω on the applied pressure and 0.2Ω on the extreme applied pressure.

3- The third FSR was made using carbon conductive ink which gave a resistance of 54MΩ on rest and decreased to 0.5Ω upon pressure.

Table 3: Resistance values of Different Conductive Inks

Solution for conductive ink	Resistance 'Ω'
Carbon Ink	5.8kΩ
Graphite Ink	1.3kΩ
Carbon+ graphite Ink	3.2kΩ

Table 4: Resistance of Low-Cost FSRs

No.	Observations		
	Type of FSR	Resistance before applying Pressure 'Ω'	Resistance after applying Pressure 'Ω'
1.	Carbon ink FSR	54MΩ	0.5Ω
2.	Graphite ink FSR	46kΩ	1.9Ω
3.	Carbon + graphite ink FSR	7.4MΩ	1.6Ω

As depicted in table 3, the graphite ink has the least resistance, and due to this the FSR designed using Graphite conductive ink also depicts the least resistance, thus it would be easy to conduct electricity through graphite ink FSR and would be an ideal choice to use in place of a commercially sold FSR.

The graphite ink FSR is then compared with commercially sold FSR using a microcontroller (Arduino Uno) to obtain sensor values and were subjected to the same amount of force at the same time as represented in figure 8. The resistance value is then obtained from the sensor values of both the FSRs using equation 4, which can be observed in table 5, after applying the

same amount of pressure at each instance on both sensors and pressure is increased gradually to the maximum.

Table 5: Change in resistance of both FSRs

Resistance values 'Ω'	
No resistance due to high pressure	No resistance due to high pressure
82	85
197	220
817	1.21kΩ
1.21kΩ	1.31kΩ
4.81kΩ	4.94kΩ
4.83kΩ	4.92kΩ
5.72kΩ	6.13kΩ
6.17kΩ	6.32kΩ
6.42kΩ	7.58kΩ
6.55kΩ	6.55kΩ
6.59kΩ	8.12kΩ
8.27kΩ	9.9kΩ
14.5kΩ	15.8kΩ
57.2kΩ	148.4kΩ
High resistance due to no pressure	High resistance due to no pressure

It can be observed from the results that the FSR created using graphite conductive ink acts almost the same as a force-sensitive resistor manufactured in factories using silver in its conductive ink (see Figure 8).
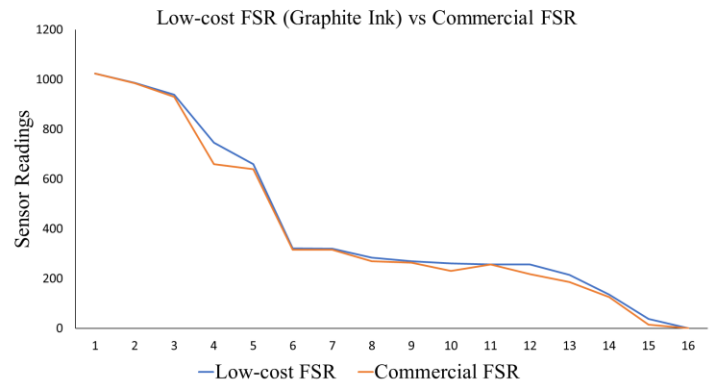
Fig. 8. Comparison of resistance values of both FSRs

3. Conclusion

In this paper, a force-sensitive resistor had been designed using a low-cost conductive ink which when compared with a commercial FSR, produced nearly the same result. Hence, this cost-effective force-sensitive resistor can be used in place of an

expensive, commercially produced FSR in designing different applications related to soft robotics.

The designed cost-effective Force sensitive resistor (FSR) can be utilized in biomedical engineering, soft robotics, and rehabilitation sector. They can be used for pressure mapping of plantar, palmar, and other surfaces of the human body as well as for gait recognition. Robotic grippers/hands/fingers, infusion pumps, tool speed control, and patient turning alarm sensor can also be designed using these low-cost force sensing resistors.

Outside the biomedical engineering domain, this FSR can be used for assembly parts detection, dynamic limit sensor, motor speed control, floor security panels, target force, accuracy detection, grip monitor, and trolling motor speed control.

4. Future enhancement

The results confirm that a single low-cost FSR is capable of detecting and measuring pressure, in future many more force-sensitive resistors can be created with this method and after screen printing the ink on them their sizes can be reduced and used in devices designed to detect pressure applied on different parts and surfaces of the human body and results in a significant cost reduction.

Acknowledgment

References

[1] C. Lebosse, B. Bayle, M. de Mathelin, and P. Renaud, "Nonlinear modeling of low cost force sensors," in *2008 IEEE International Conference on Robotics and Automation*, May 2008, pp. 3437–3442. doi: 10.1109/ROBOT.2008.4543736.

[2] A. M. Almassri *et al.*, "Pressure sensor: State of the art, design, and application for robotic hand," *Journal of Sensors*, vol. 2015. Hindawi Publishing Corporation, 2015. doi: 10.1155/2015/846487.

[3] A. Julian and V. Benjamin, "REAL-TIME MONITORING OF PROBE-TISSUE PRESSURE EFFECTS ON IN VIVO SKIN OPTICAL SPECTROSCOPY USING A PRESSURE SENSITIVE FIBEROPTIC PROBE Next generation compressed sensing techniques for quantitative MRI View project Pressure Sensitive Fiberoptic Spectroscopy View project," 2014, doi: 10.13140/RG.2.2.19433.29285.

[4] A. Pagoli, F. Chapelle, J. A. Corrales-Ramon, Y. Mezouar, and Y. Lapusta, "Large-Area and Low-Cost Force/Tactile Capacitive Sensor for Soft Robotic Applications," *Sensors*, vol. 22, no. 11, Jun. 2022, doi: 10.3390/s22114083.

[5] S. M. Biju, H. Z. Sheikh, M. F. Malek, F. Oroumchian, and A. Bell, "Design of grip strength measuring system using fsr and flex sensors using svm algorithm," *IAES International Journal of Artificial Intelligence*, vol. 10, no. 3, pp. 676–686, Sep. 2021, doi: 10.11591/IJAI.V10.I3.PP676-686.

[6] A. S. Sadun, J. Jalani, and J. A. Sukor, "Force Sensing Resistor (FSR): a brief overview and the low-cost sensor for active compliance control," in *First International Workshop on Pattern Recognition*, Jul. 2016, vol. 10011, p. 1001112. doi: 10.1117/12.2242950.

[7] S. S. Suprapto, A. W. Setiawan, H. Zakaria, W. Adiprawita, and B. Supartono, "Low-Cost Pressure Sensor Matrix Using Velostat," in *Proceedings of 2017 5th International Conference on Instrumentation, Communications, Information Technology, and Biomedical Engineering, ICICI-BME 2017*, Nov. 2018, pp. 137–140. doi: 10.1109/ICICI-BME.2017.8537720.

[8] P. Ramya, B. Padmapriya, and S. Poornachandra, "Foot pressure monitoring using single layer carbon loaded piezoresistive material," *Microprocess Microsyst*, vol. 79, Nov. 2020, doi: 10.1016/j.micpro.2020.103263.

[9] I. J. Fernandes *et al.*, "Silver nanoparticle conductive inks: synthesis, characterization, and fabrication of inkjet-printed flexible electrodes," *Sci Rep*, vol. 10, no. 1, Dec. 2020, doi: 10.1038/s41598-020-65698-3.

[10] Y. H. Wang *et al.*, "Printability and electrical conductivity of silver nanoparticle-based conductive inks for inkjet printing," *Journal of Materials Science: Materials in Electronics*, vol. 32, no. 1, pp. 496–508, Jan. 2021, doi: 10.1007/s10854-020-04828-z.

[11] W. T. Fonseca, K. R. Castro, T. R. de Oliveira, and R. C. Faria, "Disposable and Flexible Electrochemical Paper-based Analytical Devices Using Low-cost Conductive Ink," *Electroanalysis*, vol. 33, no. 6, pp. 1520–1527, Jun. 2021, doi: 10.1002/elan.202060564.

[12] S. Parmar, I. Khodasevych, and O. Troynikov, "Evaluation of flexible force sensors for pressure monitoring in treatment of chronic venous disorders," *Sensors (Switzerland)*, vol. 17, no. 8, Aug. 2017, doi: 10.3390/s17081923.

Long-Term Monitoring of the User's Condition, Using a Smart Rollator

Nazia Ejaz 1

Department of Electrical Engineering
Ziauddin University
Karachi, Pakistan
{nazia10157@zu.edu.pk}

Saad Jawaid Khan 2*

Department of Biomedical Engineering
Ziauddin University
Karachi, Pakistan
{sj.khan@zu.edu.pk}

Fahad Azim 3

Department of Electrical Engineering
Ziauddin University
Karachi, Pakistan
{fahad.azim@zu.edu.pk}

Mehwish Faiz 4

Department of Biomedical Engineering
Ziauddin University
Karachi, Pakistan
{mehwish.faiz@zu.edu.pk}

Abstract - **About 20% of the elderly population of developing countries face gait and balance disorders which lead to postural instability. Moreover, a third of every elderly person needs to use assistive devices because of this disorder. As stated by the ICF (International Classification of Functioning, Disability, and Health) disability is the limitation of activity in the gait pattern. The restricted mobility within the gait has an adverse effect on the overall quality of life. Existing gait analysis procedures are expensive, time-consuming, and confined to specific environments so usually, everyone can't able to assess their gait regularly. The smart rollator is best for users who need gait assessment for rehabilitation treatment follow-up. It's economical, easy to use, and monitors automatically, no external wearable sensors are used, no need for specific personnel and environments for monitoring. The ultrasonic sensor in the rear wheel counts the steps and the rotary encoder in the rear wheel measure distance and time while force sensors in the handle measure the upper limb forces. The observed spatiotemporal gait parameters from the rollator are Step time, Step length, Stride time, Stride length, Cadence, and walking velocity. The healthy users took less time and the minimum number of steps with greater stride length to complete the walk test so the cadence and walking speed of healthy users are greater than users with disabilities. It is also observed that muscle force decrease with the increase in age, this may lead to many muscular diseases in elderly patient e.g. muscular dystrophy.**

Keywords - Assistive Devices, Smart Walker, Gait Monitoring.

1. INTRODUCTION

In the past 50 years, a great deal of research related to gait analysis is ongoing[1]. According to the report of the year 2018 World Health Organization, it is declared that more than 15% of the world's population has some disability[2]. Moreover, it is reported that up to 190 million adults may suffer from the complications and problems of lower limb disabilities which affects gait patterns[2]. Problems related to gait are increasing due to the major factor of chronic health problems, some major issues are Parkinson's disease[3], hemiplegia[3], paraplegia[4], stroke[3], and several others. Patients related to this disease may need additional care and concern as they are not able to perform their gait properly. Gait problems are also increasing in adults due to the issues related to stress and depression, in which the most common are negative attitudes, limited social interaction, and anxiety[5]. Assistive robot use is growing in order to enhance the quality of life and independence of people with disabilities [6].

Different methodologies have been adopted for the assessment of gait parameters e.g. accelerometry-based gait analysis systems[7], electromechanical and robot-assisted gait training [8], wearable sensors[9], wearable motion sensors and smartphone technology[10], treadmills and motion capture systems[11], Inertial based measurement units [11], and instrumented walk ways[12]. All mentioned techniques are working best in their own way but these techniques are very costly and need specific environments and well-trained personnel for the test. Continuous monitoring using a rollator is the best approach [13]. This rollator provides monitoring, support, and rehabilitation but in this case, users may need to lean some weight to use this rollator so everyone cannot able to use this.

Many clinical scales are available for gait evaluation which mainly focus on gait [14], balance[15], fall risks[16], and mental disorders[17]. This test takes too much time for clinicians and patients as well and is laborious for clinicians if they have to evaluate several patients because they have to repeat the test for their progress evaluation [13]. Alternatively, other methodologies provide automatic, insight, and continuous monitoring e.g. wearable sensor-based exoskeletons and video cameras, etc.. The main drawback of this technology is to wear all the time exoskeleton which may create social discrimination and allows external noise[18]. The optoelectronic-based motion capture system cannot be used everywhere and every time, as they are fixed to some specific environments for monitoring and requires mounting tracker sensors to lower limbs for

movement[18]. So, incorporating sensors in rehabilitative devices like rollators is the best and most transparent way for continuous monitoring along with support to the patient. The user never forgets to use a device for monitoring like in the case of the wearable exoskeleton and other methods.

In this study, we presented an economical wheeled rollator for continuous assessment of gait parameters. The sensors in the rear wheel count number of steps taken by the user and the wheel odometer provide the distance covered by the user and walking speed. We extract other necessary spatiotemporal gait parameters which are used for diagnosis by applying mathematical formulas e.g. we can easily measure cadence by using the number of steps /min etc. This system is validated with 40 volunteers group of healthy and 20 elderly adults with neurological and physical conditions) with 10mWT (walk test).The advantages of this approach are:

   i.   Automatic monitoring along with support to all users with less weight bearing.

   ii.   Economical and portable, we can use it everywhere, every time, with no need for the clinician to scale gait.

2. METHODOLGY

Diagnosing different neurological conditions [9], and assessment of rehabilitative treatments for lower limb disabilities requires a gait evaluation tool. The high risk of falling in older adults is associated with changes in the gait cycle [19]. These changes are assessed by quantitative measurements of spatiotemporal parameters of gait [20]. It's advantageous if any low-cost rehabilitative aid monitor gait parameters along with providing support to the patient.

2.1. The Smart Walker

Fig. 1 Smart Walker

Fig 1. Shows a smart rollator which is a special aid device for the user's support and monitoring. This rollator is equipped with two force sensors in the handlebar to measure the forces of left and right upper limbs during walking and two more sensors which are interfaced with Arduino UNO, a rotary encoder, and an ultrasonic sensor in a rear wheel to measure the gait parameters. The rotary encoder is placed on the rear part of the rollator in contact with the right wheel to measure the walking velocity of the patient and the distance covered by the patient. We used an incremental rotary encoder a position sensor to

measure the rotation of the wheel which will help to calculate the spatiotemporal parameters. To minimize the missing rotations and get more accurate results we fixed the pulley system to make the connection between the wheel and encoder.

The ultrasonic sensor (HC-SR04) will detect the number of steps taken by the user. It offers excellent non-contact range detection with high accuracy and stable readings in an easy-to-use package from 2 cm to 400 cm or 1" to 13 feet. Its range is set from 0 to 20 cm which means that it will demean the object which is in the range of 20cm. It will calculate how many times the user has taken the steps and at the end it will sum up of all in the serial monitor.

(a)   (b)   (c)
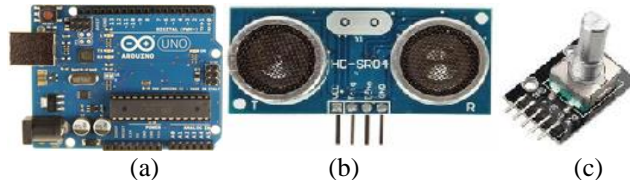
Fig. 2 (a) Arduino UNO (b) Ultrasonic Sensor (c) Rotary Encoder

Fig 2. Represent the sensors input to the microcontroller, including rotary encoder and ultrasonic sensor and the controller. Arduino UNO is connected with encoder and ultrasonic sensor which takes input from the user.

The parameters of gait will be shown on serial monitor of the Arduino software while the force applied by patients are captured by Pasco Capstone software. The parameters shown in serial monitor includes Step Length, Step Time, Stride Length, Stride Time, Cadence, Number of steps and Total time. The measured force is shown in the form of graph. The flowchart of proposed methodology is shown in Fig. 3.

Mathematical Equations for extraction of spatiotemporal gait parameters.

We have applied the following formulae in Arduino UNO code through which we have observed the values of gait parameters.

   i.   Step Time = Total time / No. of steps

   ii.   Step Length = Total distance / No. of steps

   iii.   Stride Time = Total time / No. of strides

   iv.   Stride Length = Total distance / No. of strides

   v.   Cadence = (Steps / Total time) * 60

2.2.   Users: Patients from Ziauddin Hospital, University and Old Age Home

The rollator is tested on total 40 volunteers with 20 healthy participants (Group A) and 20 participants with wide range of neurological and physiological disabilities (Group B). All volunteers are pre assed with our inclusion criteria. Our inclusion criteria for the selection of volunteer is i) Being able to walk with a rollator ii) Having experience of using rollator [20] iii) must be in between 45 to 85 years old. The healthy group of participants (Group A) were recruited from Ziauddin University and the test

was conducted at Biomechanics & Rehabilitation Lab Ziauddin University, Faculty of Engineering, Science, and Technology & Management.

12 male and 8 female with mean age of (59.45±9.98) and another group of 13 male and 7 females volunteers having neurological and physical conditions (Group B) with mean age of (62.05±10.30) were recruited from Old age home, Ziauddin Hospital, Department of Physical Therapy, Anmol e Zindagi and Faculty of rehabilitation science and Physical therapy Ziauddin University Under the supervision of physical therapist. The Informed consent was taken from all participant.
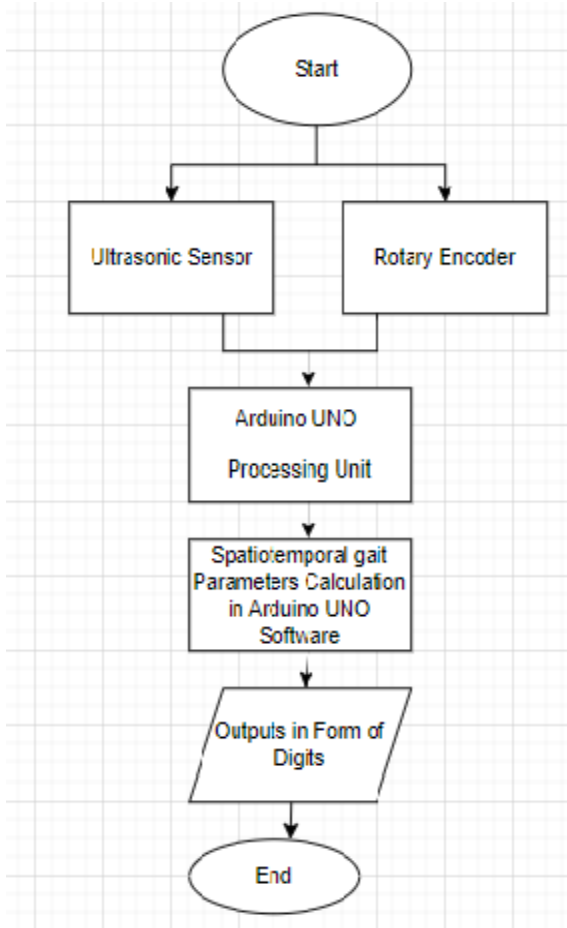
Fig 3. The Proposed Methodology

2.3 .Walk Test for Gait Parameters Estimation

There are many tests available to evaluate gait based on scale score and visual observations[21]. In many works healthy users[20]were recruited to test device in this area of study . Specific group of peoples e.g. hemiplegia[22], ataxia[23] are selected in other works. 10mWt is most widely used test for gait monitoring. For gait monitoring using a rollator, the best

outcomes can be achieved by evaluating this task on a smooth floor followed by participants in a straight line[20]. We selected a smooth titled floor of 10m marked with the starting point and ending point for walk .Marked on 2m from starting and 2m from ending for the acceleration and deceleration so users gait was analyzed in the distance of 6m. The test was conducted under the supervision of Physical therapist and a nurse. Fig 4. Shows walk test using rollator.

Fig 4. User perform walk test using smart rollator

3. RESULTS

Table 1. Shows average spatiotemporal gait parameters of user's observed by using only smart rollator. It indicates that Average Step Count are more in users with conditions versus healthy users due to fear of falling. Mostly user's takes short steps to complete the marked distance. The time taken by the users in case of healthy subjects is comparatively less than users with pathologies due to slow walk to cover the distance. The stride length and step length of users with pathologies are less than healthy users because of short steps while the step time and stride time is greater in users with pathologies .The cadence and walking velocity of users with pathologies are less versus healthy.

Table 1. Average spatiotemporal gait parameters of User;
Healthy Versus patients with different disabilities.

Gait Parameters	Healthy Subjects	Elderly Adults With Different Cerebral and Physical Conditions
	Mean ± Standard Deviation	Mean ± Standard Deviation
Age(Years)	59.45±9.98	62.05±10.30
Average Step Count	15.70±1.98	19.50±3.03
Average Distance Covered(m)	6.11±0.29	6.11±10.00
Time(sec)	10.00±0.92	15.00±0.92
Average Left Step Length(m)	0.39±0.05	0.21±0.64
Average Right Step Length (m)	0.37 ± 0.04	0.22±0.62
Average Left Step Time(sec)	0.64±0.06	1.61±0.06
Average Right Step Time(sec)	0.62 ± 0.05	1.62±0.05
Walking Speed(m/sec)	0.62±0.06	0.38±0.06
Cadence(steps/min)	94.25±8.59	55.25±0.62
Average Stride Time (sec)	1.28±0.12	3.02±0.12
Average Stride Length(m)	0.79±0.10	0.44±1.28

As presented in Fig 5. The user XIX with stroke takes short steps due to fear of falling to complete the marked distance so his cadence, stride length, step length are less and he take more time to complete walk test while the healthy user III takes large steps and less time to complete marked distance so his cadence, stride length, step length are comparatively high than Elderly user XIX.
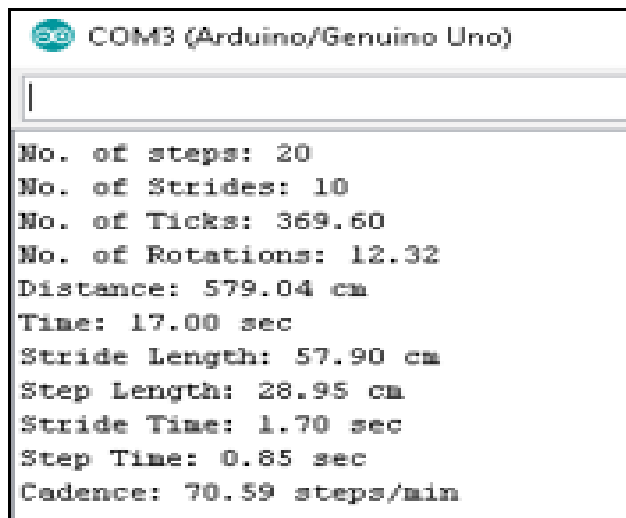
(a)
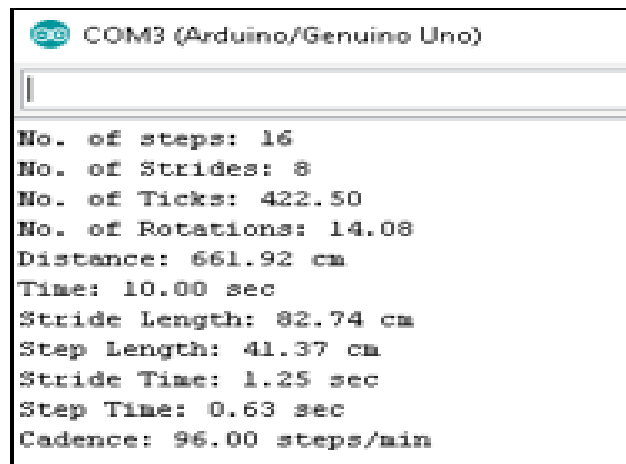
(b)

Fig. 5. (a)Elderly User XIX gait parameters with stroke (b) Healthy Users VII gait parameters.

4. CONCLUSION AND FUTURE WORK

Smart rollator equipped with wheel odometery and ultrasonic sensor is novel approach to monitor spatiotemporal gait parameters .It can be use everywhere and every time during daily living activities. Most works focus on using treadmills, video cameras, wearable sensor based exoskeletons which require specific examination area with well trained staff. Measurement of gait parameters using rollator handle bar forces is presented in[20] but the cost is comparatively high and limitation was user needs to bear weight of up to 3kg to use rollator.

Costly and complex system like motion capture systems based analysis provides in depth information of gait like joint angle rotations etc. Our system is not able to detect joint angles and rotations because this needs high resolution video cameras to capture movements of bones during walking.

We tested our proposed methodology with many volunteers with different health conditions for the most compelling gait parameters for the assessment of gait. For the validation of rollator gait parameters we compare our results with physical therapists observational gait assessment which provide approximately similar results.

The future work will focus on wireless system and extraction and classification of gait parameters using handle bar forces .We plan to use the data of number of users with different condition and healthy adults to make automatic classification systems for long term users for their rehabilitation assessment at home.

REFERENCES

[1]   J. J. J. o. b. Morrison, "The mechanics of the knee joint in relation to normal walking," vol. 3, no. 1, pp. 51-61, 1970.
[2]   K. E. Webster, J. E. Wittwer, and J. A. J. T. J. o. a. Feller, "Quantitative gait analysis after medial unicompartmental knee arthroplasty for osteoarthritis," vol. 18, no. 6, pp. 751-759, 2003.
[3]   M. Švehlík *et al.*, "Gait analysis in patients with Parkinson's disease off dopaminergic therapy," vol. 90, no. 11, pp. 1880-1886, 2009.

[4] A. R. Donati *et al.*, "Long-term training with a brain-machine interface-based gait protocol induces partial neurological recovery in paraplegic patients," vol. 6, no. 1, pp. 1-16, 2016.

[5] J. Michalak, N. F. Troje, J. Fischer, P. Vollmar, T. Heidenreich, and D. J. P. m. Schulte, "Embodiment of sadness and depression—gait patterns associated with dysphoric mood," vol. 71, no. 5, pp. 580-587, 2009.

[6] S. W. Brose *et al.*, "The role of assistive robotics in the lives of persons with disability," (in eng), *Am J Phys Med Rehabil,* vol. 89, no. 6, pp. 509-21, Jun 2010.

[7] D. Jarchi, J. Pope, T. K. M. Lee, L. Tamjidi, A. Mirzaei, and S. Sanei, "A Review on Accelerometry-Based Gait Analysis and Emerging Clinical Applications," (in eng), *IEEE Rev Biomed Eng,* vol. 11, pp. 177-194, 2018.

[8] J. Mehrholz, S. Thomas, C. Werner, J. Kugler, M. Pohl, and B. Elsner, "Electromechanical-assisted training for walking after stroke," (in eng), *Cochrane Database Syst Rev,* vol. 5, no. 5, p. Cd006185, May 10 2017.

[9] Y. Celik, S. Stuart, W. L. Woo, and A. Godfrey, "Gait analysis in neurological populations: Progression in the use of wearables," (in eng), *Med Eng Phys,* vol. 87, pp. 9-29, Jan 2021.

[10] D. Su *et al.*, "Simple Smartphone-Based Assessment of Gait Characteristics in Parkinson Disease: Validation Study," (in eng), *JMIR Mhealth Uhealth,* vol. 9, no. 2, p. e25451, Feb 19 2021.

[11] R. M. Kanko *et al.*, "Assessment of spatiotemporal gait parameters using a deep learning algorithm-based markerless motion capture system," (in eng), *J Biomech,* vol. 122, p. 110414, Jun 9 2021.

[12] D. J. Geerse, B. H. Coolen, and M. Roerdink, "Kinematic Validation of a Multi-Kinect v2 Instrumented 10-Meter Walkway for Quantitative Gait Assessments," (in eng), *PLoS One,* vol. 10, no. 10, p. e0139913, 2015.

[13] J. Ballesteros, C. Urdiales, A. B. Martinez, and M. Tirado, "Automatic Assessment of a Rollator-User's Condition During Rehabilitation Using the i-Walker Platform," (in eng), *IEEE Trans Neural Syst Rehabil Eng,* vol. 25, no. 11, pp. 2009-2017, Nov 2017.

[14] M. E. J. J. o. t. A. G. S. Tinetti, "Performance-oriented assessment of mobility problems in elderly patients," 1986.

[15] K. Berg, S. Wood-Dauphinee, and J. J. S. j. o. r. m. Williams, "The Balance Scale: reliability assessment with elderly residents and patients with an acute stroke," vol. 27, no. 1, pp. 27-36, 1995.

[16] D. Podsiadlo and S. J. J. o. t. A. g. S. Richardson, "The timed "Up & Go": a test of basic functional mobility for frail elderly persons," vol. 39, no. 2, pp. 142-148, 1991.

[17] G. Sulter, C. Steen, and J. J. S. De Keyser, "Use of the Barthel index and modified Rankin scale in acute stroke trials," vol. 30, no. 8, pp. 1538-1541, 1999.

[18] P. Chinmilli, S. Redkar, W. Zhang, and T. J. I. R. A. J. Sugar, "A review on wearable inertial tracking based human gait analysis and control strategies of lower-limb exoskeletons," vol. 3, no. 7, p. 00080, 2017.

[19] B. E. J. J. o. t. A. g. s. Maki, "Gait changes in older adults: predictors of falls or indicators of fear?," vol. 45, no. 3, pp. 313-320, 1997.

[20] J. Ballesteros, C. Urdiales, A. B. Martinez, and M. Tirado, "Gait analysis for challenged users based on a rollator equipped with force sensors," in *2015 IEEE/RSJ International Conference on Intelligent Robots and Systems (IROS)*, 2015, pp. 5587-5592: IEEE.

[21] D. A. Kegelmeyer, A. D. Kloos, K. M. Thomas, and S. K. J. P. t. Kostyk, "Reliability and validity of the Tinetti Mobility Test for individuals with Parkinson disease," vol. 87, no. 10, pp. 1369-1378, 2007.

[22] H. D. Kim *et al.*, "Analysis of vertical ground reaction force variables using foot scans in hemiplegic patients," vol. 39, no. 3, pp. 409-415, 2015.

[23] R. LeMoyne, F. Heerinckx, T. Aranca, R. De Jager, T. Zesiewicz, and H. J. Saal, "Wearable body and wireless inertial sensors for machine learning classification of gait for people with Friedreich's ataxia," in *2016 IEEE 13th International Conference on Wearable and Implantable Body Sensor Networks (BSN)*, 2016, pp. 147-151: IEEE.

PREDICTING RESPIRATORY ALLERGIES USING A MACHINE LEARNING ALGORITHM

Kehkashan Kanwal

Department of Electrical Engineering

Ziauddin University
Karachi, Pakistan
kehkashan11912@zu.edu.pk

Saad Abdullah

School of Innovation, Design, and Engineering
Mälardalens University
Västerås, Sweden
Saad.abdullah@mdu.se

Muhammad Asif*

Department of Electrical Engineering

Ziauddin University
Karachi, Pakistan
Asif.arif@zu.edu.pk

Saad Jawaid Khan

Department of Biomedical Engineering
Ziauddin University
Karachi, Pakistan
sj.khan@zu.edu.pk

Syed Ghufran Khalid*

Department of Engineering, School of
Sciences and Technology
Nottingham Trent University,
Nottingham, UK
syed.khalid@ntu.ac.uk

Abstract - **Respiratory allergies are one of the most common problems that affect the lives of millions of children and adults around the world. Even though these allergies are rarely life-threatening, it is a fact that these allergies decline the quality of life of affected individuals and are an economic burden on the healthcare setting. The confirmatory tests are usually not available in resource-scarce settings and cause misdiagnosis and delays in treatment, making such individuals susceptible to other infections and diseases. In the present work, we have proposed photoplethysmography, a non-invasive, simple, and readily available optical sensor as a prediction tool for respiratory allergies. We have collected PPG data from 26 subjects and extracted time and frequency domain features from the PPG of subjects with allergies and trained a supervised machine learning algorithm to distinguish them from features extracted from healthy individuals with no allergies. An Ensemble classifier of boosted trees gave the best training accuracy of 87.59%, test accuracy of 88.56%, sensitivity of 85.92% and specificity of 89.07%.**

Keywords - Respiratory allergies, Photoplethysmography, prediction, supervised classifier

I. INTRODUCTION

Respiratory allergic diseases are a serious global health issue that affects millions of people of all ages [1], [2] Increased environmental pollution, climate changes and industrialization are aggravating the disease rapidly [3]. Allergic disorders like asthma remain underdiagnosed and undertreated in many parts of the world [4]. These allergies usually do not pose life-threatening effects. However, the quality of life of people with allergies greatly declines because of the frequent illness episodes and economic burden [5]. However, people with respiratory allergies were found to be more susceptible to COVID-19 infection with the worst outcomes [6].

Skin prick tests and radioallergosorbent tests (RASTs) are generally used for confirming allergies as shown in Fig. 1 [7]. For asthma, a bronchoprovocation test is also done in conjunction with spirometry [8]. These testing facilities are usually not available in resource-scarce areas, this calls for alternate, yet reliable methods to predict, assess and monitor allergic diseases [9]. Ouyang, Y *et al.* established a correlation

*Corresponding Author.
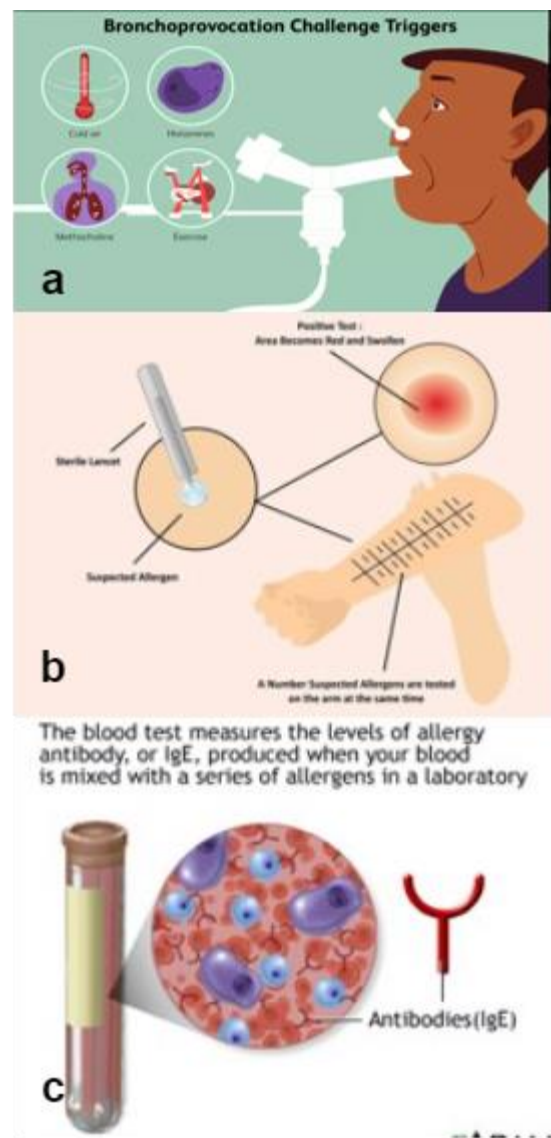
Fig. 1 Reprinted from [7]: Various diagnostic tests used for diagnosis of allergy, where (a) represents bronchoprovocation test, (b) represents skin prick test, and (c) represents serum IgE test.

exists between the incidence of allergic rhinitis and meteorological parameters [10]. D. Perna *et al.* used chest sounds to predict various respiratory disorders including allergies using advanced deep-learning networks [11].

Photoplethysmography is a simple, noninvasive, and inexpensive technique that measures volumetric changes in the blood. This simple and versatile signal contains a multitude of information about the cardiovascular system. Since the technology is readily available, it has been actively employed as a sensor of choice to measure a variety of physiological processes [12] – [20]. The advent of artificial intelligence has made medical technology take leaps that have not been imagined before. Specifically, with the computation powers of machine learning algorithms, simple technologies like PPG have been successfully correlated with a variety of biological processes and systems [21], [22].

The presented work aims to find if the PPG signal can be used to predict respiratory allergic diseases. A quick literature survey reveals that as many as 125, time and frequency domain features have been extracted from the PPG signal and the signal contains important physiological and pathological information [23]. In the proposed work, PPG recordings were taken from healthy subjects and subjects with diagnosed allergies. The signal was processed, and 35 features have been extracted from the recorded data. The features were then ranked using ANOVA and then a supervised machine learning algorithm was trained to find out if it is possible to predict the respiratory allergy with reasonable accuracy. The paper is organized as follows, section II presents the methodology for data collection, preprocessing and feature extraction. Section III presents the detailed results, the work is concluded, and future directions have been given in section IV.

II. METHODS

The PPG signal and other noninvasive physiological signals like heart rate, blood pressure and oxygen saturation have been collected from 13 healthy and 13 subjects with respiratory allergies. The patient's data has been taken from the OPD triage of the Ziauddin University Hospital. All the participants voluntarily participated after a brief review of the study. The study has been approved by the Ethical Review Committee of Ziauddin University Hospital. A 2-3-minute-long PPG signal has been recorded using CMS50D+, a commercially available oximeter. The entire methodology is summarized in Fig. 2.

A. Preprocessing
The recording device generates a csv file of the recorded PPG signal. The signal has been filtered and segmented using a python program. A bandpass fourth-order Chebyshev 2 filter has been used with low and high cut-off frequencies of 0.1 Hz and 5 Hz respectively. The data was segmented into 3-second-long segments.

B. Signal Quality Assessment
Since the data has been collected in a control setup using an FDA-approved device, the signal generated was a low-noise and high-quality signal. However, it could have sections on the signal not appropriate for the subsequent steps. A

python program was implemented that extracted and plotted individual waves from the PPG signal, upon which the user could identify it as a good or bad wave. For each category, the program would calculate skewness and Signal-to-noise ratio. The values for good and bad waves were saved as a file for each user separately in csv format. A careful inspection revealed that the majority of the good waves have positive skewness and segments of bad quality in the data had negative values for skewness. Hence skewness was selected to use as the signal quality index.

C. Feature Extraction
After preprocessing, the PPG segments were detrended and normalized. The features were extracted using a python program that extracts single waves from each segment. The features were saved as a list for each subject in a python program and then saved as an excel sheet. This way a feature table was generated for each subject and finally, all the files were merged. In the feature table, 0 was assigned for healthy subjects and 1 was assigned for allergies.

D. A Machine Learning Algorithm for Classification
Since the data was to be classified as one of the two statuses, healthy or allergic. This was a classic prediction problem of machine learning. The feature table generated in the previous step was used in the classification learner app of MATLAB 2022. This app uses supervised machine learning algorithms to classify the data. The data was selected and imported using the import option of the app. From the data pool, 25% of the data was randomly used for training and the rest was used for test. Out of the 35 features, 26 features were used for training after ranking them in order of importance using ANOVA. A cross-validation scheme was used for validation where data was divided into folds and accuracy was estimated on each fold. In the presented case, a 5-fold cross-validation scheme was implemented. This is done to ensure that the classifier is not overfitting the data. For training, initially, all the possible models were trained. This was achieved using a parallel computing toolbox, which made it possible to train 22 machine-learning algorithms in parallel. The training was done on a GPU (NVIDIA GeForce MX230) accelerated intel i7 processor. The number of total
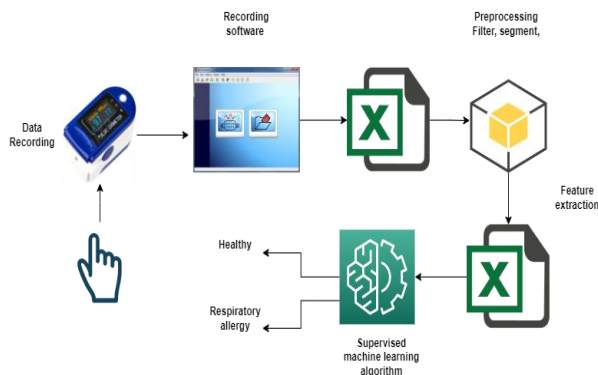
Fig. 2 The PPG data recorded using a CMS50D+ oximeter and processed in python for features extraction and machine learning classifier training to classify PPG signal from a healthy and unhealthy subject with an allergy.

observations was 4856.

III. RESULTS AND DISCUSSIONS

The PPG signal in Fig. 3 represents the segmented and filtered signal of PPG from a healthy subject. The filter is bandpass 4th order Chebyshev 2 filter. The choice of filter has been done because Chebyshev 2 filter because it filters the PPG signal most suitably and enhances the key features of the signal [24].
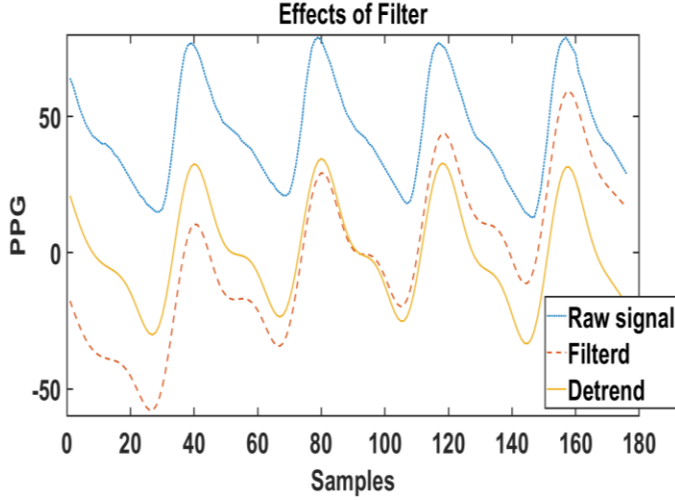
Fig. 3 Segmented and filtered PPG data from a healthy subject. The signal has been segmented into a 3-second-long data segment and filtered using the 4th-order Chebyshev 2 bandpass filter.

Table 1 lists all the features that have been calculated from each PPG wave and used as input to the supervised machine learning algorithms for classification. The classification learner app has 30 models. All the models were trained as explained above, 28 algorithms gave successful training results, and linear and quadratic discriminant could not be implemented. Boosted tree ensemble classifier gave the maximum validation accuracy of 87.59%. Fig 4. represents the confusion matrix for the training validation and the test.

Table 1 Features extracted from PPG signal and used for the classification. Features 1-4, 29, and 30 are PPG signal features. 6 to 9 are the features extracted from the first derivative of PPG, also known as the velocity PPG. Whereas a - e are the features extracted from the second derivative of PPG also known as the acceleration PPG. 1-30 are time domain features whereas 2 features are frequency domain.

	Features extracted from PPG signal		
1	Systolic Peak (S_p)	17	b
2	Onset (O)	18	c
3	Rise time	19	d
4	Pulse Interval	20	e
5	The slope between S_p and O	21	The slope between a and S_p
6	w	22	The slope between b and S_p
7	x	23	The slope between c and S_p
8	y	24	The slope between d and S_p
9	z	25	The slope between e and S_p
10	The slope between w and S_p	26	The slope between a and c
11	The slope between x and S_p	27	The slope between b and d
12	The slope between y and S_p	28	c/a
13	The slope between z and S_p	29	Total pulse area
14	The slope between w and y	30	Pulse width
15	The slope between x and z	31	Fundamental component frequency
16	a	32	Fundamental component frequency magnitude

Table 2 ANOVA importance score for the selected features. Out of 32 features, 26 were selected using ANOVA. These features were then used to train supervised machine-learning algorithms for classification. The dropped features are the c/a ratio, c, x, y, rise time, and the slope between a and S_p.

Selected feature	ANOVA Score	Selected feature	ANOVA Score
Fundamental component frequency	103.7789	b	16.9996
Pulse Interval	94.6298	Total pulse area	15.8611
Pulse width	76.6255	The slope between d and S_p	14.5415
a	31.1725	The slope between a and c	11.7462
w	30.7056	The slope between z and S_p	10.4303
Systolic Peak (S_p)	30.4119	z	10.2494
The slope between S_p and O	25.6632	Onset (O)	9.0972
The slope between y and S_p	23.7899	The slope between w and y	6.7537
e	22.7114	The slope between c and S_p	3.7219
The slope between b and S_p	20.1687	The slope between b and d	3.6246
Fundamental component frequency magnitude	19.7443	The slope between x and S_p	3.6002
The slope between e and S_p	19.3392	The slope between x and z	3.571
The slope between w and S_p	17.3219	d	3.0196

85.9% and a false negative rate (FNR) of 14.1% for allergy,
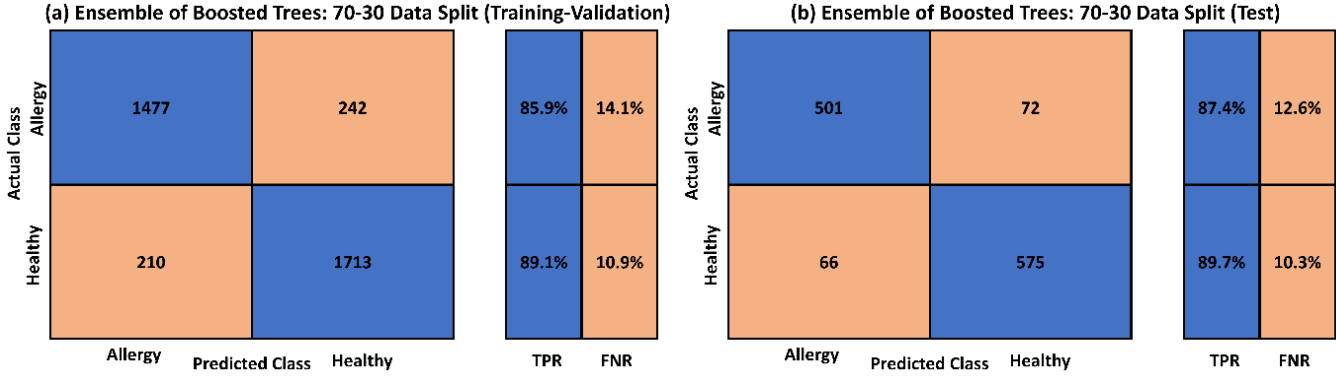
Fig. 4 Confusion matrix for (a)training validation, and (b) test. The classifier is Ensemble of boosted tree classifier.
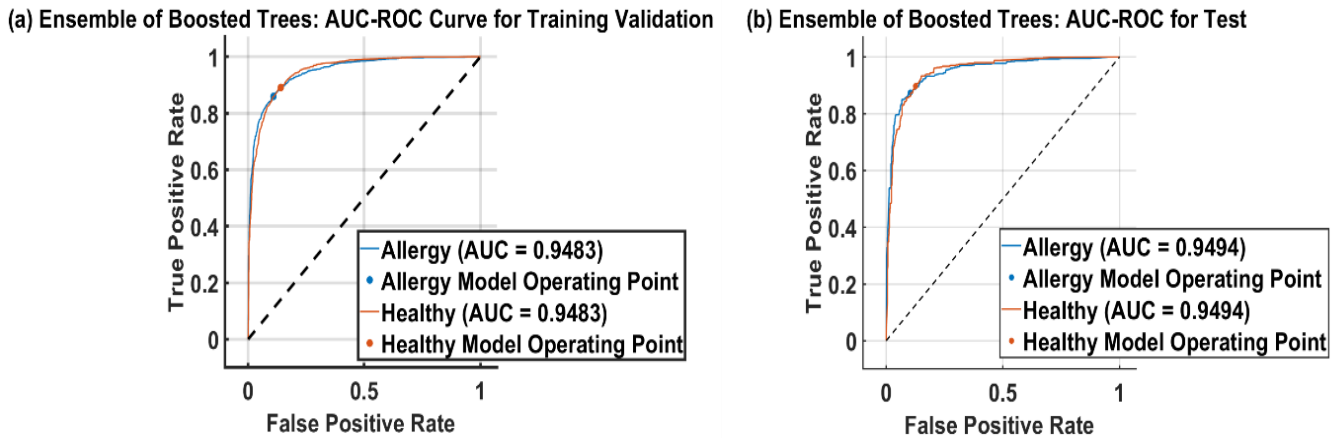
Fig. 5 AUC-ROC curves: (a) for training validation, and (b) test. The AUC value of 0.9479 indicates that the ensemble boosted classifier can separate the healthy subjects from patients with allergies.

Fig. 4 represents the confusion matrix for the ensemble of boosted tree classifier during both the training and testing phases of the study, to evaluate the performance of the algorithm, equation 1 – 6 has been used to obtain performance parameters.

$$Accuracy = \frac{TP + TN}{Total} = \frac{1477 + 1713}{3642} = 0.8759 = 87.59\%$$
(1)

$$Error = \frac{FP + FN}{Total} = \frac{210 + 242}{3642} = 0.1241 = 12.41\%$$
(2)

$$Sensitity = \frac{TP}{TP + FN} = \frac{1477}{1477 + 242} = 0.8592 = 85.92\%$$
(3)

$$Specificity = \frac{TN}{TN + FP} = \frac{1713}{1713 + 210} = 0.8907 = 89.07\%$$
(4)

$$Precision = \frac{TP}{TP + FP} = \frac{1477}{1477 + 210} = 0.8762 = 87.62\%$$
(5)

$$F1 = \frac{2 * TP}{2TP + FP + FN} = \frac{2 * 1477}{2 * 1477 + 210 + 242} = 0.8673$$
(6)

The results of the classification were evaluated using a confusion matrix, which showed a true positive rate (TPR) of

and a TPR of 89.1% for healthy during training. During testing, the TPR for allergy was found to be 87.4%, and for healthy it was 89.7%. The overall accuracy of the classification was found to be 87.59%, with an error rate of 12.41%. The sensitivity and specificity were 85.92% and 89.07%, respectively, while the precision and F1 score were 87.62% and 0.867, respectively. These results suggest that the ensemble of boosted tree classifier is an effective method for classifying between healthy and allergy classes.

Fig. 5 presents the ROC curve for the model; the AUC values were 0.9479. Table 3 represents the accuracy of validation and testing for the trained algorithm. The results indicate that the classifier achieved an accuracy of 87.6% during training and 88.6% during testing, which suggests that the classifier was able to effectively differentiate between healthy subjects and patients with allergies.

Table 3 Accuracy and total cost for training validation and test for boosted tree ensemble classifier

	Accuracy (%)	FP+FN= cost
Training	87.6	452
Test	88.6	138

PPG has been shown to be a useful tool for diagnosis and monitoring of various pathologies and physiological

parameters in recent years. Single channel PPG has been used with high accuracy as substitute for BP and heart rate estimation [25], [26]. Literature has shown PPG as a valuable signal for diagnosing risk of cardiovascular diseases [27], detecting apnea [28], and monitoring depth of anaesthesia [29] and many other applications [30], [31]. With the presented research, we have established basis to use PPG as preliminary diagnostic tool for respiratory allergies. With more data, it can be established if proposed technique can be attempted to diagnose and differentiate between different respiratory disorders like COPDs. With powerful readily available computational platforms like Jetson boards, these techniques can be turned into simple point of care devices. Such tools, in future, could aid at the triage at hospitals and health care centres.

IV. CONCLUSION

In the given work, a successful implementation of a machine learning algorithm has been presented that distinguishes healthy individuals from subjects with allergies with acceptable accuracy. To the best of our knowledge, this is the first attempt to predict respiratory allergies using a simple noninvasive optical sensor. However, more data should be collected and other features from PPG should also be investigated. In future, we intend to do comprehensive data collection for both healthy subjects and patients with allergies. Other respiratory disorders may also be investigated using a similar approach. A longitudinal study on patients with allergies could also be done to find the patterns of feature change during and after the allergic illness for the patients. This may help to rule out allergies from other related disorders like upper and lower respiratory tract infections and COPD.

REFERENCES

[1] "Facts and Stats - 50 Million Americans Have Allergies | ACAAI Patient." https://acaai.org/allergies/allergies-101/facts-stats/ (accessed Oct. 28, 2022).

[2] D.-Y. Wang, "Risk factors of allergic rhinitis: genetic or environmental?," *Ther Clin Risk Manag*, vol. 1, no. 2, p. 115, 2005, doi: 10.2147/TCRM.1.2.115.62907.

[3] H. Okada, C. Kuhn, H. Feillet, and J. F. Bach, "The 'hygiene hypothesis' for autoimmune and allergic diseases: an update," *Clin Exp Immunol*, vol. 160, no. 1, p. 1, Apr. 2010, doi: 10.1111/J.1365-2249.2010.04139.X.

[4] "Asthma." https://www.who.int/news-room/fact-sheets/detail/asthma (accessed Oct. 28, 2022).

[5] G. W. Canonica, J. Mullol, A. Pradalier, and A. Didier, "Patient Perceptions of Allergic Rhinitis and Quality of Life," *World Allergy Organization Journal*, vol. 1, no. 9, pp. 138–144, Sep. 2008, doi: 10.1097/WOX.0B013E3181865FAF/TABLES/5.

[6] J. M. Yang *et al.*, "Allergic disorders and susceptibility to and severity of COVID-19: A nationwide cohort study," *J Allergy Clin Immunol*, vol. 146, no. 4, pp. 790–798, Oct. 2020, doi: 10.1016/J.JACI.2020.08.008.

[7] K. Gallmeier *et al.*, "Prediction of new-onset asthma and nasal allergy by skin prick test and RAST in a cohort of adults," *European Respiratory Journal*, vol. 43, no. 1, pp. 92–102, Jan. 2014, doi: 10.1183/09031936.00012813.

[8] "Methacholine Challenge Test (Bronchoprovocation Test)." https://foundation.chestnet.org/lung-health-a-z/methacholine-challenge-test-bronchoprovocation-test/ (accessed Oct. 28, 2022).

[9] T. T. Ma, Y. Zhuang, H. Y. Gong, A. C. Yii, X. Y. Wang, and H. Z. Shi, "Predictive value of respiratory symptoms for the diagnosis of pollen-induced seasonal asthma among children and adults in Inner Mongolia," *Ther Clin Risk Manag*, vol. 13, p. 967, Aug. 2017, doi: 10.2147/TCRM.S138355.

[10] Y. Ouyang, J. Li, D. Zhang, E. Fan, Y. Li, and L. Zhang, "A model to predict the incidence of allergic rhinitis based on meteorological factors," *Scientific Reports 2017 7:1*, vol. 7, no. 1, pp. 1–9, Aug. 2017, doi: 10.1038/s41598-017-10721-3.

[11] D. Perna and A. Tagarelli, "Deep auscultation: Predicting respiratory anomalies and diseases via recurrent neural networks," *Proc IEEE Symp Comput Based Med Syst*, vol. 2019-June, pp. 50–55, Jun. 2019, doi: 10.1109/CBMS.2019.00020.

[12] R. Casal, L. E. di Persia, and G. Schlotthauer, "Sleep-wake stages classification using heart rate signals from pulse oximetry," *Heliyon*, vol. 5, no. 10, Oct. 2019, doi: 10.1016/j.heliyon.2019.e02529.

[13] J. L. Moraes, M. X. Rocha, G. G. Vasconcelos, J. E. Vasconcelos Filho, V. H. C. de Albuquerque, and A. R. Alexandria, "Advances in photopletysmography signal analysis for biomedical applications," *Sensors (Switzerland)*, vol. 18, no. 6. MDPI AG, Jun. 09, 2018. doi: 10.3390/s18061894.

[14] J. Xiong, L. Cai, F. Wang, and X. He, "SVM-based spectral analysis for heart rate from multi-channel WPPG sensor signals," *Sensors (Switzerland)*, vol. 17, no. 3, Mar. 2017, doi: 10.3390/s17030506.

[15] S. G. Khalid, J. Zhang, F. Chen, and D. Zheng, "Blood Pressure Estimation Using Photoplethysmography Only: Comparison between Different Machine Learning Approaches," *J Healthc Eng*, vol. 2018, 2018, doi: 10.1155/2018/1548647.

[16] R. K. Nath, H. Thapliyal, and A. Caban-Holt, "Towards photoplethysmogram based non-invasive blood pressure classification," in *Proceedings - 2018 IEEE 4th International Symposium on Smart Electronic Systems, iSES 2018*, Institute of Electrical and Electronics Engineers Inc., Jul. 2018, pp. 37–39. doi: 10.1109/iSES.2018.00018.

[17] S. A, V. Ravichandran, P. S. P, J. Joseph, and M. Sivaprakasam, "PPGnet: Deep Network for Device Independent Heart Rate Estimation from Photoplethysmogram," Mar. 2019, [Online]. Available: http://arxiv.org/abs/1903.08912

[18] M. Abdul Motin, K. Karmakar, T. Penzel, and M. Palaniswami, "Sleep-Wake Classification using Statistical Features Extracted from Photoplethysmographic Signals."

[19] T. Pereira *et al.*, "Photoplethysmography based atrial fibrillation detection: a review," *NPJ Digit Med*, vol. 3, no. 1, Dec. 2020, doi: 10.1038/s41746-019-0207-9.

[20] U. Yadav, S. N. Abbas, and D. Hatzinakos, "Evaluation of PPG Biometrics for Authentication in different states," Dec. 2017, [Online]. Available: http://arxiv.org/abs/1712.08583

[21] J. Sancho, Á. Alesanco, and J. García, "Biometric authentication using the PPG: A long-term feasibility study," *Sensors*

(Switzerland), vol. 18, no. 5, May 2018, doi: 10.3390/s18051525.

[22] J. Park, H. S. Seok, S. S. Kim, and H. Shin, "Photoplethysmogram Analysis and Applications: An Integrative Review," *Front Physiol*, vol. 12, p. 2511, Mar. 2022, doi: 10.3389/FPHYS.2021.808451/BIBTEX.

[23] M. Elgendi, "PPG signal analysis an introduction using MATLAB".

[24] Y. Liang, M. Elgendi, Z. Chen, and R. Ward, "An optimal filter for short photoplethysmogram signals," *Sci Data*, vol. 5, May 2018, doi: 10.1038/SDATA.2018.76.

[25] M. Pour Ebrahim *et al.*, "Blood Pressure Estimation Using On-body Continuous Wave Radar and Photoplethysmogram in Various Posture and Exercise Conditions," *Sci Rep*, vol. 9, no. 1, Dec. 2019, doi: 10.1038/S41598-019-52710-8.

[26] G. Prieto-Avalos, N. A. Cruz-Ramos, G. Alor-Hernández, J. L. Sánchez-Cervantes, L. Rodríguez-Mazahua, and L. R. Guarneros-Nolasco, "Wearable Devices for Physical Monitoring of Heart: A Review," *Biosensors (Basel)*, vol. 12, no. 5, May 2022, doi: 10.3390/bios12050292.

[27] M. Elgendi *et al.*, "The use of photoplethysmography for assessing hypertension.," *NPJ Digit Med*, vol. 2, no. 1, p. 60, Dec. 2019, doi: 10.1038/s41746-019-0136-7.

[28] Y. Li, H. Gao, and Y. Ma, "Evaluation of pulse oximeter derived photoplethysmographic signals for obstructive sleep apnea diagnosis," *Medicine (United States)*, vol. 96, no. 18, May 2017, doi: 10.1097/MD.0000000000006755.

[29] S. G. Khalid, S. M. Ali, H. Liu, A. G. Qurashi, and U. Ali, "Photoplethysmography temporal marker-based machine learning classifier for anesthesia drug detection," *Med Biol Eng Comput*, vol. 60, no. 11, pp. 3057–3068, Nov. 2022, doi: 10.1007/S11517-022-02658-1/TABLES/3.

[30] M. A. Almarshad, M. S. Islam, S. Al-Ahmadi, and A. S. Bahammam, "Diagnostic Features and Potential Applications of PPG Signal in Healthcare: A Systematic Review," *Healthcare (Basel)*, vol. 10, no. 3, Mar. 2022, doi: 10.3390/HEALTHCARE10030547.

[31] K. Selvakumar *et al.*, "Realtime PPG based respiration rate estimation for remote health monitoring applications," *Biomed Signal Process Control*, vol. 77, p. 103746, Aug. 2022, doi: 10.1016/J.BSPC.2022.103746.

Molecular Dynamics Study of Carbazochrome Encapsulation in Single-Walled Carbon Nanotube

Syed Hassan Sarwar*

Department of Biomedical Engineering

Ziauddin University

Karachi, Pakistan

syedhasansarwar@gmail.com

Saad Jawaid Khan

Department of Biomedical Engineering

Ziauddin University

Karachi, Pakistan

sj.khan@zu.edu.pk

Syed Faraz Jawed

Department of Biomedical Engineering
NED University of Engineering and Technology

Karachi, Pakistan

farazjawed88@hotmail.com

Abstract - **Carbon nanotubes are one of the interesting nanocarriers when it comes to targeted drug delivery and precision medicine. In this study, molecular dynamics simulation study was carried out in order to investigate the encapsulation behavior of Carbazochrome drug molecule into an armchair (12,12) Single-Walled Carbon Nanotube SWCNT) using COMPASS forcefield. It was found out the drug molecule could get inside the SWCNT very quickly and could retain its position.**

Keywords Carbon Nanotube, Carbazochrome, Encapsulate, COMPASS, Molecular Dynamics.

I. INTRODUCTION

Targeted drug delivery has become a major focus under treatment methodology in the last several years. A major reason being the side effects including toxicities, and even drug resistance of the conventional drugs and treatment methods. Precision medicine has also demanded the use of targeted and controlled drug delivery over the conventional methods[1]–[3]. Consequently, different sorts of drug delivery nanocarriers, including exosomes, hydrogels, nanotubes and nanoparticles, etc. have been developed and utilized[2], [4]–[8]. Among these employed carriers, there also exit a nanocarrier called Single-Walled Carbon Nanotube (SWCNT)[6]–[8].

Several aspects of Carbon nanotubes (CNTs) related to medicine have been reported. For instance, Wong Shi Kam et al.[9] have reported the non-toxic nature of CNTs and their cellular uptake. Similarly, CNTs have also been reported for use as part of controlled drug delivery systems[7], [10]–[12].

Along with the other studies, several research publications have also opted the methodology of computational analyses and simulations in order to investigate the interactions and behaviors of CNTs with the different polymer and drug molecules. Karimzadeh et al.[13] has reported the adsorption mechanism of an anti-cancer drug Doxorubicin on Single-Walled Carbon Nanotubes (SWCNTs) using Density Function Theory. Similarly, Yoosefian & Jahani [14] reported the Droxidopa carrier potentiality of SWCNT. Zhu & Huang [15] studied the interaction of Fluorouracil drug with functionalized CNTs using Density Functional Theory.

In addition to these analyses, a research group studied the simultaneous loading of two drugs Imatinib and Doxorubicin onto CNTs using Molecular Dynamics (MD) simulations[16]. Another research group focused on MD simulations of a single chain polymer encapsulation into the SWCNT, using COMPASS ("Condensed-phase Optimized Molecular Potentials for Atomistic Simulation Studies") forcefield and a software named "Materials Studio"[17]. The COMPASS forcefield is an advanced generalized forcefield, especially developed for condensed-phase applications at finite temperature relevant to the experimental setups, and applicable to a large number of molecular classes[18].

Another research group studied the interaction and adsorption behavior of a hemostatic agent for blood loss prevention via wound, named Carbazochrome with SWCNT using a different software[19]. They used zigzag SWCNT (4,0), and calculated the interaction energies in-between the drug and the SWCNT in different configurations and found that it was mostly attractive.

In this study, we have focused on the encapsulation behavior of drug, particularly Carbazochrome, within the SWCNT. We have decided to use MD simulations as the primary tool for analyzing the encapsulation behavior.

II. METHODOLOGY

An Armchair (12, 12) SWCNT structure having 20 repeat units and a Carbazochrome molecule structure (as per Drug Bank) were constructed (Fig. 1). Carbazochrome molecule was positioned near an opening of SWCNT (Fig. 2). The after cleaned C-C bond length was 1.54 Å and C-H length was 1.14 Å.

Table 1: Write a caption above the table

Type size (pts.)	Heading		
	Subheading 1	Subheading 2	Subheading 3
1	Contents	Contents	Contents
2			
3			

Figure axis labels are often a source of confusion. Use words rather than symbols. For example, as shown in Fig. 1, write "Magnetization," or "Magnetization (M)" not just "M." Put units in parentheses. Do not label axes only with units. In the example, write "Magnetization (A/m)" or "Magnetization (A$\square$m^{-1})." Do not label axes with a ratio of quantities and units. Figure labels should be legible, at 9-point type.
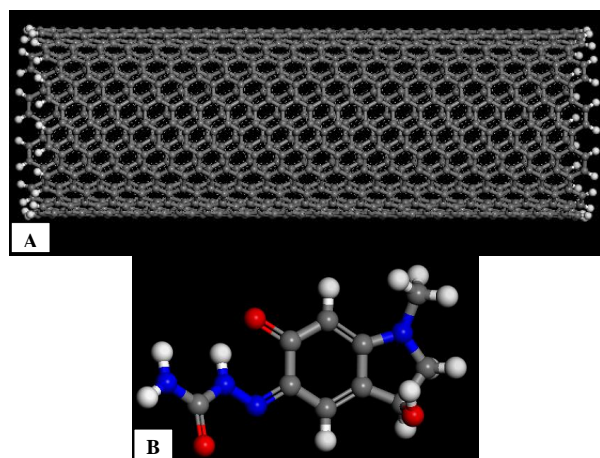
Fig. 1 Molecular models of (A) Single-Walled Carbon Nanotube (12,12); and (B) Carbazochrome molecule.
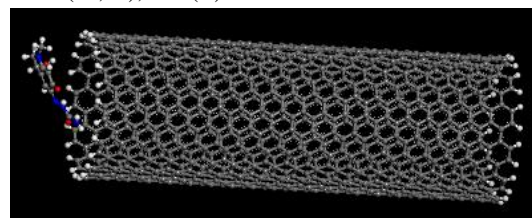
Fig. 1 Mutual positions of SWCNT and Carbaochrome molecule before MD simulation.

Biovia Materials Studio software was used for simulation. MD simulation was carried out using FORCITE module and COMPASS force field was employed. The simulation was performed in the NVT ensemble at 298 K and 1 fs was selected as the fixed time step size. The total simulation time was 40 ps with an output frame after every 1 ps.

Furthermore, interaction energies (E(int)) for the system in Fig. 2 and, the systems at 22 ps & 40 ps, were also calculated through the equation (1), using the total energy of drug-SWCNT system and the energies of drug and SWCNT, calculated using the FORCITE module and COMPASS forcefield. A negative interaction would mean that there exists a net attractive force between the molecules, otherwise, there exists a net repulsive force in case of positive interaction energy.

$$E(int) = E(system) - (E(drug) + E(SWCNT)) \qquad (1)$$

III. RESULTS

The 3D output frames of the DM simulation describe the successful encapsulation of the Carbazochrome drug molecule inside the (12,12) armchair SWCNT molecule (Fig. 3).

The total energy of the system in Fig. 2, was found to be 69408.734629 kcal/mol, while the energy of drug was 40.634906 kcal/mol and the energy of SWCNT was 69408.734629 kcal/mol. Hence, the interaction energy between drug and SWCNT was;

Fig. 3 Snapshots of MD simulation of Carbazochrome encapsulation inside SWCNT at 0 ps, 4 ps, 9 ps, 17 ps, 22 ps, & 40 ps respectively.

E(int) = 69408.734629 – (40.634906 + 69408.734629)
=> E(int) = -40.634906 kcal/mol. < 0

Similarly, the total energies of system at 20 ps and 40 ps were found to be 47403.477148 kcal/mol and 47366.646643 kcal/mol respectively. The respective interaction energies are;

$$E(\text{int @ 22ps}) = 47403.477148 - (40.634906 + 69408.734629)$$
$$\Rightarrow E(\text{int}) = -22045.892387 \text{ kcal/mol.} < 0$$
$$E(\text{int @ 40ps}) = 47366.646643 - (40.634906 + 69408.734629)$$
$$\Rightarrow E(\text{int}) = -22082.722892 \text{ kcal/mol.} < 0$$

IV. DISCUSSION

We aimed to investigate the encapsulation of Carbazochrome drug molecule inside the SWCNT. Sayiner et al.[19] reported the attractive behavior in between Carbazochrome and SWCNT. They used zigzag (4,0) SWCNT molecule of much lesser diameter and length, and showed the adsorption behavior of Carbazochrome over SWCNT. We, in this work, have emphasized on encapsulation, and have used a larger diameter SWCNT (12,12) and placed Carbazochrome molecule just out of the opening for observing the possible encapsulation (Fig. 2.2). Due to the already reported attraction between Carbazochrome and SWCNT by Sayiner et al.[19], this Carbazochrome is able to get inside and reside the SWCNT of larger diameter. As it is observable in the figure 3.1, that the drug molecule got inside the SWCNT during the first few pico-seconds, and then upon reaching a certain position at 22 pico-seconds, it has retained its position till the end of simulation.

As the interaction energy of the system before the simulation is negative, this means that there exists a net attractive force between the two molecules. Sayiner et al.[19] calculated the interaction energies of Carbazochrome and SWCNT in different formations and reported the maximum interaction energy to be -24.23 kcal/mol, while our system has shown a much higher interaction energy, leading to the successful encapsulation of the drug in the SWCNT.

As observable from the calculation of interaction energies at 22 ps & 40 ps, the attraction between the two molecules is very strong (very high negative interaction energies) and their interaction energies are nearly equal. This verifies the behavior of Carbazochrome to maintain its position within the SWCNT, as showed by the MD simulation results in Fig. 3.

V. CONCLUSION

In this study, we studied the encapsulation behavior of Carbazochrome molecule into the SWCNT. It was observed that the drug molecule was able to quickly get inside the CNT and reside in it. The interaction energies also supported the molecular dynamics results.

REFERENCES

[1] M. T. Manzari, Y. Shamay, H. Kiguchi, N. Rosen, M. Scaltriti, and D. A. Heller, "Targeted drug delivery strategies for precision medicines," *Nat Rev Mater*, vol. 6, no. 4, pp. 351–370, Apr. 2021, doi: 10.1038/s41578-020-00269-6.

[2] M. J. Mitchell, M. M. Billingsley, R. M. Haley, M. E. Wechsler, N. A. Peppas, and R. Langer, "Engineering precision nanoparticles for drug delivery," *Nat Rev Drug Discov*, doi: 10.1038/s41573-020-0090-8.

[3] Å. Flobak, S. S. Skånland, E. Hovig, K. Taskén, and H. G. Russnes, "Functional precision cancer medicine: drug sensitivity screening enabled by cell culture models," *Trends Pharmacol Sci*, vol. 43, no. 11, pp. 973–985, Nov. 2022, doi: 10.1016/J.TIPS.2022.08.009.

[4] K. Park, "Controlled drug delivery systems: Past forward and future back," *Journal of Controlled Release*, vol. 190, pp. 3–8, Sep. 2014, doi: 10.1016/J.JCONREL.2014.03.054.

[5] D. Berillo, A. Yeskendir, Z. Zharkinbekov, K. Raziyeva, and A. Saparov, "medicina Peptide-Based Drug Delivery Systems," 2021, doi: 10.3390/medicina57111209.

[6] S. Hossen, M. K. Hossain, M. K. Basher, M. N. H. Mia, M. T. Rahman, and M. J. Uddin, "Smart nanocarrier-based drug delivery systems for cancer therapy and toxicity studies: A review," *J Adv Res*, vol. 15, pp. 1–18, Jan. 2019, doi: 10.1016/J.JARE.2018.06.005.

[7] S. Adepu and S. Ramakrishna, "Controlled Drug Delivery Systems: Current Status and Future Directions," *Molecules*, vol. 26, no. 19, p. 5905, Sep. 2021, doi: 10.3390/molecules26195905.

[8] A. V. V. Nikezić, A. M. Bondžić, and V. M. Vasić, "Drug delivery systems based on nanoparticles and related nanostructures," *European Journal of Pharmaceutical Sciences*, vol. 151, p. 105412, Aug. 2020, doi: 10.1016/J.EJPS.2020.105412.

[9] N. Wong Shi Kam, T. C. Jessop, P. A. Wender, and H. Dai, "Nanotube Molecular Transporters: Internalization of Carbon Nanotube−Protein Conjugates into Mammalian Cells," *J Am Chem Soc*, vol. 126, no. 22, pp. 6850–6851, May 2004, doi: 10.1021/ja0486059.

[10] T. Lin *et al.*, "Temperature-Sensitive Hydrogels Containing Carboxylated Chitosan-Modified Carbon Nanotubes for Controlled Drug Release," *ACS Appl Nano Mater*, vol. 5, no. 8, pp. 10409–10420, Jul. 2022, doi: 10.1021/acsanm.2c01777.

[11] R. Cui *et al.*, "Antimicrobial film based on polylactic acid and carbon nanotube for controlled cinnamaldehyde release," *Journal of Materials Research and Technology*, vol. 9, no. 5, pp. 10130–10138, Sep. 2020, doi: 10.1016/J.JMRT.2020.07.016.

[12] H. Li, X. Sun, Y. Li, B. Li, C. Liang, and H. Wang, "Preparation and properties of carbon nanotube (Fe)/hydroxyapatite composite as magnetic targeted drug delivery carrier," *Materials Science and Engineering: C*, vol. 97, pp. 222–229, Apr. 2019, doi: 10.1016/J.MSEC.2018.11.042.

[13] S. Karimzadeh, B. Safaei, and T. C. Jen, "Theorical investigation of adsorption mechanism of doxorubicin anticancer drug on the pristine and functionalized single-walled carbon nanotube surface as a drug delivery vehicle: A DFT study," *J Mol Liq*, vol. 322, p. 114890, Jan. 2021, doi: 10.1016/J.MOLLIQ.2020.114890.

[14] M. Yoosefian and M. Jahani, "A molecular study on drug delivery system based on carbon nanotube for the novel norepinephrine prodrug, Droxidopa," *J Mol Liq*, vol. 284, pp. 258–264, Jun. 2019, doi: 10.1016/J.MOLLIQ.2019.04.016.

[15] X. Zhu and Y. Huang, "Theoretical study on paramagnetic amino carbon nanotube as fluorouracil drug delivery system," *J Drug Deliv Sci Technol*, vol. 75, p. 103670, Sep. 2022, doi: 10.1016/J.JDDST.2022.103670.

[16] A. Torrik, S. Zaerin, and M. Zarif, "Doxorubicin and Imatinib co-drug delivery using non-covalently functionalized carbon nanotube: Molecular dynamics study," *J Mol Liq*, vol. 362, p. 119789, Sep. 2022, doi: 10.1016/J.MOLLIQ.2022.119789.

[17] Q. Li, G. He, R. Zhao, and Y. Li, "Investigation of the influence factors of polyethylene molecule encapsulated into carbon nanotubes by molecular dynamics simulation," *Appl Surf Sci*, vol. 257, no. 23, pp. 10022–10030, Sep. 2011, doi: 10.1016/J.APSUSC.2011.06.132.

[18] H. Sun, "COMPASS: An ab Initio Force-Field Optimized for Condensed-Phase ApplicationsOverview with Details on Alkane and Benzene Compounds," *J Phys Chem B*, vol. 102, no. 38, pp. 7338–7364, Aug. 1998, doi: 10.1021/jp980939v.

[19] H. S. Sayiner, F. Kandemirli, · Serap, S. Dalgic, · Majid Monajjemi, and · Fatemeh Mollaamin, "Carbazochrome carbon nanotube as drug delivery nanocarrier for anti-bleeding drug: quantum chemical study," *J Mol Model*, vol. 1, p. 3, doi: 10.1007/s00894-021-04948-1.

Patient Telemonitoring Device For Remote Consultancy via Telecommunication

Taha Mushtaq Shaikh*
Ziauddin University Facilty
of Engineering Science Technology
and Management
Karachi, Pakistan
(taha005tms@hotmal.com)

Saad Jawaid Khan
Ziauddin University Facilty
of Engineering Science Technology
and Management
Karachi, Pakistan
(sj.khan@zu.edu.pk)

Hareem Rizwan Ahmed
Ziauddin University Facilty
of Engineering Science Technology
and Management
Karachi, Pakistan
(hareem.mr1@gmail.com)

Shehzeen Fatima
Ziauddin University Facilty
of Engineering Science Technology
and Management
Karachi, Pakistan
(syedashehzeen@gmail.com)

Hassan Arif
Ziauddin University Facilty
of Engineering Science Technology
and Management
Karachi, Pakistan
(hassan255arif@gmail.com)

Abstract—**Objective: Research in a wide range of areas, including sensor networks, medical devices, wireless communication, middleware software, and software applications, is being pursued to advance healthcare systems. To monitor patients remotely, a patient care method called telemonitoring combines several information technologies. To provide teleconsultation we have designed this telehealth monitor to ensure telemonitoring-related outcomes while monitoring body temperature, oxygen saturation, and pulse rate in real time through a touch screen LCD.**

Methods: **The telemonitor that we have built has taken the place of the conventional vital sign monitoring equipment. We have developed a tele health that measures body temperature, heart rate, and oxygen saturation and can tele-consult the patient if any of the values are abnormal.**

Results: **This tele health monitor design includes an LCD touch screen panel. The Raspberry Pi is attached to the back of the LCD panel together with all the other parts. On the front side, beneath the touch screen LCD, are the sensors. The Android GUI application is then given the patient's data.**

Conclusion: **Even though home telemetry has only recently become popular, a sizable amount of knowledge has been created and made accessible to policymakers and medical professionals. According to the results our literature review, home telemonitoring for chronic diseases appears to be a good patient care strategy that produces precise and reliable data, empowers patients, alters their behavioural patterns, and may even improve their medical conditions. The patient's heart rate, oxygen saturation, and body temperature are all tracked by this tele health monitor to prevent any life-threatening conditions. Additionally, teleconsulting services are available. Using the GUI Android application, the parameters of the patient and the state of the camera were visualised.**

Keywords: Telemedicine, telemonitoring, telemonitor, wireless patient monitoring, Internet of medical things (IoMT)

I. INTRODUCTION

The dramatic rise in the number of chronically sick patients in the face of dwindling provider numbers and significant budgetary strains necessitates a fundamental overhaul in the treatment process. We must find a technique to manage patients that assures appropriate monitoring and care while reducing expenditures. Providing care at the patient's home is an alternative. It could be considered a replacement for short-term hospitalisation, a supplement to community-based care, an alternative to long-term institutionalization, or a substitute for standard hospital outpatient or doctor visits. [1]

To advance telemedicine in Pakistan, it is necessary to build a telemonitor. If a patient's vital signs are out of the ordinary, it is required to consult with them. Additionally, pandemic-like conditions force people to stay at home and maintain their health. Patients who are unable to travel now have better access to affordable health care services. Because of this, a telemonitor that offers teleconsultation is a requirement.

Objectives: The main objective of our research is:
- To provide telemonitoring of pulse rate, oxygen saturation, body temperature in real time through Touch screen LCD.
- To provide teleconsultation through GUI Android Application from the doctor in real time.

II. MATERIALS AND METHODS
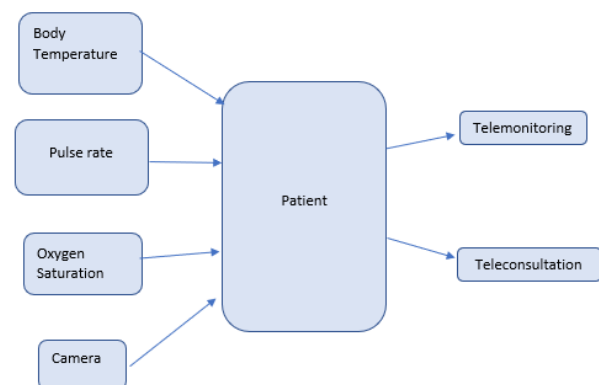
Fig 2.1: Basic Block Diagram

The tele health monitor that we have designed will help us to replace the conventional method of vital sign monitoring system that was used previously. This tele health monitor can measure pulse rate, oxygen saturation and body

temperature and tele consult the patient if the parameters are not within the normal range.

The basic hardware portion of our working prototype was based on low energy integrated circuits and sensors. The first step to initialize the project was installation of Raspberry PI software. The Raspberry PI 4 Model B was used which is a microprocessor; a mini electronic device that can perform various functions of a central processing unit present in a computer. This device can be used to learn programming skills, build hardware projects, do home automation, etc. The microprocessors are better than microcontrollers i.e., Arduino due to the high storage capability. With that, the Raspberry Pi is efficient in developing software using Python mostly, whereas Arduino is used for interfacing sensors to control LEDs and motors. Hence, the Raspberry Pi is also known as a minicomputer. The model B that we are using has a powerful processor, a USB-C power supply, micro-HDMI ports supporting 2x4K displays, Gigabit ethernet, different GB RAM, and two extra USB ports. Consequently, the touch LCD screen was interfaced with the Raspberry PI. The MCP3008 was used as a low cost 8-channel 10-bit analogue to digital (ADC) converter. It is based on CMOS technology. It had high performance and low power consumption, typically 5nA. It can take 200k samples in a second. Its applications include sensor interfacing, process control, data acquisition and battery-operated systems. MAX30105 and Waterproof NTC (Negative Temperature Coefficient) thermistor temperature sensors were used, and they were interfaced with Raspberry PI. MAX 30105 is a sensor that measures pulse rate as well as oxygen saturation. It is the combination of MAX 30101 and MAX 30100 and works on the principle of 'Photoplethysmography'. According to this principle, the changes in the volume of blood in an organ is measured by the changes in the intensity of the light passing through that organ. MAX 30105 has a high sensitivity optical reflective solution for detection of wide variety particle sizes and is capable of operating at high ambient levels. Its operating temperature range is from -40C to +85C and has robust motion artifact resilience, High SNR. It is a small sized IC without compromising on its electrical performance. The data is stored in 32-bit FIFO within the IC. It can be used as a particle sensing subsystem, temperature sensor, LED driver and proximity function.

The NTC thermistor had high precision and long-term stability. Then the software part commenced, where the GUI (Graphic User Interface) Android Application was created using Python language. The reason for using Python is that it provides multiple options for developing GUI as the user interacts more efficiently if the app contains attractive visual elements. Some of the best Python GUI frameworks for app development are PyQt5, Tkinter, Kivy, wxPython, etc. The App we designed for vital sign monitoring required login for access to patient's information and displayed pulse rate, oxygen saturation and body temperature respectively in one module. It also had an option to 'save' the data and an option to 'chat'. The other module is created to provide teleconsultation by the doctor. The doctor can easily consult through a chat option. Moreover, a 'camera' is interfaced with Raspberry Pi for the doctor to visualize the patient's condition in real time.

The microprocessors are better than microcontrollers i.e., Arduino due to the high storage capability. With that, the Raspberry Pi is efficient in developing software using Python mostly, whereas Arduino is used for interfacing sensors to control LEDs and motors. Hence, the Raspberry Pi is also known as a minicomputer. The model B that we are using has a powerful processor, a USB-C power supply, micro-HDMI ports supporting 2x4K displays, Gigabit ethernet, different GB RAM, and two extra USB ports. Consequently, the touch LCD screen was interfaced with the Raspberry PI. The MCP3008 was used as a low cost 8-channel 10-bit analogue to digital (ADC) converter. It is based on CMOS technology. It had high performance and low power consumption, typically 5nA. It can take 200k samples in a second. Its applications include sensor interfacing, process control, data acquisition and battery-operated systems. MAX30105 and Waterproof NTC (Negative Temperature Coefficient) thermistor temperature sensors were used and they were interfaced with Raspberry PI. MAX 30105 is a sensor that measures pulse rate as well as oxygen saturation. It is the combination of MAX 30100 and MAX 30102. MAX 30105 has a high sensitivity optical reflective solution for detection of wide variety particle sizes and is capable of operating at high ambient levels. Its operating temperature range is from -40 to +85C and has robust motion artifact resilience, High SNR. It is a small sized IC without compromising on its electrical performance. The data is stored in 32-bit FIFO within the IC. It can be used as a particle sensing subsystem, temperature sensor, LED driver and proximity function. The principle of measuring oxygen saturation is measured by pulse oximeter also known as SpO2. The pulse oximeter can noninvasively measure SpO2. Waterproof NTC thermistor changes resistance to measure temperature. When resistance decreased, temperature increased and vice versa but we have taken DS18b20 for a temperature sensor because it works on extreme conditions like it have an amazing range between -55 degrees to +125 degrees centigrade.

Now we have installed the latest software in raspberry pi 4. After installing the software, we have to work on the interfacing and as for the oxygen saturation we have used MAX30105 because it is a flexible and powerful sensor enabling sensing of distance, heart rate, particle detection, even the blinking of an eye. Now after interfacing all these sensors, we have to work on wireless interfacing and for that we have to use the virtual network computing (VNC). It is a cross platform screen sharing system that was created to remotely control another computer. The focus is on wireless real-time vital signs monitoring device, whether it be in smart homes; for elderly patients or in E-Ambulance on international level. However, the focus of our research is to design such a telemonitor that performs wireless monitoring in real-time and displays it on touch LCD screen as well as perform teleconsultation through GUI Android Application. It is mainly for Pakistan. This is the innovation that we are coveting to bring in our project.
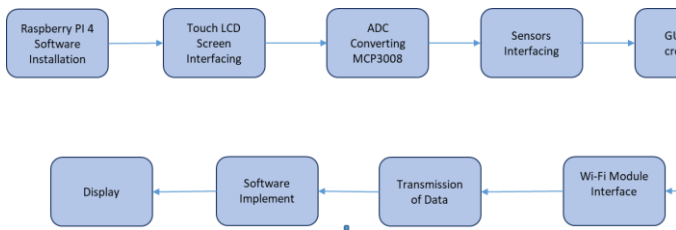
Fig 2.2: Methodology Block Diagram

III. RESULTS

After getting done with raspberry Pi software installation, temperature sensor interfacing, camera interfacing and wireless interfacing. We tested them and got preliminary results. We collected the data for temperature interfacing. In first round we collect the data of around 17 people from mercury thermometer and digital thermometer and then we compared the results from our temperature sensor. The results showed +-1.5 difference that could be considered as near to the accurate readings.

Figure 3.1 Comparison result with mercury thermometer
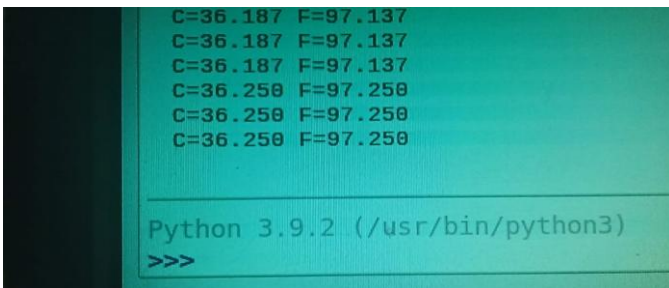
Fig 3.2 Temperature monitoring

In the second round we did the test for wireless and camera interfacing and the results we got can be seen below in the picture.

Fig 3.3 Real-time monitoring and camera recording.

IV. DISCUSSION

The health monitoring system is important to keep a check and balance of health of a person. The deviation from the normal ranges might result in some severity later. Hence, telemonitoring is an easy way to assess the health of a patient whilst being at home. It is cost effective and provides patient a reliable way to cure themselves. The smart health care systems are nowadays on the top for research work. The advancement in these services improve sensor networks, wireless connections, medical devices, software, etc. The telemedicine can be used for both indoor and outdoor monitoring and is now a topic of attraction for many researchers. [2] Telemedicine is described as the direct provision of clinical care for a patient at a distance via telecommunications, including diagnosis, treatment, and consultation [4]. In a more limited sense, home telemonitoring refers to the use of audio, video, and other communications technologies to monitor patient status from a distance. Amala A. Louis et al. stated that telemonitoring, either employed alone or as part of a multidisciplinary approach, has been shown in observational studies to reduce hospitalization and readmission rates in patients. Telemonitoring could be an important aspect of a plan for providing patients with effective health care. This is a key indicator of home telemonitoring's success in providing timely access to the highest data for clinical decision-making. With the advancement of telecommunication technologies, telemonitoring has never been easier. [11] GUY PARÉ et al. found out the given technical advancements and the current body of evidence on the influence of telemonitoring on data quality, they suggest researchers should instead focus on other telemonitoring effects that are still unknown. Furthermore, the studies included with this review found that the effects of home telehealth on patients' attitudes and actions were consistent. This approach to clinical outcomes appears to be well received and embraced by patients. It allows them to actively participate in the care process, improves their knowledge and sense of security, and, eventually, strengthens them. Despite the current evidence on the attitudinal and behavioural effects of telemonitoring, little is known about the conditions that would support the development of patient's empowerment and enhance their participation in the telemonitoring process, particularly considering the reported decrease in patients' compliance over time that has been noted in several studies. Because of the supply and demand curve in health care, the challenge becomes even more complex. Indeed, while the number of chronically ill patients is increasing dramatically, there are global provider shortages. Patients were generally amenable to telemonitoring as a patient care strategy and had a favourable attitude toward it. Blood pressure and heart rate can help you keep track of your health. Our objective is to use a touch screen LCD, that will give real-time telemonitoring of pulse rate, oxygen saturation, and body temperature. And to provide true teleconsultation from the doctor to use a GUI Android application. The telemonitor design has a touch screen LCD display. The Raspberry Pi with all of the miscellaneous items is attached at the backside of the LCD screen. The sensors are kept on the front side below the touch screen LCD. The data taken from

the patient is then transferred to the GUI Android Application. The data is saved there by creating a private account of the patient. The doctor can access the condition of the patient by the results of their vital signs. If needed, the doctor can provide teleconsultation as well through the camera or the App as per the need. [1]

LIMITATION: Telemonitoring may be hampered by the relatively steep learning curve associated with the implementation for both patients and families. Clearly, home telemonitoring's full potential has yet to be realized, and more clinical trials are required. To summarize, telemonitoring may play a significant role in the delivery of effective health care to patients, but further evidence of usefulness is needed before it can be recommended for broad use. Furthermore, to assess the potential benefits and cost-effectiveness of this emerging strategy, existing research and new large multicentre, randomized controlled trials are required.

V. Conclusion

Despite the short history of home telemetry, a substantial body of knowledge has been developed and made available to policymakers and physicians. Based on the findings of this study, home telemonitoring for chronic diseases appears to be a promising patient care strategy that generates accurate and trustworthy data, empowers patients, impacts their behavioral patterns, and may improve their medical conditions. Nonetheless, more research is needed in this field to provide a comprehensive body of knowledge about its clinical effects, cost effectiveness, impact on health-care expenditures, and acceptance by health-care professionals. It is critical to demonstrate the feasibility of this patient care method at the statistical level for insurance companies and governments to contemplate future endorsement and subsequent reimbursement for the services delivered. More thorough study on home telemonitoring would produce stronger evidence that would lead to impact on the practice and management of these chronic illnesses, payer and practitioner acceptance of this patient management approach, and its future inclusion into the overall care process. So that's why we are designing the telehealth monitor device. The telemonitor is designed to keep track of the pulse rate, oxygen saturation and body temperature of the patient to avoid any crucial circumstances. In addition to this, it can proffer the services of tele consultation as well. The GUI Android application was created to access the parameters of the patient and the camera to visualize the condition of the patient.

References

[1] GUY PARÉ, PHD, MIROU JAANA, PHD, CLAUDE SICOTTE, PHD Systematic Review of Home Telemonitoring for Chronic Diseases: The Evidence Base 2007

[2] Leili Lind, Erik Sundvall, Daniel Karlsson, Nosrat Shahsavar, Hans Ahlfeldt Requirements and prototyping of a home health care application based on emerging JAVA technology/ 2002

[3] Yu Fua, Jian Liub System design for wearable blood oxygen saturation and pulse measurement device/ 2015

[4] Haider Mshali, Tayeb Lemlouma, Maria Moloney, Damien Magoni A survey on health monitoring systems for health smart homes/ 2018

[5] P. Finet , R. Le Bouquin Jeannès, O. Dameron Interoperable Infrastructure and Implementation of a Health Data Model for Remote Monitoring of Chronic Diseases with Comorbidities/ 2018

[6] Festus Oluseyi Oderanti, Feng Li, Marija Cubric, Xiaohui Shi Business models for sustainable commercialisation of digital healthcare (eHealth) innovations for an increasingly ageing population/ 2021

[7] G.C. Lamprinakos, S. Asanin, T. Broden, A. Prestileo , J. Fursse, K.A. Papadopoulos, D.I. Kaklamani, I.S. Venieris An integrated remote monitoring platform towards Telehealth and Telecare services interoperability/ 2015

[8] Basem Almadania, Manaf Bin-Yahyaa, Elhadi M. Shakshukib E-Ambulance: Real Time Integration Platform for heterogenous medical telemetry system/ 2015

[9] Lili Liua, Eleni Stroulia, Ioanis Nikolaidis, Antonio Miguel-Cruz, Adriana Rios Rincona Smart homes and home health monitoring technologies for older adults: A systematic review/ 2016

[10] Alessandra Angelucci, Andrea Aliverti Telemonitoring system for respiratory patients: technological aspects/ 2020

[11] Amala A. Louis, Tracy Turner, Marcia Gretton, Angela Baksh, John G.F. Cleland* A systematic review of telemonitoring for the management of heart failure. 2003

Mobile Servo Robotic Arm

Nida Abdullah
Department of
Biomedical Engineering
Salim Habib University
Karachi,Pakistan
nidaamir1120@gmail.com

Maryam Furqan
Department of
Biomedical Engineering
Salim Habib University
Karachi,Pakistan
maryamfurqan50@gmail.com

Hassan Ali
Department of
Biomedical Engineering
Salim Habib University
Karachi,Pakistan
hassan.ali@shu.edu.pk

Tooba Khan
Department of
Biomedical Engineering
Salim Habib University
Karachi,Pakistan
tooba.khan@shu.edu.pk

Abstract- **Trauma, cancer, vascular disease, congenital abnormalities, and other orthopedic diseases can restrict the range of motion of joints such as hinges, ball and socket joints, shoulder joints, and pivot joints. According to studies, Seventy percent of individuals with upper limb loss have their limbs amputated below the elbow, with ten percent having their limbs amputated at the hand or wrist. Any type of amputation in these joints affects patients' emotional well-being along with their ability to perform their daily activities. This study aims to develop a prototype mobile servo robotic arm that could be used to assist such patients. A mobile servo robotic arm that can be controlled with the other limb, assisting in mimicking the motions of a normal human limb and allowing for the completion of all daily activities. Servo motors are particularly useful for applications where precise positioning is essential, such as controlling and moving a robotic arm into a specific range. It was achieved in this study by coupling two servo motors that can rotate up to 180 degrees each which produced the pitch and roll motion for the robotic arm.**

Keywords - Amputation, Robotic arm, Servo motors, Range of motion, Pitch and roll.

I. INTRODUCTION

Amputation of the upper limb, orthopedic diseases, and trauma cause major structural and functional alterations in the body. Robotic devices are suited for use in such situations. In nonindustrialized countries, the most common cause of amputation is trauma. Injuries involving machinery, powered tools and appliances, weapons, and motor vehicle crashes have been identified as the primary causes of trauma-related amputations. It has been reported that amputations occur globally at a rate of 17-30 per 100,000 people [1]. Nonindustrialized countries have a higher incidence because of war, trauma, and inadequate medical systems.

A robotic arm is essentially a machine resembling a human hand and comprises a series or parallel arrangement of linkages. It can be programmed to do different tasks and has a wide range of applications in fields such as health care, mechanical engineering, industries, and manufacturing [2].

Robots are commonly utilized to undertake tasks that are dangerous, repetitive, and unpleasant. The robots are powered by servomotors that are controlled by a sophisticated control system that includes a few microprocessors and sophisticated software [3]. Therefore, the major focus in designing the mobile servo robotic arm, is that is high precision, low-cost, accurate, and easy to handle. The task is to create a human-like movement

that can be attached securely to the bone. As a result, the bone is treated as a fixed object, simplifying control of the robotic system.

II. METHODOLOGY

A. Hardware:

To design the mobile servo robotic arm, the following hardware components had been required:

1. MPU6050
2. Servo Motors
3. Arduino Mega
4. Jumper Wires
5. Breadboard
6. Arduino IDE (Software)

1. MPU6050

MPU-6050 is a 6-DOF IMU chip with a 3-axis Accelerometer which is an acceleration sensor and also has a 3-axis Gyroscope which is a balance regulator. The I2C serial interface is used [4]. It communicates using I2C, which is a single-ended, multi-master, multi-slave serial computer bus with highly low speed but great utility because it only has two wires: SCL (clock) line and SDA (data) line [5]. Furthermore, MPU-6050 contains Digital Motion Processors which process the raw data/signal from each of the sensors. The MPU6050's DMP also helps reduce the number of errors.

2. Servo Motors

Servo motors are actuators that can be controlled precisely in terms of rotation and angular position. The servomechanism is used to control the servomotor. A servo motor can be either a DC or an AC motor. PWM, or Pulse Coded Modulation, determines the angle by the duration of the applied pulse to the signal wire. Servo motors rotate up to 180 degrees and are employed in robotics applications due to their simplicity, affordability, and dependability of microprocessor control [6].

3. Arduino Mega 2560

The Arduino Mega 2560 microcontroller board is based around the ATmega2560. It contains 54 pins for digital input and

output, including a crystal oscillator of 16 MHz, 4 hardware serial ports, 14 PWM output pins, 16 analog inputs, a USB port, a power jack, a reset button, and an ICSP header [7].

4. Arduino IDE (Software)

The Arduino development board is a hardware device, while the Arduino IDE (Integrated Development Environment) is software that facilitates code writing. These microcontrollers are equipped with Atmel's 8-bit AVR microcontrollers or a 32-bit Atmel ARM microcontroller and can be easily programmed using the C or C++ language through the Arduino IDE. The Arduino IDE provides a user-friendly integrated platform that can be installed on a regular personal computer and enables users to create Arduino programs in C or C++ [8].

B. The System Architecture:

The specification of the components such as Arduino Mega 2560, MPU-6050, and servo motor for the project: "Mobile servo robotic arm" are shown in Table 1. The main aim of these specifications is to emphasize important aspects of this project.

Table 1: Specification of Mobile Servo Robotic Arm

Modules	Specifications
Interface	Arduino Mega 2560
Main controller	MPU-6050
Programming Software	Arduino IDE
Controller (Actuator)	Servo Motor

C. Structural Design:

The main structure of the robotic arm was designed on the Autodesk fusion 360 to get an idea of how the project will be presented. For the arm, the sheets are that to be attached to the servo motors were also designed with the help of Autodesk Fusion 360, and the sheets were 3D printed by Flashforge 3D printer, as the 3d- printed sheets are lightly weighted and can rotate easily. The sheet dimensions that is the width (X), length (Y), and height (Z) respectively, and scaling in millimeters (mm), are shown in Table 2.

Table 1: The dimensions and scaling of the sheet

Dimensions	Scaling (mm)
Width (X)	49.05
Length (Y)	107.92
Height (Z)	5.89

Figure 1 shows the design of the mobile servo robotic arm with (a) the fundamental structure of the robotic arm and (b) The designed sheet to be attached to the servo motor. Two servo motors, two sheets, plus a base and stand will make up the robotic arm. The servo motor is attached to the stand that holds the other servo motor to form the arm and the stand is placed together with the base to form the complete structure.
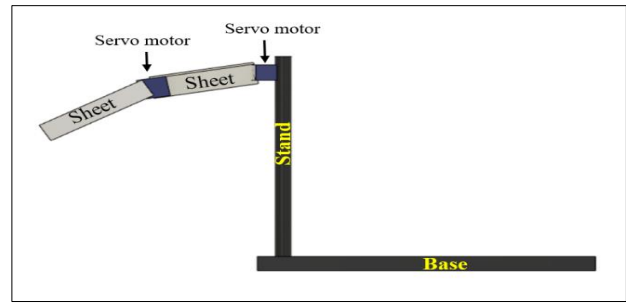
Fig. 1(a) The fundamental structure of the robotic arm.
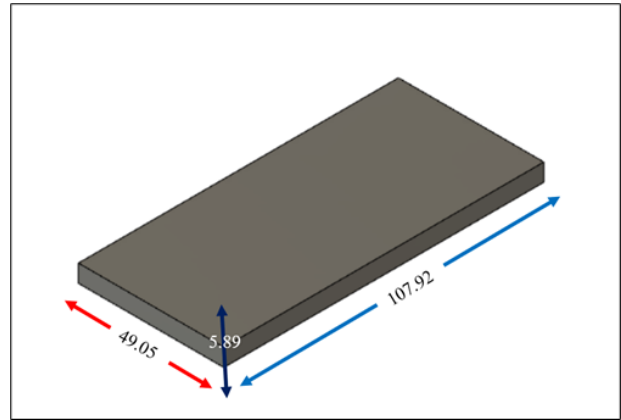
Fig. 1(b) The designed sheet to be attached to the servo motor.

The project combines the hardware and software functions to make the system reliable, precise, and accurate. The Arduino Mega 2560 will interface with the servo motors and MPU-6050, and the MPU-6050 will give signals to the board, which will be forwarded to the servo motors that will control the movement of the robotic arm. The schematic diagram is shown in Fig. 3.
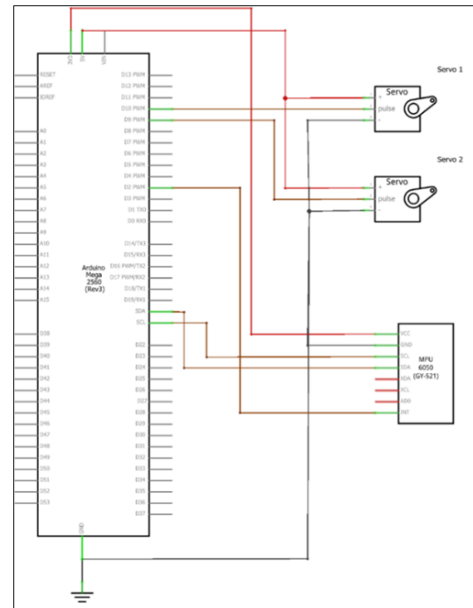
Fig. 3 The Schematic Diagram.

D. Modelling Implementation:

The mechanism of a robotic arm is summarily shown in Fig. 4.
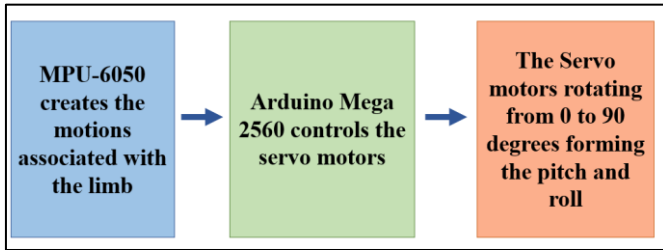
Fig. 4 Block Diagram.

The two servo motors are connected with the help of strong glue and 3D-printed sheets to form the base of the arm. A sheet is placed on the top of the first servo motor and above it, a second servo motor is placed and glued on the same sheet. Servo motors have three wires: signal, power and ground. To link the servo motors with the Arduino board, connect the positive wires of both servos to the 5-volt pin. Connect the negative wires of both servos to the ground pin of the board. The signal pin is typically yellow, white or orange and is connected to the digital pin of the Arduino Mega 2560 that controls the rotation. These are connected in a way that the servo motors can rotate freely up to 90 degrees. It requires a servo library, as this library allows an Arduino board to control servo motors. Also, to interface MPU-6050 with Arduino, need to must download the MPU-6050 library. To create the motions, MPU-6050 pins: SDA and SCL are connected to the same-named pins of the Arduino Mega board. SDA that is serial data wire used for data exchange occur between master and slave devices, while SCL (serial clock) wire is used for synchronizing clocks. INT pin of MPU-6050 is connected to the digital pin of the Arduino Mega board. The interrupt pin enables notification of available data to the MCU/MPU. The sensor interrupt can be used as a wake-up signal to bring the CPU back from sleep mode in some applications where the processor goes into sleep mode to save power. Then upload the project-specific code to the Arduino Mega board and create the different movements by operating MPU-6050 and observing the rotation changes in the robotic arm.

Fig. 5 The robotic arm setup.

III. RESULTS AND DISCUSSION

The robotic arm was tested at different angles by moving and controlling the motions through the MPU-6050 that is attached to the glove. As the gloved hand moves, the robotic arm mimics the same motion through the rotation of the servo motors. When the gloved hand is at the horizontal level (0°), the direction of the robotic arm is toward the left; with the procedure of the gloved hand moving towards 90°, the robotic arm rotates in the anti-clockwise direction. At the complete 90°, the robotic arm direction is downward. When the output spline of the motor reaches the desired position, the power supplied to the motor is decreased, and the servo maintains that position until instructed otherwise.

A servo motor will actively work to maintain a specific position when halted. The speed of rotation of a servo motor is limited to the extent necessary for it to move from its current position to the requested position. The robotic arm rotates in two axes: pitch and roll. The rotation of an arm about its transverse axis is known as pitch (X-axis). An arm rotates about its longitudinal axis when it rolls (Y axis).

The different motions by the gloved hand and rotations by the robotic arm are shown in Fig. 6.
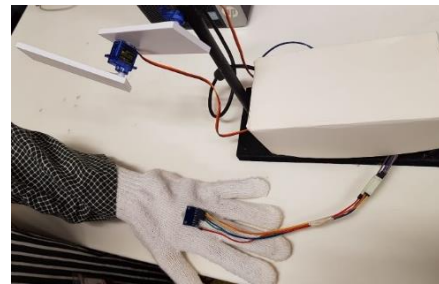
Fig. 6(a) The direction is towards the left.
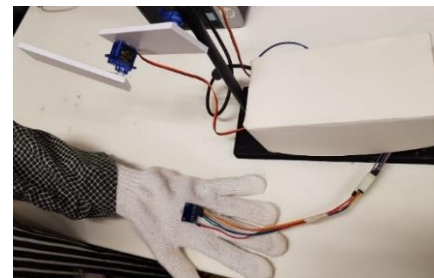
Fig. 6(b) The direction is rotating anticlockwise.
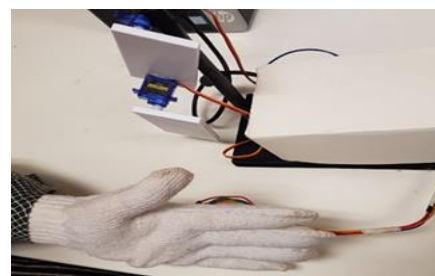
Fig. 6(c) The direction is downwards.

IV. CONCLUSION

The objective has been achieved by designing a robotic arm and implementing the pitch and roll system operation. It is evident from the testing and analysis that its movement is precise, accurate, simple to regulate, and user-friendly. Moreover, if it is developed with extreme precision, it then is capable of carrying out difficult surgical procedures. The MPU6050 was selected as the inertial measurement unit because it is a low-cost, high-accuracy device that integrates a gyroscope and an accelerometer onto a single chip.

REFERENCES

[1] Brigham and Women's Hospital, "Standard of Care : Lower Extremity Amputation," Brigham Women's Hosp. Dep. Rehabil. Serv., pp. 1–46, 2011.

[2] G. R. Reddy and V. K. P. Eranki, "Design and Structural Analysis of a Robotic Arm," p. 101, 2016.

[3] N. Barai and S. Manekar, "Review on design and development of intelligent robotic arm," *Proc. 2015 IEEE 9th Int. Conf. Intell. Syst. Control.* ISCO 2015, vol. 3, no. 3, pp. 527–529, 2015.

[4] E. V Board and U. Guide, "MPU-6000 / MPU-6050 9-Axis Evaluation Board User Guide," vol. 1, no. 408, pp. 1–13, 2011.

[5] B. A. Sawalkar, N. Kasat, and M. E. Student, "A Review on Analysis and Reusability of FPGA Implementation for I2C Protocol," vol. 7, no. 2, pp. 440–443, 2016.

[6] Swamardika A, Budiastra IN, Setiawan N, IndraEr N. Design of mobile robot with robotic arm utilizing microcontroller and wireless communication. *Int. J. Eng. Technol.* 9(2):838-46, 2017.

[7] D. Mellis, "Arduino Mega 2560," Retrieved November., p. 2560, 2011.

[8] L. Louis, "Working Principle of Arduino and Using it as a Tool for Study and Research," *Int. J. Control. Autom. Commun. Syst.*, vol. 1, no. 2, pp. 21–29, 2016.

Design of a Computer Assisted Diagnosis System for Brain Tumor Detection

Rafia Jabbar

Biomedical Engineering
NED University of Engineering & Technology
Karachi, Pakistan

rafiajabbar999@gmail.com

Abstract **- The most common and serious condition, a brain tumor, has a life expectancy of only a few months. A range of imaging modalities, including CT, MRI, and ultrasound, have been utilized to assess cancers in the prostrate, breast, lung, and brain. MRI images are mostly used in this study to identify malignancies in the brain. An MRI scan collects so much data that manual classification of cancers vs. non-tumors is unfeasible at any given time. It does, however, have significant limitations due to the small quantity of pictures available (i.e., precise quantitative measurements). An automated classification system is necessary to avoid human fatalities. Because of the spatial and structural diversity of brain tumors, automatically identifying them in the tumor region is difficult. AlexNet, VGG16, GoogleNet, and RestNet50 were four deep learning models used to classify brain tumors in this study. RestNet50 was determined to become the most appropriate prediction, with a 95.7 percent accuracy, and AlexNet had the quickest performance, with a 1.2 second processing time. Using the k-fold approach for separating the data and a processing time of roughly 1 second for each fold calculation, we were possible to forecast the presence of tumors with 79 percent accuracy.**

Keywords – MRI Scans, k-fold, algorithms, brain tumour, automatic diagnosis.

1. INTRODUCTION

The body participates in different types of cells. Each type of cell has an express limit. Most cells in the body develop and divide systematically to form new cells because they are expected to function robustly and adequately in the body. When cells lose the ability to control their development, they continue to divide without structure. The structure of the extra cell is a mass of tissue called a tumor. There are two types of brain tumors: benign and malignant.

Benign tumors are not aggressive. They do not penetrate the surrounding tissue or spread anywhere else. Still, if they grow near vital organs, press on a nerve, or restrict blood flow, they can cause serious problems. They usually respond well to treatment. Benign tumors may need to be surgically removed. They can grow very large and sometimes weigh pounds. On the other hand, malignant brain tumor is a fast- growing cancer that spreads to other areas of the brain and the spine.

2. METHODOLOGY

With the help of TensorFlow, machine learning is used to develop models for high precision applications that handle images, text, video, or audio. TensorFlow is a deep learning framework from Google. CNN is a deep learning subgroup of machine learning whose techniques are used to process large amounts of data.

TensorFlow allows developers to launch applications quickly. In our model a transfer learning strategy is used.

Transfer learning refers to the retraining of a model that has already been trained in a different problem to fit our data. This saves us time and effort by not having to start from scratch.

2.1. Data Understanding

The first step is to analyze the MRI data. There is a total of 253 MRI images related to this problem. There are 155 marked "yes" which means there is a tumor and 98 which are marked "no" which means there is no tumor. Now, to use CNN, we must first train a neural network, which can be thought of as a set of algorithms that can detect and classify relationships between images in a dataset.

2.2. Data Augmentation

We use a technique called data augmentation to address this problem [1]. This is vital in medicine, as there will be multiple instances of data imbalance. To generate more images, we use data augmentation to take a single MRI image and apply various image enhancements such as rotating, mirror, and reflect. We are using more magnification for the class with fewer images, so both classes have roughly the same number of images.

2.3. Splitting the Data

The next step is to divide our data into two sets: training and testing. The training set receives 80% of the scans that are used to train our neural network. The remaining 20% is used in the test set where we apply our trained neural network and categorize it to see if our neural network is correct. We have used 5-fold distribution.

2.4. Building the CNN Model

The next step is to create a neural network with multiple layers of convolution and grouping using the Keras library.

$$ReLU = f(x) = \max(0, x) \qquad (1)$$

$$Sigmoid = \sigma(x) = 1 / 1+e{-x} \qquad (2)$$

Equation (1) and (2) are the two activations used in our model, ReLu is used with Conv2D layer while sigmoid is used at the end with dense layer.

2.5. Pre-Training the CNN Model

We then created a "train generator" and a "test generator" to split the photos of the training and test sets into two classes (yes and no). As you can see, the 4047 photos are divided into 3238 (80%) for the "train generator" and 809 (20%) for the "test generator".

2.6. Training the CNN Model

Finally, we come to the stage of adapting the image data to the trained neural network. We train the image data for approximately 50 "epochs". An era can be imagined as an iteration in which we repeatedly feed the training photos into the neural network so that it is better trained with the training images.

2.7. Study the CNN Model

Finally, we record the "precision" and "loss" of the "train generator" for every k-fold 10 epochs after training (iterations). Finally, this model allows you to feed in a single magnetic resonance image and determine whether you have a tumor or not.

3. RESULTS

We have used python language to build this model. Worked on sequential model as it gives better results. We have chosen splitting method as k-fold validation method because this method doesn't vary the accuracy after we again run our model. While array method shuffles the dataset every time we run the model, and that is the main reason for not giving a constant accuracy again and again.

At the initial stage the dataset was not so big, so we gave 15 parameters to be applied on every image present in that dataset to increase the dataset so that classification can be done easily.

Below are tables for accuracy results for training and testing of model.

TABLE 1. CROSS VALIDATION SCORE – (TRAINING)

Model	Iteration 1	Iteration 2	Iteration 3	Iteration 4	Iteration 5	Average
Sequential	96.06 %	96.82 %	98.85 %	97.10 %	98.21 %	97.354 %

TABLE 2. CROSS VALIDATION SCORE – (TESTING)

Model	Iteration 1	Iteration 2	Iteration 3	Iteration 4	Iteration 5	Average
Sequential	55.57 %	69.01 %	85.29 %	93.82 %	97.78 %	80.294 %
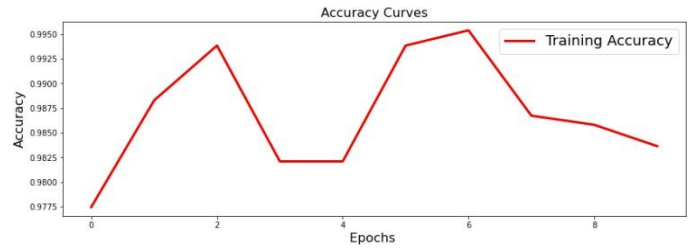
Fig. 1. Graphical Representation of Training Accuracy
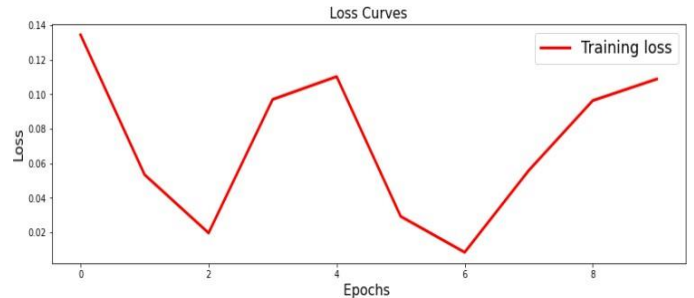
Fig. 2. Graphical Representation of Training Loss

4. DISCUSSION

Tumors develop in the brain and other areas of the body as a result of unchecked cell division. Neurofibromatosis, Epstein-Barr virus, vinyl chloride, and ionizing radiation are all potential causes of brain tumors. An intracranial tumor, often known as a brain tumor, is an abnormal mass of tissue where cells reproduce and develop uncontrollably, seemingly independent of the systems that regulate normal cells.

About 24,530 harmful brain or spinal cord tumors are analyzed (13,840 in men and 10,690 in women). These numbers would be much higher if the considered (non- pathological) tumors were also included. In addition, approximately 18,600 people (10,500 men and 8,100 women) will bite the dust from the brain and spinal cord tumors. This measurable study comes from the US. The probability that a person will develop a life-threatening brain or spinal cord tumor in their lifetime is less than 1%.

4.1. Symptoms of Brain Tumor

The following are the symptoms of a brain tumor:

4.1.1. **Headache:** With 46% of the patients experiencing headaches, this was the most prevalent symptom. They gave various descriptions of the headaches; no one pattern was a surefire indicator of a tumor.

4.1.2. **Seizures:** A seizure was reported by 33% of the patients, making it the second most frequent symptom to be recorded. A seizure is a rapid, unconscious alteration in awareness, sensation, muscular control, and/or behavior. The signs of a seizure might include muscular twitching or minor shaking of a limb to abrupt, in-

tense shaking and complete loss of consciousness.

4.1.3. Nausea and Vomiting: Similar to headaches, nausea and vomiting are non-specific, hence the majority of sufferers do not have a brain tumor. 22 percent of those who responded to our survey listed nausea and/or vomiting as a symptom.

4.1.4. Vision or hearing problems: 25 percent of people said they had eyesight issues. This one is simple: if you suspect a hearing or vision issue, have it evaluated.

4.1.5. **Behavioral, cognitive, and neuromuscular problems:** There have been numerous reports of behavioral and cognitive changes, including issues with recent memory, difficulty focusing or finding the right words, acting out, lack of patience or tolerance, and loss of inhibitions, which can result in saying or doing things that are inappropriate for the circumstance. issues with muscular weakness in your arms, legs, or face, as well as odd feelings in your hands or brain. 25% of people felt weakness in their arms or legs. 9% of people said they had unusual emotions in their hands, while 16% said they had strange feelings in their heads. This might lead to a different stride (way of walking), dropping things, falling, or an asymmetrical look on the face.

Many different ways have come across for diagnosing the brain tumor; automatic and semi-automatic.

4.2. Semi – Automatic Systems

A semi - automatic system is defined as any system which requires both machines and human participation in performing any task. It includes.

4.2.1. Magnetic Resonance Imaging (MRI): A comprehensive three- dimensional anatomical picture may be produced using the non-invasive imaging technology known as MRI. It is frequently used to locate the disease, provide a diagnosis, and monitor its development [2]. It employs powerful magnets to produce a powerful magnetic field that compels the body's protons to align with it. The patient is pulsed with a high-frequency current, which activates and unbalances the protons. When the RF field is absent, the energy produced when protons realign with the magnetic field may be detected by MRI sensors.

Bloch's phenomenological equations are useful for describing the motion of the magnetization vector of uncoupled spins like protons in water:

$$\frac{dM}{dt} = \gamma M \times H - \frac{M_{xy}}{T_2} - \frac{M_z - M_o}{T_1} \qquad (3)$$

Where γ is the gyromagnetic ratio, H is the effective field, $M0$ is the equilibrium magnetization and $T1$ and $T2$ are the relaxation time.

4.2.2. Computed Tomography (CT): A patient is subjected to a small X-ray beam that rapidly rotates around the body, creating signals that are then evaluated by the computer of the device to create cross-sectional pictures, or "slices," of the body. Because they offer more information than standard X-ray pictures, these slices are known as tomographic images. It operates by rotating a motorized X-ray source around the donut- shaped gantry's circular aperture.

4.2.3. Positron Emission Tomography (PET): PET is a non-invasive imaging technique that uses the injection of radioactive chemicals (radiotracers), radiation detection, and reconstruction of the radiotracer distribution to provide physiological information. This is because radiolabeled molecular imaging agents are used to provide clinically valuable information on the function and status of tissues and organs. Screening, categorization, staging, prognosis, treatment planning, therapy response monitoring, and monitoring based on imaging agents and disease can be offered [3].

On the other hand, an automatic system is a mix of both programming and equipment which is planned and modified to work naturally without the need for any human administrator to give information sources and guidelines for every activity. It includes artificial intelligence, machine learning, and deep learning.

4.3. Automatic Systems

An automatic system is a mix of both programming and equipment which is planned and modified to work naturally without the need for any human administrator to give information sources and guidelines for every activity. It includes different models of convolutional neural networks like AlexNet, VGG16, GoogleNet, ResNet50 and many more [4].

4.3.1. AlexNet: One of Alex Krizhevsky's convolutional neural network (CNN) architectures is known as AlexNet. Not the first quick GPU deployment by CNN to win an image recognition competition, AlexNet. AlexNet had eight layers, the first five of which were convolutional, the next few of which were maxpooling layers, and the final three of which were fully linked. He made use of the non-satiating ReLU activation function, which outperformed Tanh and Sigmoid in terms of exercise performance. The permeability of vacuum has a subscript of zero with subscript formatting, not a lowercase letter, as do other widely used scientific constants [5].

4.3.2. VGG16: One of the convolutional neural network

models that K. Simonyan and A. Zisserman have suggested is VGG16. It is currently one of the best vision model designs available. The most distinctive feature of VGG16 is that it prioritized convolution layers of a 3x3 filter with stride 1 rather than multiple hyper-parameters and consistently employed the same padding and maxpool layer of a 2x2 filter with stride 2 [5].

4.3.3. GoogleNet: Researchers at Google created GoogleNet. It is a deep convolutional neural network with 22 layers that was created as a variation on the Inception Network. It is used for many PC visual tasks like face recognition and identification, adversary preparation, and so forth [5].

4.3.4. ResNet50: Remaining network is referred to as ResNet. Kaiming He, Xiangyu Zhang, Shaoqing Ren, and Jian Sun introduced it in 2015. It is a residual network with 50 layers. Character easy route associations or skip associations that skirt at least one layer are used to address the evaporating slope issue [5].

5. CONCLUSION

Comparing accuracy results of same model i.e., Sequential Model with different number of layers on same number of images, it has been noticed that the model with 10 layers gives us highest accuracy among all i.e., 92%. Hence, we are now clear that CNN Sequential Model can be used for diagnosing presences of tumor using MRI Scans.

ACKNOWLEDGMENT

REFERENCES

[1] L. Nanni, M. Paci, S. Brahnam, and A. Lumini, "Feature transforms for image data augmentation," Neural Comput. Appl., pp. 1–12, Aug. 2022, doi: 10.1007/S00521-022-07645- Z/FIGURES/4.

[2] R. A. Kauppinen and A. C. Peet, "Using magnetic resonance imaging and spectroscopy in cancer diagnostics and monitoring: Preclinical and clinical approaches," Cancer Biol. Ther., vol. 12, no. 8, pp. 665–679, 2011, doi: 10.4161/cbt.12.8.18137.

[3] L. Hou et al., "Positron Emission Tomography Imaging of the Endocannabinoid System: Opportunities and Challenges in Radiotracer Development HHS Public Access," J Med Chem, vol. 64, no. 1, pp. 123–149, 2021, doi: 10.1021/acs.jmedchem.0c01459.

[4] S. S. Roy, N. Rodrigues, and Y. H. Taguchi, "Incremental Dilations Using CNN for Brain Tumor Classification," Appl. Sci. 2020, Vol. 10, Page 4915, vol. 10, no. 14, p. 4915, Jul. 2020, doi: 10.3390/APP10144915.

[5] A. A. Abbood, Q. M. Shallal, and M. A. Fadhel, "Automated brain tumor classification using various deep learning models: A comparative study," Indones. J. Electr. Eng. Comput. Sci., vol. 22, no. 1, pp. 252–259, Apr. 2021, doi: 10.11591/IJEECS.V22.I1.PP252-259.

An IoT-Based Innovus Health Monitoring System*

Khalid Mahmood*

Department of Biomedical Engineering
Hamdard University
Karachi, Pakistan

khalidmalik1120@gmail.com

Nameerah Nafees

Department of Biomedical Engineering
Hamdard University
Karachi, Pakistan

namirahkhan26@gmail.com

Waleed Haider

Department of Biomedical Engineering
University Name
Karachi, Pakistan

walidhyder912@gmail.com

Hareem Shakeel

Department of Biomedical Engineering
Hamdard University
Karachi, Pakistan

hareemshakeel33@gmail.com

Tariq Javid

Department of Biomedical Engineering
Hamdard University
Karachi, Pakistan

tariq.javid@hamdard.edu.pk

Tayyaba Khalid

Department of Biomedical Engineering
Hamdard University
Karachi, Pakistan

tayyaba.khalid@hamdard.edu.pk

Abstract – **In recent days, mainly after Covid-19 spread, the Internet of Things (IoT) is performing a significant part in healthcare systems where health-related data of a patient can be monitored 24/7 remotely. IoT-enabled technologies develop the possibility of designing innovative and non-invasive clinical support systems as it is a crucial part of telemedicine, particularly for COVID-19 patients, where continuous monitoring of vital signs is required. This paper is about the design and prototype of an IoT-based Innovus Health Monitoring System to facilitate sick and older people. For instant results, this system provides the facility to measure vital signs at home in less time. The proposed system consists of two devices Thermometer and Pulse Oximeter, which are assembled and turned into a device. A temperature sensor and heartbeat rate sensor are deployed to determine the temperature and heartbeat rate. Proteus 8 Professional is initially used to simulate these two devices individually and measure the results. After the validation of the simulation, the model is practically implemented by using different sensors with Arduino UNO board, LCD, Wi-Fi module, Alarm and indicators. Finally, all the individual circuits are designed on the breadboard. In addition, two channels for the Heartbeat rate and temperature are created on the ThingSpeak cloud to visualise the real-time transmitted data from the Wi-Fi module. A Wi-Fi connection is required to transmit the information to the ThingSpeak. This data is fetched from the cloud and stored in a spreadsheet. When temperature and heartbeat rate parameters go out of normal ranges, an alarm begins to sound, and LED illuminates. This system also sends an emergency email in case of an alarming situation. Thus, this IoT-based innovus health monitoring system effectively monitors the vital signs of a patient and facilitates both the healthcare system and the patient.**

Keywords – Healthcare, IoT, ThingSpeak, Vital signs, Wi-Fi

I. INTRODUCTION

Health is always a foremost priority in every technological advancement the human race makes. In the past, the fixed-installed system was used for health monitoring, which could only work if the patient was in a hospital or clinic. Recently portable systems have been widely used only in hospitals [1]. But now IoT based systems are used to send patient health-related data to the telehealth systems and doctors. Telehealth is helpful for both the patient and doctor alike because it is cost-effective, low power, time-saving, and easily accessible. Furthermore, patient understanding and participation in data collection can promote healthy habits and interest in pursuing health. After the Covid-19 emergence, telehealth monitoring technology is a better approach to monitoring medical vital signs. As per the need of the hour, a health monitoring system based on IoT is the only prime solution [2]. The paper's primary purpose is to track patient data using a sensor network with minimum contact with the body and the internet to inform telehealth systems in case of any problem. It can reduce healthcare costs by minimizing physician clinic visits, hospitalizations, and diagnosis processes. The sensors' network is linked to a microcontroller that converts the amplified analog data to digital form, processes to interface with LCD and adds an alarm and indicator. It also transmits dynamic and real-time data to ThingSpeak cloud through Wi-Fi simultaneously. The system continuously shows patient status over IoT and indicates the pulse rate and temperature in the cloud visualizations. The normal range of heartbeat rate is in between 60-120 beats per minute (BPM) for healthy people [3]. If there is a sudden deviation in the normal set range of heartbeat or temperature, the system alarms the doctors.

II. LITERATURE REVIEW

A number of researches on the idea of designing a remote healthcare system using IoT in connection with wireless sensors were done in the past as projects or research articles. Few are discussed here.

In the first system, a design was assembled using a microcontroller and a wireless sensor network was made. A heartbeat, temperature, and blood pressure sensor network was used to monitor a patient's vital signs. These parameters were sent to the doctor via GSM. This system had a sensor network, a microcontroller, an LCD, and a GSM device to send information to the physician. Similarly, a GSM module was installed at the

hospital. GSM modem created a connection between the patients and the doctor's servers. LCD was attached to display the result to the patient [4].

In the second system, health parameters were sensed by designing the same monitoring design using GSM and Bluetooth. This system allowed patient blood pressure to be monitored. The health parameter was transmitted directly to the physician using GSM and UTMS. A microcontroller unit was used to read the patient's Tag ID and vital signs. The client's mobile device received real-time data via Bluetooth. Also, these health parameters were directly transmitted remotely to healthcare systems using GSM and wireless technology. This system also stored the previous data [5].

In the third system, two significant vital signs, the heart rate and the body temperature, were monitored by designing a tele-health system using a microcontroller (C8051F0200, Zigbee. The sensors were used to collect data from the body and transfer it to the microcontroller. It was used to transmit the data to the Zigbee module, which could send this real-time data to the healthcare system [6].

An e-health system was designed to monitor the heartbeat rate, blood pressure and body temperature using Microcontroller (AT-Mega 32) and GSM module. Sensor modules collected health parameters from the patient's body and transferred them to the microcontroller. A GSM module was used to send an emergency SMS to the physician if any parameter was out of the normal range [7].

A remote health monitoring system was designed using the heartbeat rate sensor and temperature sensor wired to the Arduino UNO. The Arduino Ethernet module was attached to the Arduino UNO motherboard for internet connectivity. The health data collected by the sensors was transferred to the Arduino UNO board, which transmitted the data to the cloud via the Ethernet module. The health data were obtained from the cloud on the mobile application Blynk where health data was shown in tables, real-time graphs or numeric values [8].

A temperature monitoring system using LM35 and Arduino UNO board was created to track human body temperature. The Arduino board was wired to the sensor to receive the patient data and transmit it to a secure website database [9].

III. WORKING

The IoT-based innovus health monitoring system operates on the principle of monitoring temperature and heart rate. A temperature sensor LM35 and a heartbeat sensor network are used to sense the temperature and heartbeat rate, respectively. These sensors are attached to analog pins of the Arduino Uno board. These sensors convert the physical signals into analog electrical signals, amplified and transmitted to the Arduino board. The Arduino Uno board has a 10-bit ADC that converts analog electrical signals into digital ones. After processing, these values are displayed on LCD and simultaneously transmitted to the IoT system through a Wi-Fi module to analyze the data graphically; ThingSpeak cloud is used to visualize the data in this system. The block diagram illustrates the outline of the system operation in Fig. 1. A Wi-Fi connection is needed to operate this system. Wi-Fi module transmits the real-time data to the ThingSpeak channel by accessing its specific API key. An API key is used to write and read the data from the channels of ThingSpeak. The doctor can track the patient's heartbeat rate and temperature data graphically and numerically from anywhere using a specific API key for the particular channel. If any value deviates from the normal set range of values, an email will be delivered to the physician's desk. The flowchart of the whole model is displayed in Fig. 2.

Fig. 1. Basic Block Diagram of the Proposed Model

Fig. 2. Flowchart of the IoT-Based Health Monitoring System

IV. System Architecture

The prototype system has two primary components: hardware infrastructure and software infrastructure.

A. Hardware Infrastructure

The Hardware Infrastructure of the system has a sensor network with other components for vital operation. Following is the model prototype used here:

Pulse Sensor: The pulse sensor SEN-11574 has three pins, an analog pin, a VCC, and a GND pin, as shown in Fig. 3. It works on the photoplethysmography principle. According to the principle, variations in the blood volume of an organ are calculated by the variations in light intensity transmitted to that organ. This sensor has a light-emitting diode & a light sensor on its first side and amplification with noise cancellation on the second side [10]. The pulse sensor transmits light to the finger and measures the reflected light through a photodiode. The oxygen in the blood haemoglobin can absorb a certain amount of light. The more oxygen in the blood maximizes the absorption rate of light and minimizes the reflection. The change in the amount of reflected light creates an oscillating waveform [11]. The heartbeat rate can be measured by the waveform. The amplitude of this analog waveform is very low and noisy. It is filtered and amplified using an operational amplifier and then read by the Arduino Uno board. The basic principle of the heartbeat sensor is shown in Fig. 4.

Fig. 3. Pulse Sensor SEN-11574 Pin Configuration

Fig. 4. Block diagram of the working principle of the Pulse Sensor

Temperature Sensor: LM35 is an analogue temperature sensor with the pins VCC, GND, and Out as shown in Fig. 5. It operates on temperature ranges of -55° C - 150° C. The output

of LM35 changes by 10 mV to every centigrade, increase decrease in temperature and is proportional to the change [12]. It can be operated on a 5 V or 3.3 V source voltage.

Fig. 5. Pin Configuration and working principle of LM35 Sensor

Wi-Fi Module: Wi-Fi transmitter ESP8266, is a microcontroller developed by Espressif Systems. It can perform Wi-Fi-related tasks, e.g., WIFI transmitter. Here it is wired to the transmitting (Tx) and receiving (Rx) pins of the Arduino board shown in Fig 6. AT commands check data transmission from Arduino to ESP01 [13].

Fig. 6. Pin Configuration of ESP8266-01 WiFi Module

Arduino UNO Board: It is a microcontroller with 14 digital pins (input/output), from which 6 pins are PWM output supported. It has 6 analog inputs (A0 to A5), as shown in Fig. 7. to read analog data. It has a 10-bit built-in ADC to differ 1024 analog values. It has 16 MHz clock frequency [14].

Fig. 7. Pin Configuration of Arduino Uno Board

B. The Software Infrastructure

It includes Integrated Development Environment (IDE), Proteus software and the ThingSpeak cloud by MATLAB.

Integrated Development Environment: IDE is a valuable tool for researchers, programmers, and project development experts to create projects with sensors. The Arduino IDE is a commonly used Integrated Development Environment that is freely accessible and designed for programming and wiring projects. IDE has features like finding and switching, cutting-pasting, automated programming and indentation. It can compile and upload the code to an Arduino Uno board. C and C++ languages are used to code in Arduino IDE [15].

Setting the ThingSpeak: ThingSpeak is a cloud-based platform that allow users to collect, analyse, and visualize data from Internet of Things (IoT) systems. It gives the user-friendly interface for IoT applications. Using ThingSpeak, developers can easily create real-time dashboards that display critical health metrics and alerts, making it an ideal platform for remote patient monitoring and other healthcare applications [16]. In this paper, it is used to collect and store data from health sensors such as heart rate and temperature monitors. It obtains the data from the sensor's network connected to the Arduino UNO through a Wi-Fi module. Data can be analysed and visualized using its built-in tools.
a) Link for ThingSpeak (https://thingspeak.com)
b) Created an account.
c) Then created a channel and made Field1 as temperature and Field2 for Heart Rate shown in Fig. 8.

Fig. 8. Channel Creation in the ThingSpeak Cloud

d) API key is generated as shown in Fig. 9. which is used for reading and writing data to the cloud.
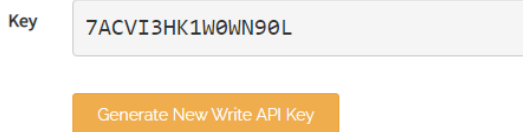
Fig. 9. Generating API Key to Write Data to the ThingSpeak

e) Used this API key in the code to write the data to the specific channel created in ThingSpeak. The code is uploaded to an assembled circuit with Arduino Uno. It will start transmitting the data through Wi-Fi [17].

Proteus Circuit Simulation: Proteus is a software tool that provides a virtual environment for designing, simulating, and testing electronic circuits. Proteus includes a library of pre-built components, such as sensors, microcontrollers, and communication modules, that can be easily dragged and dropped into a circuit design [18]. It can test the functionality and performance of the health monitoring system. In this paper, Proteus 8.12 Pro is used to simulate the circuitry and connectivity of the sensors, Arduino UNO, Wi-Fi module, alarms, LEDs and LCD display that are used in the system. The pulse sensor and LM35 temperature sensor are used with Arduino UNO board and other components are wired according to the model. The simulation is run using Proteus 8.12 Professional, and simulated results are obtained. as shown in Fig. 10.
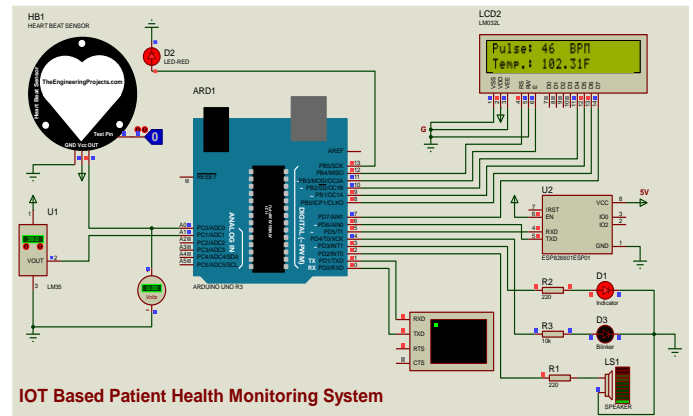
Fig. 10. Proteus Simulation of the combined circuit with results

Proteus Serial Monitor: It shows the simulated results of the pulse and temperature sensors were obtained by simulating the designed software model, as shown in Fig. 11.
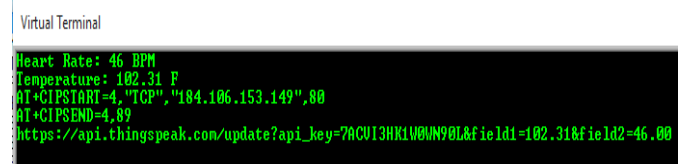
Fig. 11. Simulated results on proteus serial Monitor

Arduino IDE Serial Monitor: It also displays the results, obtained through the designed hardware prototype being used, as shown in the Fig. 12.

Fig. 12. Hardware results on Arduino Serial Monitor

Code Flowchart:
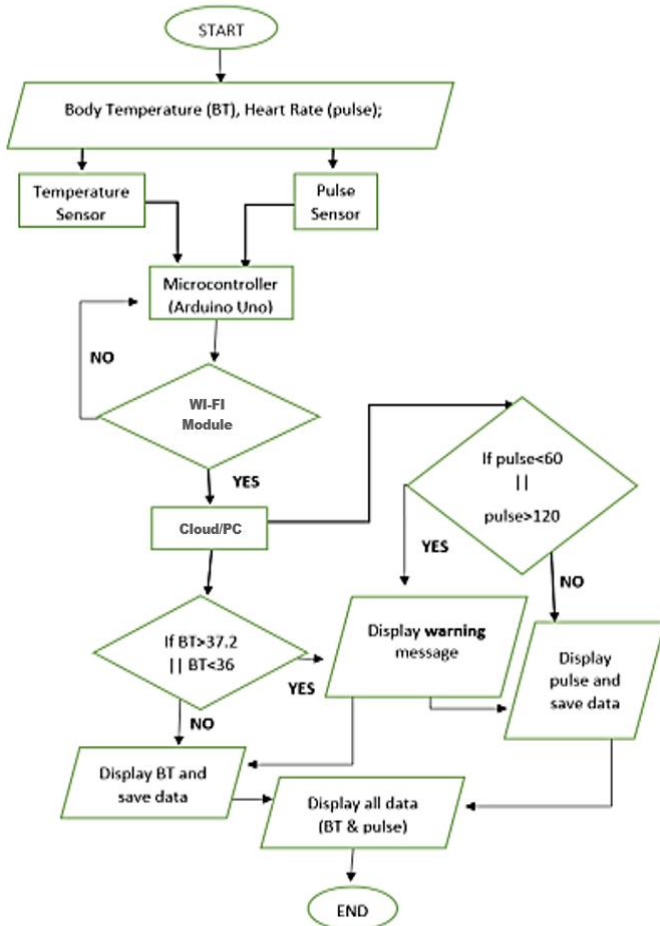
Fig. 13. Code Flowchart of the IoT-Based Health Monitoring System

V. HARDWARE PROTOTYPE

The hardware prototype for the proposed design has sensors, Arduino UNO board, LCD, a Wi-Fi module, an alarm, and indicators. All the connections made in the sensors, Arduino board, and other components (LCD, Wi-Fi module, alarms, indicators, and power supply) are visible in Fig. 14.
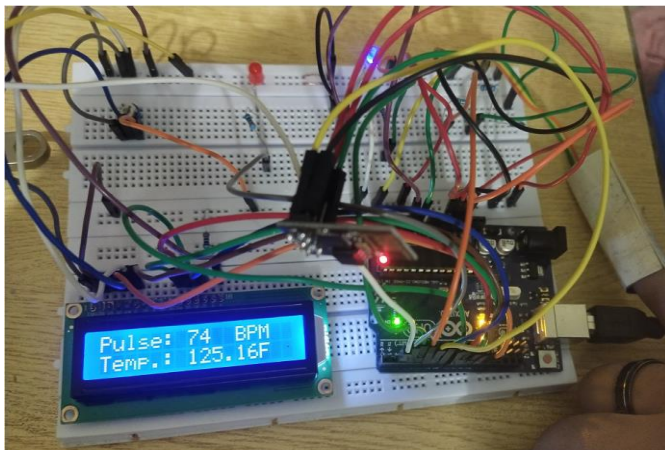
Fig. 14. Designed Hardware Prototype being used

VI. RESULT AND DISCUSSIONS

The collected results from the model are attached below. The microcontroller receives the data from the heart and temperature sensors. It transmits via the Wi-Fi Module to the ThingSpeak cloud to monitor the individual's health in real-time. The data is received after every 30 seconds through a Wi-Fi transmitter. If any abrupt changes or the values of the parameters deviate from the normal ranges, then an alarm would be sent off to the custodian and the doctor. Collected values from each of the sensors were stored and accessed by the ThingSpeak cloud server is attached here.

A. Analysis of Body Temperature on ThingSpeak

When the patient was monitored in different situations, pattern of the body temperature alterations in real time is shown in Fig. 14. When the patient was active and stressed; the temperature started to go high. When the patient was at rest and relaxed, the body temperature started to go low to its optimum value. When any data value deviated from the normal range of 97-99 F, the system identified it and sent an email to the doctor. Fig. 15. displays the last body temperature value in pie chart format, and Fig. 16. displays the current body temperature value in numeric quantity.
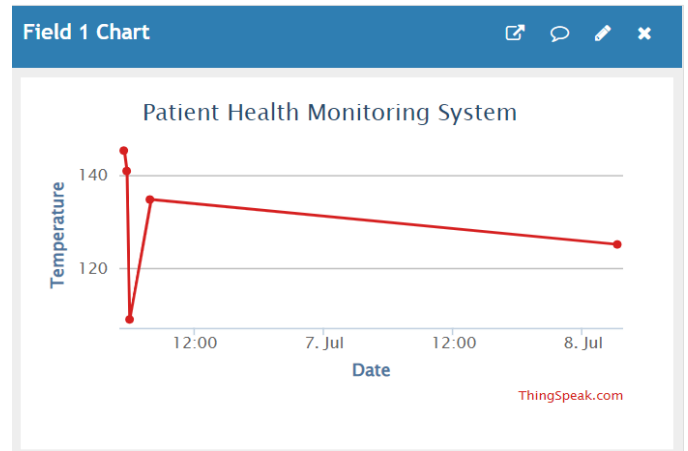
Fig. 14. Chart format of real-time values of Body Temperature
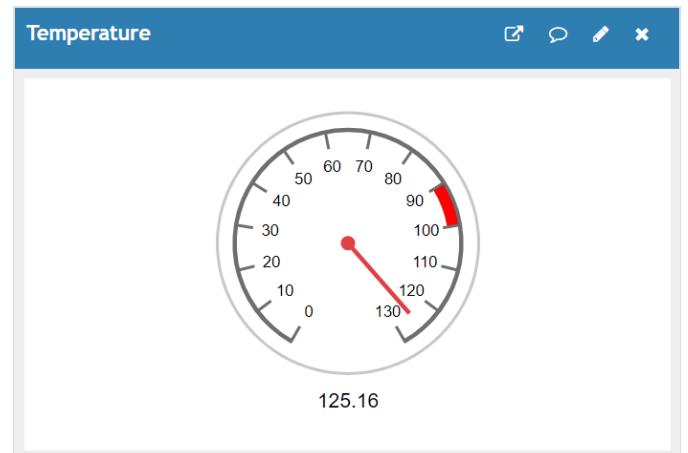
Fig. 15. Pie Chart of body temperature value in Fahrenheit
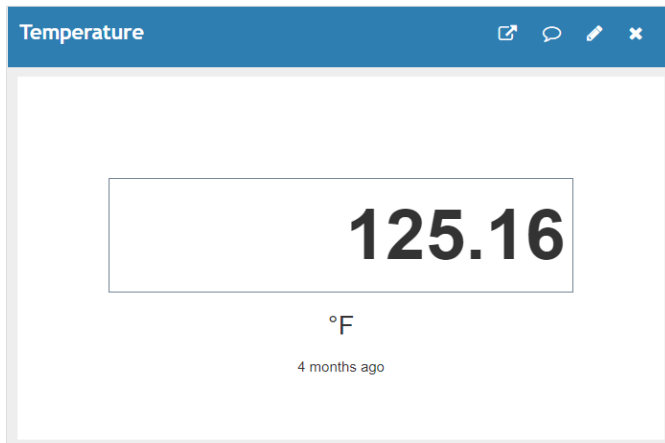
Fig. 16. Numeric value of body temperature in Fahrenheit

B. Analysis of Heartbeat Rate on ThingSpeak

When a patient was monitored under different conditions, pattern of the heartbeat rate alterations in real time is shown in Fig. 17. Heartbeat rate started to go high when the patient was active and stressed. Heartbeat rate started to go low to its normal value when the patient was at rest and relaxed. When any value deviated from the normal range of 60-100 BMP, the system identified it and sent an email to the doctor. Fig. 18. shows the last value of the heartbeat rate in pie chart format, and Fig. 19. shows the current value of heart rate in numeric quantity.
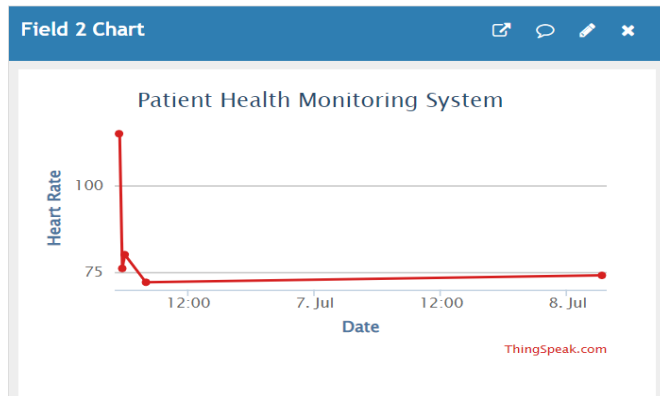
Fig. 17. Chart format of real-time values of heartbeat rate
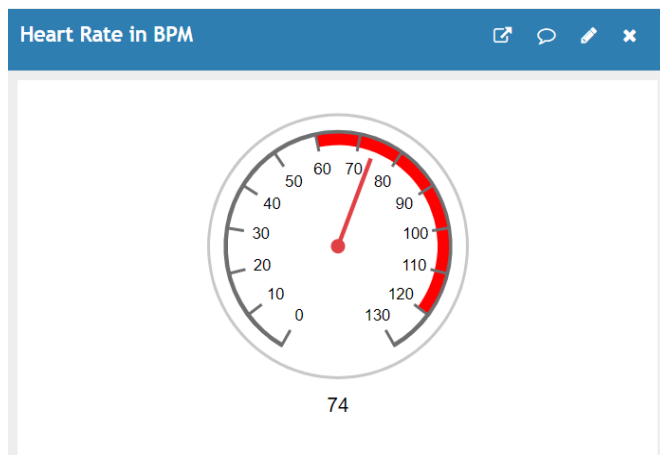
Fig. 18. Pie chart of heartbeat rate in BPM

Fig. 19. Numeric data of heartbeat rate in BPM

VII. CONCLUSIONS

In this paper, an IoT-based prototype for telehealth monitoring has been proposed. The proposed system efficiently monitors patients' real-time vitals data like body temperature and heartbeat rate at home or remotely from anywhere using internet connectivity. It informs the custodians and the doctors about the health status of their patients. The system is low-power and cost-effective, lessening hospital burden by reducing the visits and minimizing the patient's time.

VIII. FUTURE SCOPE

Although the design is a valuable and cost-effective tool for telehealth services, it may be improved to be more efficient. The future scope of the design can be a multipara meter patient monitor to measure additional vital signs, e.g., ECG, glucose level, blood pressure, and respiration rate and transmit it to any other better and safer cloud such as Arduino Cloud, Google Cloud, or Microsoft Azure. Contactless sensors can be used to improve future design.

REFERENCES

[1]. Bhardwaj, Vaneeta, Rajat Joshi, and Anshu Mli Gaur. "IoT-based smart health monitoring system for COVID-19." *SN Computer Science* 3, no. 2 (2022): 137.

[2]. Valsalan, Prajoona, Tariq Ahmed Barham Baomar, and Ali Hussain Omar Baabood. "IoT based health monitoring system." Journal of critical reviews 7, no. 4 (2020): 739-743.

[3]. Ahmed, Mobyen Uddin, Mats Björkman, Aida Čaušević, Hossein Fotouhi, and Maria Lindén. "An overview on the internet of things for health monitoring systems." *Internet of Things. IoT Infrastructures: Second International Summit, IoT 360° 2015, Rome, Italy, October 27–29, 2015, Revised Selected Papers, Part I* (2016): 429-436.

[4]. Mahalle, S. M., and P. V. Ingole. "Design and implementation of wireless body area sensor network-based health monitoring system." *International Journal of Engineering Research & Technology* 2, no. 6 (2013): 105-113.

[5]. Gajare, Mansi Mhalsakant, Manas A Dani, Payal D Deshmukh, and Pritesh Chaudhari. "IOT Based Health Monitoring System." ResearchGate, January 4, 2021.

[6]. Malhi, Karandeep, Subhas Chandra Mukhopadhyay, Julia Schnepper, Mathias Haefke, and Hartmut Ewald. "A zigbee-based wearable physiological parameters monitoring system." *IEEE sensors journal* 12, no. 3 (2010): 423-430.

[7]. Jain, Nitin P., Preeti N. Jain, and Trupti P. Agarkar. "An embedded, GSM based, multiparameter, realtime patient monitoring system and control—An implementation for ICU patients." In *2012 World Congress on Information and Communication Technologies*, pp. 987-992. IEEE, 2012.

[8]. Kaur, Amandeep and Ashish Jasuja. "Cost Effective Remote Health Monitoring System Based on IoT Using Arduino UNO." (2017).

[9]. Mansor, Hasmah, Muhammad Helmy Abdul Shukor, Siti Sarah Meskam, Nur Quraisyia Aqilah Mohd Rusli, and Nasiha Sakinah Zamery. "Body temperature measurement for remote health monitoring system." In *2013 IEEE International conference on smart instrumentation, measurement and applications (ICSIMA)*, pp. 1-5. IEEE, 2013.

[10]. Arora, Jatin, Amandeep Singh, Narinder Pal Singh, Sarvesh SS Rawat, and Gurvinder Singh. "Heartbeat rate monitoring system by pulse technique using HB sensor." In *International Conference on Information Communication and Embedded Systems (ICICES2014)*, pp. 1-5. IEEE, 2014.

[11]. Yuen, Man-Ching, Shin Ying Chu, W. Hong Chu, H. Shuen Cheng, H. Lam Ng, and S. Pang Yuen. "A low-cost IoT smart home system." *Int. J. Eng. Technol* 7, no. 4 (2018): 3143-3147.

[12]. Oyebola, Blessed, and Odueso Toluwani. "LM35 Based digital room temperature meter: a simple demonstration." *Equatorial Journal of Computational and Theoretical Science* 2, no. 1 (2017).

[13]. Shekhar, J., D. Abebaw, M. A. Haile, M. A. Mehamed, and Y. Kifle. "Temperature and heart attack detection using IOT (Arduino and ThingSpeak)." *International Journal of Advances in Computer Science and Technology* 7, no. 11 (2018): 75-82.

[14]. Badamasi, Yusuf Abdullahi. "The working principle of an Arduino." In *2014 11th international conference on electronics, computer and computation (ICECCO)*, pp. 1-4. IEEE, 2014.

[15]. O. E. Amestica, P. E. Melin, C. R. Duran-Faundez and G. R. Lagos, "An Experimental Comparison of Arduino IDE Compatible Platforms for Digital Control and Data Acquisition Applications," 2019 IEEE CHILEAN Conference on Electrical, Electronics Engineering, Information and Communication Technologies, 2019, pp. 1-6.

[16]. Jebane, P., P. Anusuya, M. Suganya, S. Meena, and M. Diana. "IoT based health monitoring and analysing system using Thingspeak Cloud & Arduino." *Int. J. Trendy Res. Eng. Technol* 5 (2021): 1-6.

[17]. M. A. A. Razali, M. Kassim, N. A. Sulaiman and S. Saaidin, "A ThingSpeak IoT on Real Time Room Condition Monitoring System," 2020 IEEE International Conference on Automatic Control and Intelligent Systems (I2CACIS), 2020, pp. 206-211.

[18]. Fan, Chengcheng, Xiang Liu, Ronghua Ling, and Boyu Si. "Application of Proteus in experimental teaching and research of medical electronic circuit." In *2018 3rd International Conference on Modern Management, Education Technology, and Social Science (MMETSS 2018)*, pp. 512-515. Atlantis Press, 2018.

Simulation of Suitable Carbon Nanotube as a Drug Delivery System: A Molecular Dynamics Study

Muhammad Jawad Shafique[1]
Biomedical Engineering
Sir Syed University of Engg. & Tech.
Karachi, Pakistan
Ziauddin University, Karachi, Pakistan
jawad.shafique@zu.edu.pk

Muhammad Usman Baig[2]
Biomedical Engineering
Sir Syed University of Engg. & Tech.
Karachi, Pakistan

baigmuhammadusman@gmail.com

Mariam Raziq[3]
Biomedical Engineering
Sir Syed University of Engg. & Tech.
Karachi, Pakistan

mraziq@ssuet.edu.pk

Syed Faraz Jawed[4]
Biomedical Engineering
NED University of Engineering and Technology
Karachi, Pakistan
farazjawed@neduet.edu.pk

Abstract: A significant use of nanotechnology is preferred in drug delivery systems, especially in the case of targeted delivery of anti-cancer drugs using carbon nanotubes (CNTs). Molecular dynamics (MD) simulations have been used to study the anti-cancerous carbon nanotubes drug delivery system that supports single-walled carbon nanotubes (SWCNTs), including pristine SWCNTs. Important geometries and properties have also been identified. In contrast to complex states with SWCNT, however, no appreciable change in drug structure is seen in the free form. One promising strategy for achieving controlled drug release involves placing carboplatin within the pristine nanotubes at the tube's tip. When the drug moved outside of the pristine SWCNT, it typically moved down the end to about a third of the tube's length, but the group of carboxylics on the functionalized SWCNT held the drug in the tube's midline. It has also been found that the binding free energy of carboplatin in the SWCNT is the lowest of all the possible binding free energies due to van der Waals interactions. Thus, the molecular dynamics study supports, in contrast to earlier experimental findings, that pristine SWCNTs are the optimal CNT for an anticancer drug delivery system.

Keywords—molecular dynamics, carbon nanotubes simulation, drug delivery system

I. INTRODUCTION

Cancer is on the rise nowadays. In cancer detection and treatment, carbon nanotubes (CNTs) have become a prominent tool because of their unique physical-chemical features [6]. So far, they have been regarded as one of the most promising nanomaterials for identifying malignant cells as well as delivering medications or tiny therapeutic compounds to these cells. Photothermal therapy (PTT) and photodynamic therapy (PDT) have also been employed to directly kill cancer cells by the application of these carbon nanotube mediators [2]. For a more molecular grasp on carbon nanotubes, carbon nanotubes (CNTs) have gained interest among researchers who are considering them as a drug delivery system. CNT's size, shape, and surface properties make it an ideal drug delivery vehicle. CNT's surface charge, the chemistry of the surface, and ability to cross biological barriers within the body have also made it an intriguing cancer therapeutic and diagnostic tool. CNT can permeate biological tissues because of its tiny size [4]. CNTs have now also become ideal for transporting medicines, proteins, and vaccines because of their mobility and excellent penetration [4, 5]. CNT's large surface area makes it easy to

modify the surface's properties and make them more useful. It can have pharmaceutical substances loaded on or inside its surface [1].

The word "cancer" refers to a wide range of disorders where cells proliferate uncontrollably [8]. Each form of cancer has a distinct nomenclature depending on the type of tissue from which the cell arises [4]. There are approximately 200 different types of cancer. For a large number of cancer patients, death is caused by the systemic consequences of metastases in distant organs rather than the primary tumour itself. Preventing metastasis as early as possible is one of the goals of cancer treatment [3]. Current clinical trials and recent advancements in biotechnology add confidence to nanotechnology's ability to aid in the battle against cancer. Many different types of nanomaterials, such as carbon nanotubes, have unique features that may be used for a variety of applications, including cancer diagnostics, thermal ablation, and medication administration [6]. Tubular CNTs with widths in the nanometer range have unique features that may be used in the detection and treatment of cancer. It is also possible to deliver medications directly to the cells and tissues that need them. The toxicity of nanoparticles must be studied alongside the fast advancements in the production of nanotechnology-based technologies. Since CNTs may be used as therapeutic platforms in cancer, this research will focus on the biological uses of CNTs [7].

The main objective of the study is to study the molecular dynamics of carbon nanotubes as a drug delivery system.

II. METHODOLOGY

A. Setting Modular Framework for Simulation

The COMPASS (condensed-phase-optimized molecular potentials for atomistic simulation studies) force field will be used in the Forcite module of the Materials Studio 8.0 software to assign potentials and charges to each atom, which is proven to forecast the condensed properties and structural units of carbon nanotubes precisely.

B. Material Procedure for further Simulation

At 300K, the method of Verlet integration will be used with the integrative steps of velocity and Maxwell-Boltzmann random starting velocity distributions to maintain the system

under the canonical ensemble. This trend of the system works under potential energy, which shows the equilibrium. Every 10,000 steps, the frame is produced, and the atomic trajectories are stored to display behaviour progression. An atom-based summing approach for Van der Waals interactions with a cut-off distance of 15.5 nm will be utilized for Van der Waals interactions, while another method, i.e., Ewald, will be used for long-range electrostatic interactions.

It is necessary to set the 3-dimensional Cartesian coordinates of SWNTs in order to simulate non-covalent modification by following the track of H2O molecules and the development of SDS behaviour near SWNTs. In order to avoid the 3-dimensional periodic boundary conditions between M-SWNTs and SiO2 (1 0 0), another vacuum slab with a thickness of thirty is put on top of the M-SWNTs after they have been transferred onto F-surfaces for the self-assembly simulation. M-SWNTs are composed of SWNTs and SDS molecules, whereas F-surfaces are made up of 60 silane molecules and 60 SiO2 cells with 11 layers of thickness.

III. RESULTS

Simulations using the standard (60,0) SWCNT model will show encouraging results so far. However, additional CNT (m, n) and length simulations need to be done before a final conclusion can be drawn about Young's modulus at 1.4 TPa. If 1-2, 1-3, and 1-4 atom interactions are not switched off or weighted, then the comparatively high Young's modulus may be owing to this fact. Bond length computations using LAMMPS commands or independent code that uses LAMMPS output to determine bond length could be included in future simulations, helping to better understand failures in systems with weighted atom interactions.

The limitations of the study are huge research gap in past 10 years, software 'temp' errors, codeworks, inaccuracy in maintaining geometries (software configuration default), and variable results due to featured functions/features.

IV. DISCUSSION

The usage of nanotechnology in drug delivery systems is ideal, particularly in the context of targeted delivery of anti-cancer drugs using carbon nanotubes [8]. The anti-cancerous carbon nanotubes drug delivery system that supports single-walled carbon nanotubes, including pristine SWCNTs, has been studied using molecular dynamics simulations [9]. In contrast to complex states with SWCNT, however, there is no discernible change in drug structure in the free form. Carboplatin's binding free energy in SWCNT was also discovered to be among the lowest of all possible binding free energies due to van der Waals interactions. In contrast to previous empirical evidence, the molecular dynamics study supports the idea that pristine SWCNTs are the best CNT for an anticancer drug delivery system [10]. CNTs have been determined to be a reliable drug delivery system for the treatment of cancer. Because of their unique attributes, they have generated intense interest in the field of targeted drug delivery for cancer treatment. However, when

compared to pristine CNT, basic CNT has not been shown to be beneficial in cancer prevention [10]. Because of their natural geometrical properties, they are not only useful as drug carriers for transporting a variety of anticancer cancer drugs but also as phototherapy mediators.

A. Obtained Geometries

To achieve the ideal outcomes, the rate of Young Modulus should be justified accordingly. The obtained geometries for CNTs before simulation have been shown in Fig 1, 2, and 3.
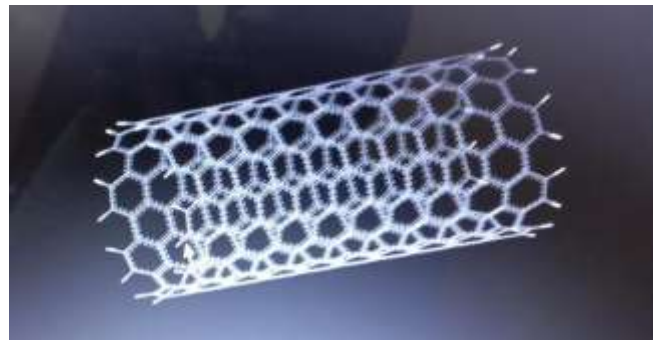
Fig. 1. CNT Geomertical Optimisation
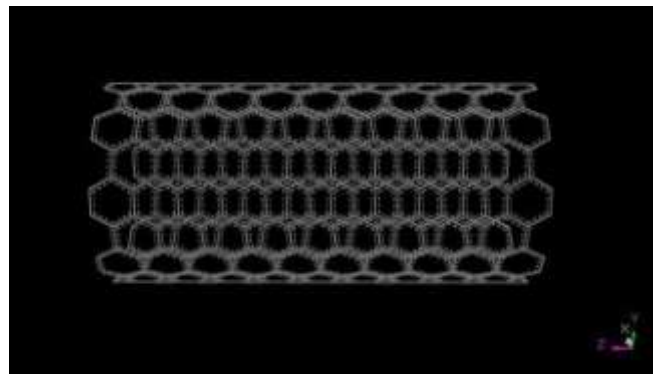
Fig. 2. CNT Geomertical Optimisation (with pre-set dimensions)
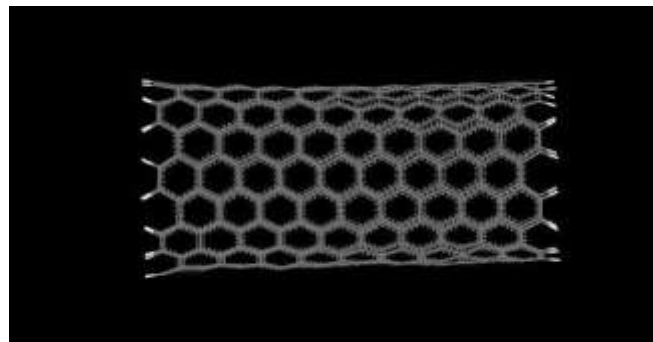
Fig. 3. CNT Geomertical Optimisation (with final placement)

TABLE I.   TABLE TYPE STYLES

Material Input	Geometries with Properties		
	CNT	Pre	Post
YM	Basic CNT	0.9	1.1

Material Input	Geometries with Properties		
	CNT	Pre	Post
YM2	Pristine CNT	1.3	1.4

Table 1. Magnitude of CNTs

CONCLUSION

It has been concluded that CNTs are a proven drug delivery system for treating cancer. Because of their unique characteristics, they have attracted much research in the field of targeted drug delivery for cancer treatment. However, as compared to pristine CNT, basic CNT has not been shown to be beneficial in preventing cancer's spread. Because of their natural geometrical properties, they are not only useful as drug carriers for transporting a wide range of anticancer cancer drugs but also make for good mediators in phototherapy.

REFERENCES

[1] Li, S., Sajadi, S. M., Alharbi, K. A. M., El-Shorbagy, M. A., & Tlili, I. (2022). The molecular dynamics study of vacancy defect influence on carbon nanotube performance as drug delivery system. Engineering Analysis with Boundary Elements, 143, 109-123.

[2] Zhang, L., Peng, G., Li, J., Liang, L., Kong, Z., Wang, H., ... & Shen, J. W. (2018). Molecular dynamics study on the configuration and arrangement of doxorubicin in carbon nanotubes. Journal of Molecular Liquids, 262, 295-301.

[3] Chaban, V. V., Savchenko, T. I., Kovalenko, S. M., & Prezhdo, O. V. (2010). Heat-driven release of a drug molecule from carbon nanotubes: a molecular dynamics study. The Journal of Physical Chemistry B, 114(42), 13481-13486.

[4] Wang, J., Dong, H., Leng, T., Yu, Y., & Li, Y. (2022). Turning the structure of the Aβ 42 peptide by different functionalized carbon nanotubes: a molecular dynamics simulation study. Physical Chemistry Chemical Physics, 24(7), 4270-4279.

[5] Seif, M., & Montazeri, A. (2022). Molecular dynamics simulation reveals the reliability of Brij-58 nanomicellar drug delivery systems for flurbiprofen. Journal of Molecular Liquids, 119496.

[6] Lobato, J. C. M., da Silva Arouche, T., Del Nero, J., Andrade Filho, T., dos Santos Borges, R., & Neto, A. M. D. J. C. (2022). Interactions between carbon nanotubes and external structures of SARS-CoV-2 using molecular docking and molecular dynamics.

[7] Alexiadis, A., & Kassinos, S. (2018). Molecular simulation of water in carbon nanotubes. Chemical reviews, 108(12), 5014-5034.

[8] Ivanovskii, A. L. (2020). Non-carbon nanotubes: synthesis and simulation. Russian chemical reviews, 71(3), 175-194.

[9] Du, Y., Zhou, T., Zhao, C., & Ding, Y. (2022). Molecular dynamics simulation on thermal enhancement for carbon nano tubes (CNTs) based phase change materials (PCMs). International Journal of Heat and Mass Transfer, 182, 122017.

[10] Von Ranke, N. L., Castro, H. C., & Rodrigues, C. R. (2022). Molecular modelling and dynamics simulations of single-wall carbon nanotube as a drug carrier: New insights into the drug-loading process. Journal of Molecular Graphics and Modelling, 113, 108145.

Critical Thinking and Problem Solving Intelligent Agent for High-Precision Simulated Image-Guided Cardiac Interventions

Faisal Mujtaba

Dept. of Biomedical Engineering
Faculty of Engg. Sci. and
Technology Hamdard University
Karachi, Pakistan

faisalmujtaba29@gmail.com

Sumaiya Aziz

Dept. of Biomedical Engineering
Faculty of Engg. Sci. and
Technology Hamdard University
Karachi, Pakistan

sumaiyaaziz91@gmail.com

Ayesha Hasany

Dept. of Biomedical Engineering
Faculty of Engg. Sci. and
Technology Hamdard University
Karachi, Pakistan

ayesha.hasany99@gmail.com

Tariq Javid

Dept. of Biomedical Engineering
Faculty of Engg. Sci. and
Technology Hamdard University
Karachi, Pakistan

tariq.javid@hamdard.edu.pk

Muhammad Faris

Dept. of Biomedical Engineering
Faculty of Engg. Sci. and
Technology Hamdard University
Karachi, Pakistan

m.faris@hamdard.edu.pk

Jawwad Sami

Dept. of Biomedical Engineering
Faculty of Engg. Sci. and
Technology Hamdard University
Karachi, Pakistan

jawwad.rehman@hamdard.edu.pk

Abstract— This research is to incorporate an intelligent agent in cardiac coronary intervention simulator for critical thinking and problem solving. The simulator is an incorporated hardware and software program system. The learner makes use of a catheter wire to carry out the preferred intervention. The use of an embedded system records the catheter wire actions. The measured values are then communicated to the software program that animates the catheter function in the computer simulation. The problem solving agent identifies the problem in order to solve it and critical thinking agent determines how to solve the problem during a cardiac intervention procedure. The software program intervention module has different alternatives. These alternatives are both, to amplify the coronary artery or stent application. The animation suggests the entire coronary intervention's overall performance once the user selects the desired option].

Keywords— *Precision, cardiac interventions, medical simulators, cardiac catheterization, image-guided interventions.*

I. BACKGROUND

Computer simulation has been adopted by the medical community, due to the complex nature of human body and difficulty in experimentation based approaches. Owing to this, much progress has been made in the medical industry toward computer simulation and especially for surgical training systems. The aim of this research work is to add into the existing body of research literature a new theme, that is, artificial intelligence in surgical simulators. There are highlights similar contributions that simulation has made to the study of different physiological systems over the past few years. Simulation based studies show an ease adoption to investigate the problem. In [2], the project was a modified version of a simulator and described the layout and improvement of a medical simulator for the cause of cardiac surgical treatment training. The authors have studied the available contemporary model to layout the expansion of a cardiac intervention simulator for plaque elimination via coronary expansion and stent placement tasks.

The catheter movement is measured through infrared (IR) sensors which are interfaced with the embedded system, that is, an Arduino UNO board. This constitute the hardware part of the simulator used in this research work. This embedded system measures the length of wire during movement. The recorded values are then communicated to the software part which is coded in the Python language. The communication among both parts of the simulator is established through a Universal Serial Bus (USB) cable.

The purpose of coronary intervention simulator is to train the cardiac surgeons at the beginner level to use catheter wire in order to perform the tasks of plaque removal [1]. The previous project provided great assistance in this breakthrough technique of performing cardiac simulations and with the modification the performance will get more precise and give desired output.

As the medical science is getting advanced day-by-day, there is a dire need for more advance technologies which can perform tasks with an acceptable level of precision and accuracy. In this case, there exists high risks and chances of errors. To overcome the problem a realistic computer-based training system that includes hand-eye coordination, catheter and guided-wire choices, three-dimensional anatomic representations, and an integrated learning system are designed, in order to permit learning to occur safely, without putting patients at risk [3]. Many commercial simulators are available in the market which can perform such tasks, one such example is Mentice software and hardware. These simulators are scientifically validated and have been specifically developed for healthcare providers [4]. The most commonly used simulator is Mentice VIST-G7, See Fig. 1.

Fig. 1. Mentice Simulator

Cardiac interventions refer to a broad term of clinical procedures, practices and activities done by cardiologists to prevent heart diseases and treat cardiovascular diseases. Cardiac interventions primarily involve the application of catheters for the process. Catheters enable cardiac surgeons view human heart through minimal invasive method. Catheters pave way to examine various heart conditions and to check for plaque deposition in veins or arteries. Cardiac interventions are non-surgical and mostly non-invasive. Some of the cardiac interventions include heart valve surgery, angioplasty, catheter ablation, bypass operation, stent placement, etc., See Fig. 2.
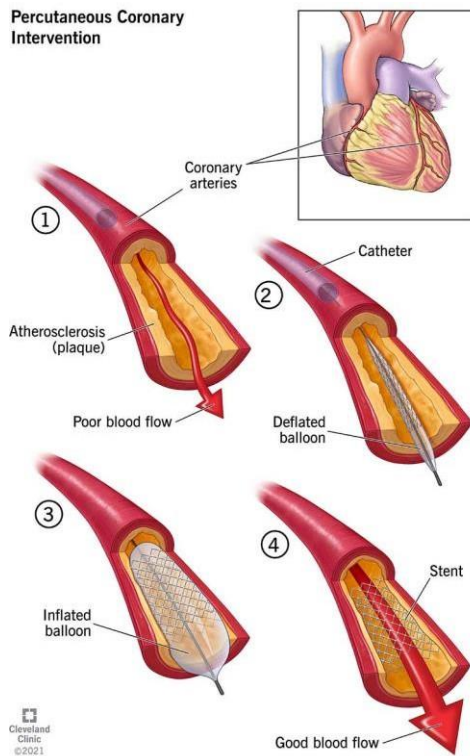
Fig. 2. Cardiac intervention including angioplasty and stent placement [5]

The most common heart diseases occur due to deposition of fat in blood vessels causing plaque deposition which leads to narrowing and hardening of blood vessels of heart. As a result, heart is unable to pump blood efficiently. This leads to heart attack in severe cases. So the most common intervention for this domain is angioplasty which removes plaque from blood vessels ensuring proper blood flow through heart. The other most common intervention is stent placement. When the heart vessel is constricted due to some reasons such as a prior plaque deposition, a stent is placed insuch blood vessel so that it might not constrict and block theflow of blood. These two interventions are the basis of this project and enables medical professionals in gaining expertise in this.

In critical thinking agents a problem is defined. A logic is applied related to the problem. The issues are defined and situation evaluated using the logic. Previous experiences are used in this process. A decision is made using logic and evaluation. Finally, the decision is updated and performance is made, See Fig. 3.

In problem solving agents, a problem is first defined. The problem faced by agent is guided towards dictionary. The possible solution for the problem is looked into the dictionary. That solution is applied and checked whether the problem is solved or not, See Fig. 4.
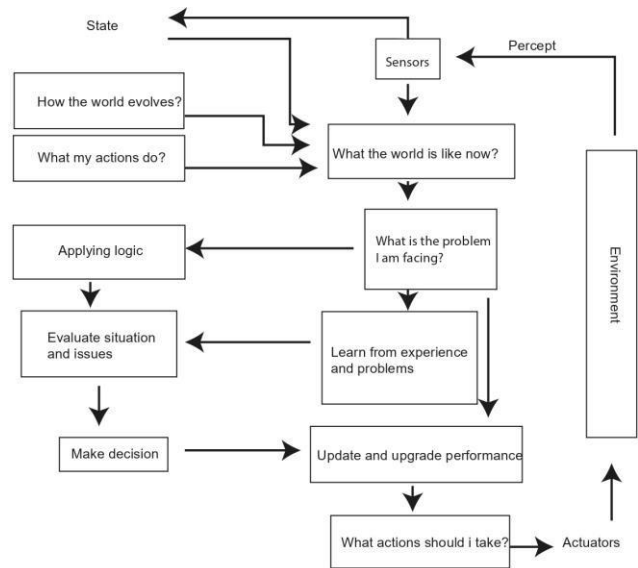
Fig. 3. Block diagram of critical thinking intelligent agent
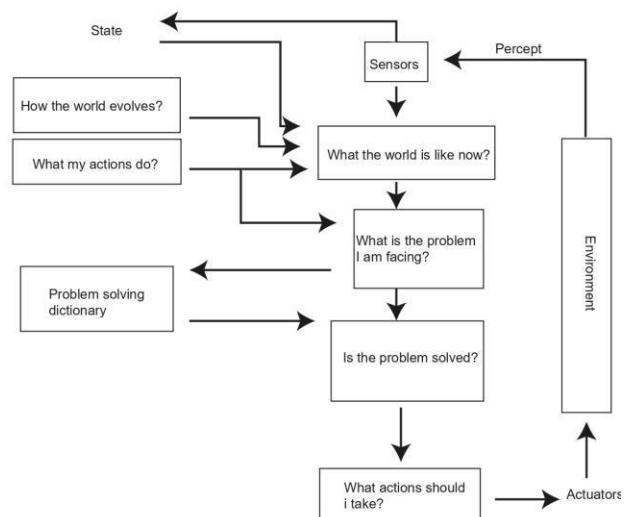
Fig. 4. Block diagram of problem solving intelligent agent

Precision refers to the closest possible results taken at different times. When a system produces similar outcomes at multiple iterations, then the system is said to be precise. Medical equipment requires the best precision due to its implementation for people's health. The cardiac intervention simulator must be exact to allow the catheter to move seamlessly through the blood vessels toward the heart, See Fig. 5.
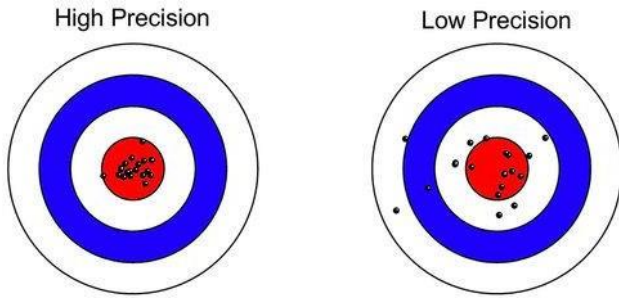
Fig. 5. The depiction of precision [9]

In this project precision is checked by two steps. Firstly, an ideal iteration of cardiac intervention will be performed on simulator via cardiac catheter which will be set as astandard. Then as we perform further iterations these values will go to database and compared with standard. The closer the performed value is to standard; a higher precision will be achieved.

II. METHODS

This project is done by doing a thorough research on cardiac interventions, medical simulators and intelligent agents. This process is extension of project 'Cardiac catheterization simulator [6]. A hardware model is made in which the motion of catheter is identified by embedded system and simulated images of the cardiac intervention process are generated. The intelligent agents are introduced in such a way that whenever a problem arises, it is identified by problem solving agent and critical agent then uses critical thinking in order to mitigate that problem. In this way, high-precision images are obtained and intervention is performed through intelligent agents.

A. Hardware Configuration

The hardware has to be simulated beforehand to evaluate and rectify the results. The aim is to get as precise results as possible to gain realistic outcomes. The movement of the inserted catheter will be sensed via multiple infrared sensors interfaced with the Arduino Mega board. Similarly, with the help of the encoded system, the sensors will measure the length of the catheter. They will forward the data to the software part for further processing to obtain visual results.

B. Software Composition

The coding has to be in Jupyter notebook to facilitate Python language. The data collected in the hardware will be received by software through a graphical user interface to animate the movement of the catheter and show the simulated results on display.
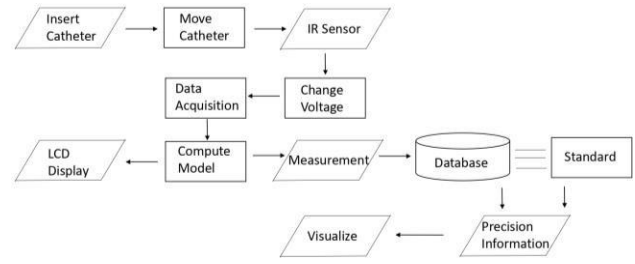
Fig. 6. Block diagram of the process

This block diagram in Fig. 6 summarizes the whole process of cardiac intervention which is performed in the project. The insertion of catheter is detected by IR sensor whose signal is processed by Arduino and finally images of the process are obtained. The database stores the data and compares it with standard to ensure maximum precision [6].

C. Verification and Validation of Image-Guided Interventions

Verification is the checking and confirmation a process. It is the mechanism used during the process of research to contribute to ensuring reliability and validity. Verification is the extent to which a concept is accurately measured in a quantitative study [7], See Fig. 7.
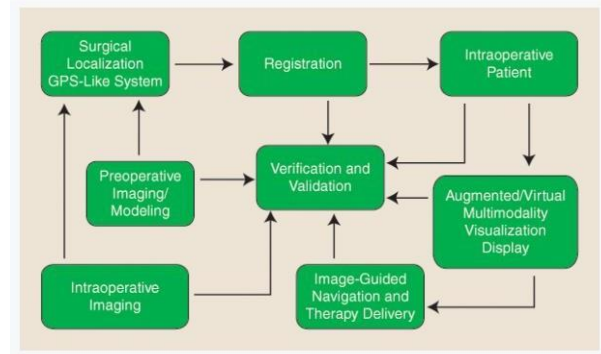
Fig. 7. Verification and validation of image-guided interventions [8]

D. Incorporation of Critical Thinking Agents And Problem Solving Agents

In critical thinking agents a problem is defined first. The system identifies the problem. A logic is applied related to the problem. The issues are defined and situation evaluated using the logic. The system does critical thinking in three ways. In first approach, the intelligent agent does no thinkingon its own, instead it uses previous experiences and solves the problem. A decision is made using logic and evaluation. In second approach, the intelligent agent uses previous experiences and takes data from database as well. In the third approach, the intelligent agent uses previous experiences and data from database. If it is still unable to do critical thinking, the intelligent agent goes one step further and does thinking on its own to critical thinking and identify the problem. Finally, the decision is updated and performance is made, See Fig. 8.

Fig. 8. Critical thinking agent depiction of the project

In problem solving agents, a problem is first defined. The problem faced by agent is guided towards dictionary. The nature of the problem is looked into the dictionary. The possible solution for the problem is looked by problem solving agent. That solution is applied and checked whether the problem is solved or not. This is done in hand along with the critical thinking agent, See Fig. 9.

Fig. 9. Problem solving agent depiction of the project

III. RESULTS

The results are presented in Figs. 10 – 13. In Fig. 10, the region of intervention is shown at the display of the system. In Fig. 11, the catheter wire reached at the region. In Fig. 12, the removal of plaque through balloon is shown with success. In Fig. 13, the placement of stent is animated. Theseresults are generated from the software section of the system.

The onscreen section is at the very initial stage, See Fig. 14. The onscreen display shows a number of parameters related to the performance by the user. These include success rate, performance level, standard, problem-solving agent utilization, and critical-thinking agent utilization. The display on top left corner show the standard by which the performance of user is compared and results are generated according to the evaluation. As stated earlier, these results are at the very initial stage.

Fig. 10. An artery with plaque deposition

Fig. 11. Insertion of catheter in the artery

Fig. 12. Removal of plaque and widening of artery via balloon

Fig. 13. Stent placement

Fig. 14. Indicators for procedure evaluation by problem solving and criticalthinking agents.

IV. CONCLUSIONS

The aim of the research project was to achieve a higher degree of precision in evaluation of training and how closestpossible results for image-guided cardiac interventions and to solve any problem that encountered through the implementation of intelligent agents. The simulator mimics the movement of the catheter sensed and measured through multiple infrared sensors. The project's design has been discussed in terms of its hardware and software and artificial intelligence incorporation. High-precision simulated image- guided cardiac intervention simulator enables cardiac surgeons to polish their skills by incorporating them into educational and learning purposes. A realization of the proposed research in this work is a future task.

ACKNOWLEDGMENT

REFERENCES

[1] T. Javid et al., "Cardiac Coronary Intervention Simulator," 2021 IEEE 18th International Conference on Smart Communities: Improving Quality of Life Using ICT, IoT and AI (HONET), 2021, pp. 66-70, doi: 10.1109/HONET53078.2021.9615446

[2] S. Dawson, S. Cotin, D. Meglan, D. Shaffer, and M. Ferrell, "Designing a Computer-Based Simulator for Interventional Cardiology Training: Catheterization and cardiovascular interventions," Official journal of the Society for Cardiac Angiography & Interventions. 2001, vol. 51, pp. 522-527. 10.1002/1522-726X(200012)51:43.0.CO;2-7.

[3] Cleveland Clinic, "Cleveland Clinic," 11 06 2021. [Online]. Available: https://my.clevelandclinic.org/health/treatments/22066- percutaneous-coronary-intervention.

[4] T. Hafsa, M. Kinat, J. Tariq, "Design and development of a cardiac coronary intervention simulator," IEEC 2021, NEDUET, Karachi, Pakistan

[5] R. Pankaj, Differences between Verification and Validation, Geeks for Geeks, 2020.

[6] L. A. Cristian, R. Y., Ziv, "Image-Guided Interventions," IEEE Pulse, 2016. Online available, Last accessed on 3rd November 2021.

[7] S. Luck, "Why experimentalists should ignore reliability and focus on precision," Luck Lab, Chicago, 2019.

[8] T. Javid, M. Faris, M. D. Mujib, T. Ansari, H. Iftikhar, T. Khalid, and W. Saadat, " Cardiac Coronary Intervention Simulator," IEEE HONET 2021, ISBN: 978-1-6654-2385-4